pathfood Se

University of Warsaw

Biological and Chemical Research Centre

Winter School on Capillary Electrophoresis

Danilo Corradini

Institute for Biological Systems

Consiglio Nazionale delle Ricerche

Montelibretti (Rome) Italy

Funded by the European Union

Winter School on Capillary Electrophoresis

Overview

The five-day Winter School on Capillary Electrophoresis, held as part of the PATHFOOD project at University of Warsaw, is designed for researchers, PhD students and partners of the Project. It is aimed at providing an in-depth exploration of fundamental and practical aspects of capillary electrophoresis (CE) and how this separation technique can be employed to answer scientific questions. Attendees will gain theoretical knowledge and hands-on experience with various CE separation techniques, including capillary zone electrophoresis (CZE), micellar electrokinetic chromatography (MEKC), and capillary electrochromatography (CEC). Key topics will include the influence of operational conditions on separation performance, the role of background electrolyte solutions (BGE) in the separation process, detection, and online preconcentration methods. The school will highlight the versatility of CE in analyzing complex and/or small-quantity samples, including diluted ones, emphasizing its cost-effectiveness, minimal use of hazardous chemicals, and alignment with green chemistry principles. The utility of CE in real-world, practical scenarios will be evidenced in diverse scientific and practical contexts, particularly in food and phytochemical research.

Presenter

Danilo Corradini, PhD, investigates fundamental and practical aspects of capillary electromigration techniques and high performance liquid chromatography (HPLC), applied to analytical chemistry, life science, and phytochemistry. His fundamental studies are devoted to shed light on the physical-chemical mechanisms leading to the separation of biomolecules in capillary electrophoresis (CE), as well as in conventional and micro-scale analytical HPLC. His first involvement in Separation Science was in 1976 during his Ph. D. studies conducted under the scientific direction of Prof. Michael Lederer, founder and first Editor of Journal of Chromatography.

He received postdoctoral education in separation science at the Department of Chemical Engineering of Yale University (USA), where he held several appointments as Postdoctoral fellow (1983-84), Associate researcher (1986) and Visiting scientist (1996), working with Csaba Horváth, pioneer of HPLC and eminent separation scientist, with whom he has conducted a twenty years long fruitful collaboration in the framework of numerous Italy-USA Bilateral Research Projects he was the Principal Investigator.

In recognition of his significant contributions to Analytical Chemistry and Separation Science, he has received several awards and honours, including the Csaba Horváth Memorial Award from the Hungarian Society for Separation Science in 2009, the Central European Group for Separation Sciences Award in 2011, the Arnaldo Liberti Medal from the Italian Chemical Society in 2014, the Giovanni Dugo Medal from the Italian Chemical Society in 2021, the Prof. Andrzej Waksmundzki Award from the Polish Academy of Sciences in 2023, and the Medal Award for Lifetime Achievements from the Central European Group for Separation Science in 2025. Currently, he is the chairmen of the Separation Science Group of the Italian Chemical Society (2025-2027 term), is a Member of the Central European Group for Separation Sciences (CEGSS) and of the International Strategy & Evaluation Board (ISEB) of the Austrian Drug Screening Institute (ADSI), Innsbruck, Austria. Previously (April 2006 – February 2012), he has been a Member of the General Scientific Advisory Board of Consiglio Nazionale delle Ricerche (CNR) and served in the scientific advisory board of the Institute of Chromatography (1996-2000) and of the Institute for Chemical Methodologies (2002-2008), both belonging CNR.

pathfood Se

Pathfood Winter School on Capillary Electrophoresis Program (February 16–20, 2026)

Biological and Chemical Research Centre, University of Warsaw, Żwirki i Wigury 101, 02-089 Warsaw, Poland

Day 1 – Monday, February 16
09:00 – 11:00 Welcome, Objectives, Introduction to Capillary Electrophoresis (CE)
11:00 – 11:30 Coffee break
11:30 – 13:00 Session 1 – Basic Concepts of Electrokinetic Phenomena
13:00 – 14:00 Lunch break
14:00 – 16:00 Session 2 – Instrumentation for CE, Key Operational Steps, Data handling

Day 2 – Tuesday, February 17
11:30 – 13:00 Laboratory – Overview of CE Equipment and Software for System Control (on-site only)
13:00 – 14:00 Lunch break
14:00 – 16:00 Session 3 – Electroosmotic flow (EOF) and Factors Influencing Performance and Separation

Day 3 – Wednesday, February 18
09:00 – 11:00 Session 4 – Dynamic and Chemical Coating of Bare Fused-silica Capillaries - Control EOF
11:00 – 11:30 Coffee break
11:30 – 13:00 Session 5 – Main Separation Modes of CE (Part 1)
13:00 – 14:00 Lunch break
14:00 – 16:00 Laboratory – Measurement EOF (on-site only)

Day 4 – Thursday, February 19
09:00 – 11:00 Session 6 - Main Separation Modes of CE (Part 2)
11:00 – 11:30 Coffee break
11:30 – 13:00 Session 7 – Online Sample Preconcentration. Method Development and Validation
13:00 – 14:00 Lunch break
14:00 – 16:00 Laboratory – CZE plant secondary metabolites (on-site only)

Day 5 – Friday, February 20
09:00 – 11:00 Laboratory – CZE plant primary metabolites (on-site only)
11:00 – 11:30 Coffee break
11:30 – 13:00 Session 8 – Multidimensional CE. Hyphenation of CE with Mass Spectrometry.
13:00 – 13:30 Summary and Closing

Additional information
Lectures on-site and online.
Laboratory sessions on-site only.

Helpdesk contact: pathfood@cnbc.uw.edu.pl

- D. Corradini “Capillary Electromigtration Techniques”. Handbook of HPLC, Second Edition, D. Corradini Ed. Chapter 6, CRC Press, 2010, pp 155-206.

- D. Corradini “Buffering agents and additives for the background electrolyte solutions used for peptide and protein capillary zone electrophoresis”. Trends in Analytical Chemistry 164 (2023) 117080. https://doi.org/10.1016/j.trac.2023.117080

- D. Corradini, F. Orsini, I. Nicoletti, L. De Gara “Capillary Electromigration Techniques for the Analysis of Phenolic Compounds in Plants and Plant-Derived Food, Part 2: Capillary Electromigration Techniques”. LC GC EUROPE 32 (2019) 8-14.

6 Capillary Electromigration Techniques

Danilo Corradini

CONTENTS

6.1 INTRODUCTION

Liquid-phase separation techniques using columns of capillary size have recently gained large acceptance for qualitative and quantitative analyses as well as physicochemical characterizations. High throughput, small sample amount requirement, and high separation efficiency are the major advantages of these microscale separation techniques. Additional advantages include straightforward optimization of separation, use of small amounts of chemicals, reduced waste, and a wide

range of possible detection methods, which include absorbance, fluorescence, electrochemical, nuclear magnetic resonance spectroscopy, and mass spectrometry.

A variety of microscale separation methods, performed in capillary format, employ a pool of techniques based on the differential migration velocities of analytes under the action of an electric field, which is referred to as capillary electromigration techniques. These separation techniques may depend on electrophoresis, the transport of charged species through a medium by an applied electric field, or may rely on electrically driven mobile phases to provide a true chromatographic separation system. Therefore, the electric field may either cause the separation mechanism or just promote the flow of a solution throughout the capillary tube, in which the separation takes place, or both.

The electrically driven flow of a liquid within a capillary tube, either open or packed or filled with a solid medium bearing a stationary phase, is caused by electroosmosis, which originates from the action of the electric field on the electric double layer formed at the plane of share between the inner surface of the capillary tube and the surrounding liquid (see Section 6.2). The flow of liquid caused by electroosmosis is termed electroosmotic flow (EOF) and displays a plug-like profile because the driving force is uniformly distributed along the capillary tube. Consequently, a uniform flow velocity vector across the capillary occurs. The flow velocity approaches zero only in the region of the capillary tube close to its inner surface. Therefore, no peak broadening is caused by sample transport carried out by the EOF. This is in contrast to the laminar or parabolic flow profile generated in a pressure-driven system where there is a strong pressure drop across the capillary caused by frictional forces at the liquid–solid boundary. A schematic representation of the flow profile due to electroosmosis in comparison to that obtained in the same capillary column in a pressure-driven system, such as a capillary HPLC, is displayed in Figure 6.1.

Separations in capillary electromigration techniques take place according to different separation modes in either open or packed or monolithic capillaries of typical inner diameter and length of 20–100 μm and 20–100 cm, respectively. The ends of the capillary are inserted into two distinct vessels (electrolyte compartments) containing the electrolyte solution, usually of same composition of that filled into the capillary, and the electrodes connected to a high-voltage power supply, typically up to 30 kV. The capillary format enables the application of high electric fields with minimal generation of Joule heat, which is efficiently dissipated by transfer through the tube wall as a result of the large surface-to-volume ratio of the capillary and, in open capillaries, ensures the absence of convective mixing of the separated zone in the electrolyte solution.

Samples are introduced into the capillary by either electrokinetic or hydrodynamic or hydrostatic means. Electrokinetic injection is preferentially employed with packed or monolithic capillaries whereas hydrostatic injection systems are limited to open capillary columns and are primarily used in homemade instruments. Optical detection directly through the capillary at the opposite end of sample injection is the most employed detection mode, using either a photodiode array or fluorescence or a laser-induced fluorescence (LIF) detector. Less common detection modes include conductivity [1], amperometric [2], chemiluminescence [3], and mass spectrometric [4] detection.

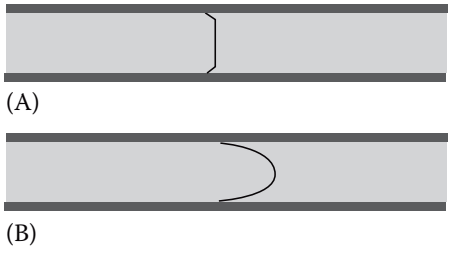

FIGURE 6.1 Schematic representation of the flow profile generated by (A) electroosmosis and (B) a mechanical pump.

On-line coupling of capillary electromigration techniques with nuclear magnetic resonance spectroscopy [5] and matrix-assisted laser desorption/ionization (MALDI) time-of-flight (TOF) mass spectrometry [6] has also been reported.

This chapter illustrates basic concepts, instrumental aspects, and modes of separation of electromigration techniques performed in capillary format. It should be noted that most of the fundamental and practical aspects of the electromigration techniques performed in capillary tubes also apply when the techniques are carried out in microchannels fabricated on plates of reduced dimensions, communally referred to as chips.

6.2 BASIC CONCEPTS OF ELECTROKINETIC PHENOMENA

The word electrokinetic implies the joint effects of motion and electrical phenomena. We are interested in the electrokinetic phenomena that originate the motion of a liquid within a capillary tube and the migration of charged species within the liquid that surrounds them. In the first case, the electrokinetic phenomenon is called electroosmosis whereas the motion of charged species within the solution where they are dissolved is called electrophoresis. This section provides a brief illustration of the basic principles of these electrokinetic phenomena, based on text books on physical chemistry [7–9] and specialized articles and books [10–12] to which a reader interested to study in deep the mentioned theoretical aspects should refer to.

6.2.1 Electroosmosis

Electroosmosis refers to the movement of the liquid adjacent to a charged surface, in contact with a polar liquid, under the influence of an electric field applied parallel to the solid–liquid interface. The bulk fluid of liquid originated by this electrokinetic process is termed electroosmotic flow. It may be produced either in open or in packed or in monolithic capillary columns, as well as in planar electrophoretic systems employing a variety of supports, such as paper or hydrophilic polymers. The origin of electroosmosis is the electrical double layer generated at the plane of share between the surface of either the planar support or the inner wall of the capillary tube and the surrounding solution, as a consequence of the uneven distribution of ions within the solid/liquid interface.

6.2.1.1 Electric Double Layer

Usually a solid surface acquires a superficial charge when it is brought into contact with a polar liquid. The acquired charge may result from one or a combination of the following mechanisms: dissociation of ionizable groups on the surface, adsorption of ions from solution, by virtue of unequal dissolution of oppositely charged ions of which the surface is composed. This superficial charge causes a variation in the distribution of ions near the solid–liquid interface. Ions of opposite charge (counterions) are attracted toward the surface whereas ions of the same charge (co-ions) are repulsed away from the surface. This, in combination with the mixing tendency of thermal motion, leads to the generation of an electric double layer formed of the charged surface and a neutralizing excess of counterions over co-ions distributed in a diffuse manner in the polar liquid. Part of counterions are firmly held in the region of the double layer closer to the surface (the compact or Stern layer) and are believed to be less hydrated than those in the diffuse region of the double layer where ions are distributed according to the influence of electrical forces and random thermal motion. A plane (the Stern plane), located at about one ion radius from the surface separates these two regions of the electric double layer.

Certain counterions may be held in the compact region of the double layer by forces additional to those of purely electrostatic origin, resulting in their adsorption in the Stern layer. Specifically

adsorbed ions are attracted to the surface by electrostatic and/or van der Waals forces strongly enough to overcome the thermal agitation. Usually, the specific adsorption of counterions predominates over co-ions' adsorption.

The variation of the electric potential in the electric double layer with the distance from the charged surface is depicted in Figure 6.2. The potential at the surface (ψ_0) linearly decreases in the Stern layer to the value of the zeta potential (ζ). This is the electric potential at the plane of shear between the Stern layer (and that part of the double layer occupied by the molecules of solvent associated with the adsorbed ions) and the diffuse part of the double layer. The zeta potential decays exponentially from ζ to zero with the distance from the plane of shear between the Stern layer and the diffuse part of the double layer. The location of the plane of shear a small distance further out from the surface than the Stern plane renders the zeta potential marginally smaller in magnitude than the potential at the Stern plane (ψ_δ). However, in order to simplify the mathematical models describing the electric double layer, it is customary to assume the identity of (ψ_δ) and ζ. The bulk experimental evidence indicates that errors introduced through this approximation are usually small.

According to the Gouy–Chapman–Stern–Grahame (GCSG) model of the electric double layer [12], the surface density of the charge in the Stern layer is related to the adsorption of the counterions, which is described by a Langmuir-type adsorption model, modified by the incorporation of a Boltzmann factor. Considering only the adsorption of counterions, the surface charge density σ_S of the Stern layer is related to the ion concentration C in the bulk solution by the following equation:

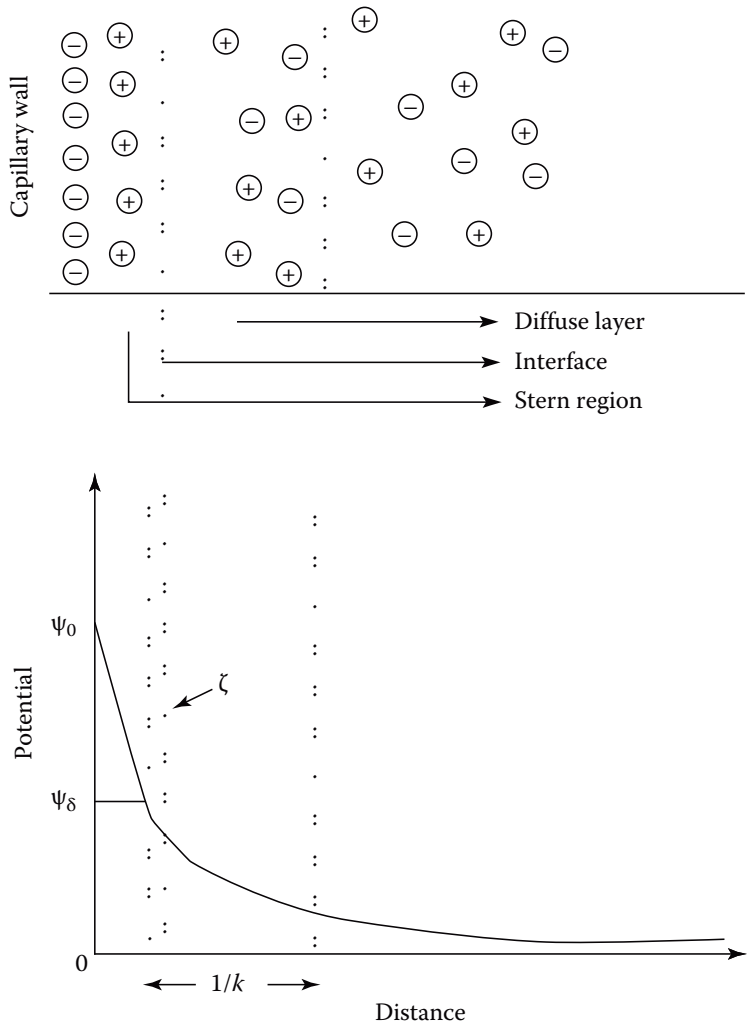

FIGURE 6.2 Graphical representation of the electric double layer at the solid–liquid interface within a capillary tube and diagram of the decay of the electric potential with distance from the capillary wall.

$$\sigma_S = \frac{zen_0 \frac{C}{V_m} \exp\left(\frac{ze\xi + \Phi}{kT}\right)}{1 + \frac{C}{V_m} \exp\left(\frac{ze\xi + \Phi}{kT}\right)} \tag{6.1}$$

where
e is the elementary charge
z is the valence of the ion
k is the Boltzmann constant
T is the temperature
n_0 is the number of accessible sites
V_m is the molar volume of the solvent
Φ is the specific adsorption potential of counterions

The surface charge density of the diffuse part of the double layer is given by the Gouy–Chapman equation:

$$\sigma_G = \left(8\varepsilon kTc_0\right) \sinh\left(\frac{ze\xi}{2kT}\right) \tag{6.2}$$

where
ε is the permittivity of the electrolyte solution
c_0 is the bulk concentration of each ionic species in the electrolyte solution

At low potentials, Equation 6.2 reduces to

$$\sigma_G = \frac{\varepsilon\xi}{\kappa^{-1}} \tag{6.3}$$

where κ^{-1} is the reciprocal Debye–Huckel parameter, which is defined as the "thickness" of the electric double layer. This quantity has the dimension of length and is given by the following equation:

$$\kappa^{-1} = \left(\frac{\varepsilon kT}{2e^2 I}\right)^{1/2} \tag{6.4}$$

in which I is the ionic strength of the electrolyte solution.

Equation 6.3 is identical to the equation that relates the charge density, voltage difference, and distance of separation of a parallel-plate capacitor. This result indicates that a diffuse double layer at low potentials behaves like a parallel capacitor in which the separation distance between the plates is given by κ^{-1}. This explains why κ^{-1} is called the double layer thickness.

Equation 6.2 can be written in the form

$$\xi = \frac{\sigma_G \kappa^{-1}}{\varepsilon} \tag{6.5}$$

which indicates that the zeta potential can change due to variations in the density of the electric charge, in the permittivity of the electrolyte solution, and in the thickness of the electric double layer, which depends, according to Equation 6.4 on the ionic strength and consequently on the

concentration and valence of the ions in solution. Sign and value of the zeta potential determine direction and velocity of the EOF, generated by applying an electric field.

6.2.1.2 Dependence of EOF on the Zeta Potential

The dependence of the velocity of the EOF (v_{eo}) on the zeta potential is expressed by the Helmholtz–von Smoluchowski equation [13]:

$$v_{eo} = -\frac{\varepsilon_0 \varepsilon_r \zeta}{\eta} E \tag{6.6}$$

where

E is the applied electric field
ε_0 is the permittivity of vacuum
ε_r and η are the dielectric constant and the viscosity of the electrolyte solution, respectively

This expression assumes that the dielectric constant and viscosity of the electrolyte solution are the same in the electric double layer as in the bulk solution.

The Helmholtz–von Smoluchowski equation indicates that under constant composition of the electrolyte solution, the EOF depends on the magnitude of the zeta potential, which is determined by various factors influencing the formation of the electric double layer, discussed above. Each of these factors depends on several variables, such as pH, specific adsorption of ionic species in the compact region of the double layer, ionic strength, and temperature.

The specific adsorption of counterions at the interface between the surface and the electrolyte solution results in a drastic variation of the charge density in the Stern layer, which reduces the zeta potential and hence the EOF. If the charge density of the adsorbed counterions exceeds the charge density on the surface, the zeta potential changes sign and the direction of the EOF is reversed.

The ratio of the velocity of the EOF to the applied electric field, which expresses the velocity per unit field, is defined as electroosmotic coefficient or more properly, electroosmotic mobility (μ_{eo}) [13]:

$$\frac{v_{eo}}{E} = \mu_{eo} = -\frac{\varepsilon_0 \varepsilon_r \zeta}{\eta} \tag{6.7}$$

Using the SI units, the velocity of the EOF is expressed in meters/second (m s^{-1}) and the electric field in volts/meter (V m^{-1}). Consequently, the electroosmotic mobility has the dimension of m^2 V^{-1} s^{-1}. Since electroosmotic and electrophoretic mobility are converse manifestations of the same underlying phenomena, the Helmholtz–von Smoluchowski equation applies to electroosmosis, as well as to electrophoresis (see below). In fact, it describes the motion of a solution in contact with a charged surface or the motion of ions relative to a solution, both under the action of an electric field, in the case of electroosmosis and electrophoresis, respectively.

6.2.1.3 Factors Influencing the EOF

According to Equation 6.6, the velocity of the EOF is directly proportional to the intensity of the applied electric field. However, in practice, nonlinear dependence of the EOF on the applied electric field is obtained as a result of Joule heat production, which causes the increase of the electrolyte temperature with consequent decrease of viscosity and variation of all other temperature-dependent parameters (protonic equilibrium, ion distribution in the double layer, etc.). The EOF can also be altered during a run by variations of the protonic concentration in the anodic and cathodic electrolyte solutions as a result of electrophoresis. This effect can be minimized by using electrolyte

solutions with high buffering capacity, electrolyte reservoirs of relatively large volume, and by frequent replacement of the electrolyte in the electrode compartments with fresh solution.

Velocity and direction of the EOF also depend on the composition, pH, and ionic strength of the electrolyte solution. Both pH and ionic strength influence the protonic equilibrium of fixed charged groups on the surface and of ionogenic substances in the electrolyte solution, which affect the charge density in the electric double layer and consequently, the zeta potential. In addition, the ionic strength influences the thickness of the electric double layer (κ^{-1}). According to Equation 6.4, increasing the ionic strength causes a decrease in κ^{-1}, which is currently referred to as the compression of the double layer, with consequential reduction of the zeta potential. Hence, the practical effect in increasing the ionic strength is decreasing the EOF.

6.2.2 Electrophoresis

Section 6.2.1 has briefly examined the electrokinetic phenomena of electroosmosis, which refers to the motion of a liquid relative to a surface under the action of an electric field. This section examines the motion of ions in an applied electric field relative to the solution that surrounds them.

6.2.2.1 Electrophoretic Mobility

Under the action of an electric field, ions in solution migrate toward the electrode of opposite sign, i.e., positively charged ions migrate toward the cathode and negatively charged ions migrate toward the anode. The velocity v at which each ion migrates toward the electrode of opposite sign is proportional to the strength of the electric field E, which is expressed as the electric potential gradient in volts per unit length (in m) across the capillary tube:

$$v = \mu E \tag{6.8}$$

The constant of proportionality in Equation 6.8 is called the electrophoretic mobility and expresses the velocity of the ion (in m s^{-1}) in the considered medium per unit electric field (in V m^{-1}):

$$\mu = \frac{v}{E} \tag{6.9}$$

Therefore, the electrophoretic mobility is expressed in $m^2\ V^{-1}\ s^{-1}$, and is a characteristic constant for any given couple "ion–medium."

The value of the electrophoretic mobility can be calculated considering the migration of an ion in an electrolyte solution at infinite dilution where no ionic interactions occur. Under the action of an electric field, the ion is accelerated by a force F_{el}, directed toward the appositively charged electrode, which is given by

$$F_{el} = qE \tag{6.10}$$

where

q is the electrical charge of the ion
E is the electric field strength

This force is contrasted by an opposite force (F_v), due to the viscosity resistance of the solution, which increases as the ion velocity (v) increases:

$$F_v = fv \tag{6.11}$$

The proportional constant f in Equation 6.11 is called the friction factor. When the two forces equal each other, the ion moves with a constant migration velocity, which is expressed by the following equation:

$$v = \frac{qE}{f} \tag{6.12}$$

Isolated ions can be assimilated to spherical particles for which, according to Stokes law, the friction factor is given by

$$f = 6\pi\eta r \tag{6.13}$$

where

η is the viscosity of the solution

r is the radius of the solvated ion, the so-called Stokes or hydrodynamic radius

Substitution of Equation 6.13 into Equation 6.12 yields

$$v = \frac{q}{6\pi\eta r} E = \mu^0 E \tag{6.14}$$

where μ^0 expresses the velocity of the ion per unit electric field.

6.2.2.2 Absolute and Effective Mobility

The constant of proportionality of Equation 6.14 is defined the absolute mobility or mobility at infinite dilution (μ^0):

$$\mu^0 = \frac{q}{6\pi\eta r} \tag{6.15}$$

Equation 6.15 is valid only for rigid, spherical ions. In addition, it originates from Equation 6.14, which is applicable only if the electric field at the ion is due to the applied electric field only, undisturbed by the effects of the other ions in solution. Consequently, Equation 6.15 ignores other forces originating in the counterion atmosphere, leaving the influence of the medium on the mobility unexplained.

In practice, electrophoresis is not performed at infinite dilution and other ions are present in the electrolyte solution. In addition, each ion is surrounded by oppositely charged counterions, forming the so-called ionic atmosphere, which tends to move in the opposite direction of the ion and, therefore, contrast the migration of the ion toward the electrode of opposite sign, lowering its electrophoretic mobility. Logically, the electrostatic interactions between ions of same sign and between each ion and its counterions are stronger with increasing electrolyte concentration with the result that the electrophoretic mobility at finite dilution is lower than that at infinite dilution.

In order to consider the influence of the ionic atmosphere on the electrophoretic mobility, the theoretical electrical charge of the ion q in Equation 6.14 is replaced by the smaller effective charge Q_{eff} and the hydrodynamic radius r by the effective radius R of the ion, which includes its ionic atmosphere:

$$\mu = \frac{Q_{\text{eff}}}{6\pi\eta R} \tag{6.16}$$

where μ is the effective mobility, which is always lower than the absolute mobility.

The effective mobility of ionogenic substances present in solution in different forms, which are in a fast dynamic equilibrium, is expressed as

$$\mu_A = \frac{1}{c_A}\sum_{i=1}^{n} C_i\mu_i = \sum_{i=1}^{n} x_i\mu_i \tag{6.17}$$

where

μ_A is the effective mobility of the considered substance A
C_A is the analytical concentration
C_i, x_i, and μ_i, are concentration, molar fraction, and effective mobility of the component i, respectively

Under this condition, the ionogenic substance migrates as a single substance.

It has been pointed out above that electroosmotic and electrophoretic mobilities are converse manifestations of the same underlying phenomena; therefore the Helmholtz–von Smoluchowski equation based on the Debye–Huckel theory developed for electroosmosis applies to electrophoresis as well. In the case of electrophoresis, ξ is the potential at the plane of share between a single ion and its counterions and the surrounding solution.

6.3 INSTRUMENTATION FOR CAPILLARY ELECTROMIGRATION TECHNIQUES

6.3.1 Separation Unit

The instrumentation employed to perform capillary electromigration techniques is basically the same for all separations modes, either based on an electrophoretic or on a chromatographic separation mechanism. A schematic representation of a typical instrument for capillary electromigration techniques is reported in Figure 6.3. Commercially available instruments are equipped with a power supply allowing to apply up to 30 kV. Such limit depends on the possible corona discharges through the capillary and elsewhere in the instrument that may take place at values of applied voltage higher than 30 kV. Besides the applied voltage, the resulting driving current mainly depends on the composition of the electrolyte solution and is commonly maintained at values lower than 100–200 μA by regulating the applied voltage, which is usually set at a constant value. However, almost all commercially available instruments allow operation at constant current or constant power across the capillary, as well. Another desired feature of the power supply is the possibility to reverse the polarity, which allows to ground either electrode by a remote control.

The power supply is connected by a pair of isolated cables to the two electrodes that are immersed into the reservoirs containing the electrolyte solution and the ends of the capillary, either open

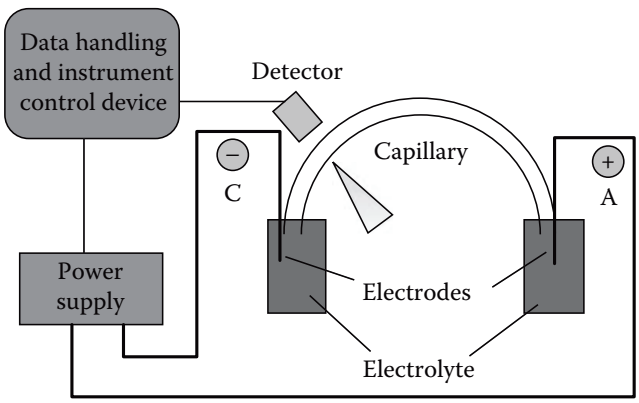

FIGURE 6.3 Scheme of a basic instrument for capillary electromigration separation techniques.

or containing a suitable chromatographic support (see Section 6.5), usually filled with the same electrolyte solution enclosed in the electrode compartments.

Tubular fused-silica capillaries, externally coated with a polyimide film to alleviate the fragility of this material, are generally employed. A small section of the polyimide coating is removed to generate a window in correspondence to the optical center of the detector to allow on-capillary detection. Capillaries made from organic synthetic material (e.g., Teflon or related materials, poly(etheretherketone) [PEEK], poly(vinylchloride), and polyethylene) have found limited applicability [14–16] due to the superior properties of fused-silica tubing, which include high thermal conductivity, high electrical resistance, good chemical inertness, good flexibility, high mechanical strength, and good UV-visible transparency in the zone where the polyimide external coating is removed. Also rarely employed are fused-silica capillaries of rectangular cross sections in spite of the significant improvements in absorbance detection sensitivity due to the flat walls that produce less optical distortion than circular capillary walls [17,18].

In most commercially available instruments, the capillary is mounted on a cartridge that is part of the cooling system devoted to maintain the capillary in an environment at constant temperature, either by circulating air or a cooling fluid through the cartridge, which also guarantees reliable alignment of the capillary detection windows in the optical center of the detector. An inert gas or air supply is used to rinse and fill the capillary with the electrolyte solution, to introduce the sample by hydrodynamic injection, and for the pressurization of packed and monolithic capillary column to prevent air bubble formation. In the case of rinsing and filling the capillary with solutions or introducing sample by hydrodynamic injection, only one electrolyte reservoir is pressurized, whereas the same pressure is applied on both reservoirs for the pressurization of capillaries filled or packed with a chromatographic support.

Other common sample injection techniques include siphoning and electrokinetic sampling, whereas the use of sampling devices, such as miniaturized sampling valve [19], rotary-type injectors [20], or electric sample splitter [21] have found very limited applications. Sample injection by siphoning is performed by introducing the appropriate end of the capillary into the sample vial and raising it up to a defined level above the electrolyte reservoir for a certain time. The resulting hydrostatic pressure generates a hydrodynamic flow that allows the introduction of a volume of the sample solution into the capillary proportional to the level and duration of raising the sample vial, pending on the fast and repeatable execution of all operations. In brief, the procedure comprises moving the capillary end from the electrolyte reservoir to the sample vial, raising the sample vial, returning it back to the reservoir level after the sampling time, and moving back the capillary end into the electrolyte reservoir. Therefore, the repeatability of these operations is low when they are done manually, as in the case of homemade apparatus. On the other hand, this injection mode allows introducing an aliquot of the sample representative of its composition.

Electrokinetic sampling is based on electrophoretic migration of charged components of sample and introduction of the sample solution into the capillary by the EOF. The main drawback of this sampling technique is the selective introduction of sample, which depends on the polarity of applied voltage, electrophoretic mobility of each sample component, and velocity of the EOF. For example, injecting at the anodic end in presence of cathodic EOF implies that positively charged analytes are selectively introduced into the capillary at a greater extent than negatively charged ones, which are introduced into the capillary only if their electrophoretic mobility is lower than the EOF, otherwise they do not enter the capillary at all. In such a case, the analytes introduced into the capillary tube are not representative of the sample composition.

In commercially available instruments, all vials containing either the sample solution or the solutions employed for separation and for rinsing the capillary between runs are held in an autosampler, which in most instruments can be thermostated at a desired temperature. The autosampler can also be programmed to carry out the collection of separated fractions for micropreparative applications. The operations performed by the autosampler and by the other equipments of the separation unit

are controlled by suitable software loaded on a personal computer, also performing data acquisition and processing.

6.3.2 Detection

Typically, sample detection in electromigration techniques is performed by on-column detection, employing a small part of the capillary as the detection cell where a property of either the analyte, such as UV absorbance, or the solution, such as refractive index or conductivity, is monitored. This section briefly describes the major detection modalities employed in capillary electromigration techniques, which are accomplished using UV-visible absorbance, fluorescence spectroscopy, and electrochemical systems. The hyphenation of capillary electromigration techniques with spectroscopic techniques employed for identification and structural elucidation of the separated compounds is also described.

6.3.2.1 Absorbance

As in HPLC, the primarily used detector is based on the absorbance of UV or visible light, due to the great number of substances that absorb these radiations. The photometric on-column detection is performed through a "window" obtained by removing a small portion of the polyimide external coating at one end of the capillary tube. The UV or visible light is focused though the central bore (lumen) of the capillary tube by either fiber optics or high-quality lens, and is then detected by a suitable photosensor. The high transparency of fused silica allows detection at wavelength as low as 190 nm. The most common photometric detectors employed in electromigration techniques comprise fixed wavelength, variable wavelength, scanning monochromator, and photodiode array detectors. Similarly to the detectors used in HPLC, low pressure discharge lamps are employed as the sources of intensive line UV radiations, such as mercury (254 nm) or cadmium (229, 326 nm), whereas deuterium lamps, covering the range 190–700 nm, are employed in variable-wavelength and photodiode array detectors, where a tungsten–halogen lamp may be also employed to improve the performance in the visible region.

The main drawback of photometric on-column detection is the short distance the light travels through the capillary (the optical path length), which corresponds to the internal diameter of the capillary tube. This is because, according to the Beer's law, the sensitivity in photometric detection is proportional to the optical path length, which in the on-column detection is in the range of 20–100 µm, compared to the usual 1.0 cm path length of standard HPLC detectors. Moreover, the incident radiation enters the detection zone through a curve surface, which leads to light intensity loss. Even with detectors having noise levels as low as 10^{-5} absorption units (au), concentration detection limits are rarely lower than 10^{-6} M. However, since the injected sample volume is in the range of nanoliters (nL), for a 10.0 nL volume of injected sample at 10^{-6} M concentration, the corresponding injected sample mass is in the range of 10^{-14} mol. Therefore, at a relatively poor concentration, detection limit of 10^{-6} M corresponds an excellent mass detection limit of 10^{-14} mol.

Improvements in photometric detection obtained by increasing the optical path length include the use of capillaries having bubble shape at the detection zone [22], which is fabricated directly into the fused-silica tube, capillaries bent to a Z-shape configuration [23] or with modified surface to realize a multireflective absorption cell at the detection region of the capillary tube [24] (see Figure 6.4). Increasing the inner diameter of the capillary tube only at the detection window ("bubble" cell) offers the sensitivity of a wide inner diameter capillary and the low-current generation of a narrow one. The improvement in sensitivity is 3–5-fold over a capillary of same inner diameter, whereas resolution and peak shape are practically not affected. According to Beer's law, the sensitivity gains in a Z-shaped capillary of 50 µm inner diameter can exceed a factor 100 for an optical path length of 5 mm. However, the gain in sensitivity is at expenses of resolution that is lost for adjacent peaks. Resolution is also sacrificed using the multireflective absorption cell, which is made directly onto the capillary by silver coating a short portion of the capillary at the detection

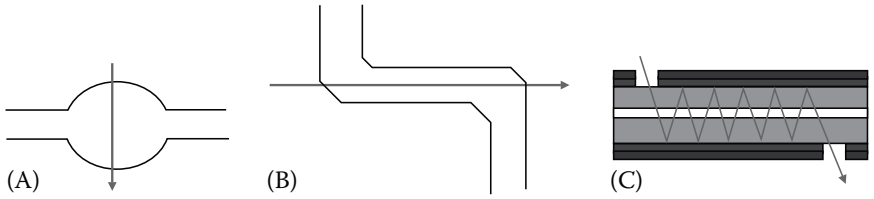

FIGURE 6.4 Schematic representation of capillaries with (A) bubble shape, (B) Z-shape, and (C) multireflective absorption detection zone configuration. The arrow indicates how the light beam travels through the capillary at the detection zone.

region in order to enlarge the volume of solution probed by the incident light, whose entrance is 1.5 mm apart from the exit port made in correspondence to the photosensor. Detection sensitivity improvement of 40 fold has been reported using laser illumination and multireflective absorption cell, in comparison to direct on-column detection [24].

A high-sensitivity detection cell that can be fully decoupled from the separation capillary, either open or packed has been introduced by Agilent [25]. The cell is constructed from silica parts fused together and is flanked by flat, clear windows in order to minimize stray light. The optical path length is 1.2 mm and a 20-fold increase in detection sensitivity is reported, however, resolution is lost when the interpeak volume is lower than the cell volume (1.2 nL).

Furthermore, as it has been mentioned above, the effects of limited optical path length can be alleviated using capillaries of rectangular cross sections and performing the detection through the long axis of the capillary with the additional advantage that the flat walls of rectangular capillaries produce less optical distortion and scatter compared to the walls of circular capillaries. However, higher cost and minor availability of rectangular capillaries over the circular ones have limited their use.

Besides the short optical path length, further sources of poor absorbance detection are the high background noise level due to low light intensity and challenging optical coupling resulting from the small size of the detection window, which may be improved using optical fibers to focus the incident radiation and to collect the light passed through the capillary. Other attempts to improve absorption detection include the use of light-emitting diodes (LEDs) as alternative light sources. LEDs are particularly attractive in absorbance detection due to their excellent output stability, reasonable monochromaticity, and the option of emission at a variety of wavelengths, covering UV, visible, and near-infrared region (280–1300 nm) [26]. The improvement in sensitivity in using a LED is primarily due to its low noise compared to traditional UV-visible light sources, its high intensity at nearly monochromatic output, and small size, which make easy the efficient coupling between light source, capillary, and photodiode detectors [27,28]. The reduced size of LEDs, their exceptional performance, long lifetime, and low cost have greatly contributed to increase the recent attention on these light sources [29,30], which are cool emitters and can be used to realize miniature absorbance detection systems for portable electrophoretic instrumentation [31]. Up to 10 time detection sensitivity improvement have been reported in absorbance detection with LEDs light sources, in comparison to traditional UV-visible light emitters [32]. However, also with LED light sources, the limits of detection are still in the range of 10^{-5} to 10^{-6} M [26].

6.3.2.2 Fluorescence and Laser-Induced Fluorescence

Fluorescence detection is widely employed in electromigration techniques for samples that naturally fluoresce or are chemically modified to produce molecules containing a fluorescent tag. Indirect detection incorporating a fluorescent probe into the electrolyte solution is also employed. One of the most common fluorophores used for this purpose is fluorescein, which is a water soluble, stable, and relatively cheap compound.

In a typical fluorescence detector, the excitation radiation emitted by the high-energy source passes through a suitable filter or monochromator and then is focused though the lumen of the

detection window, which is made at the detection end of the capillary. The emitted fluorescence radiation is collected orthogonally to the excitation beam and passes a slit, to eliminate the scattered excitation radiation, and a second filter or monochromator, to select the emission wavelength, prior to be focused on the photosensor, which usually is either a photomultiplier or a photodiode. Typically, a mercury–xenon arc lamp is employed as the emitter of the excitation radiation.

The signal measured by the photosensor expresses the intensity of the emitted fluorescence (I_F), which depends on the intensity of the incident light (I_0) and sample concentration c, among other factors, such as the fluorescence (or quantum) yield (Φ), the molar absorption coefficient (ε), and the optical path length (d). At low concentration, the intensity of emitted fluorescence is given by the following equation [33]:

$$I_F = I_0 \varphi \, (2.3025 \varepsilon d c) \tag{6.18}$$

which indicates that at otherwise constant conditions the intensity of the emitted fluorescence directly augments with increasing the intensity of the incident light. Therefore, high-intensity monochromatic beams as lasers are preferred excitation sources due to their brightness and spatial beam properties, which allow the excitation energy to be efficiently focused in a very small area, such as the lumen of the on-column detection windows, whereas the high monochromaticity reduces stray light levels. These excitation light emitters are largely employed to realize LIF detectors, which usually employ microscope objectives or optic fibers to collect the fluorescence signal at the exit port of the detection window, as it has been firstly reported by Gassmann et al. [34].

LIF is to date the most sensitive commercially available detection system developed for electromigration techniques, having concentration detection limits ranging between 10^{-11} and 10^{-13} M and mass detection limits in the order of few molecules with ultrasensitive LIF detectors [35]. However, also the LIF detectors may suffer from various drawbacks, which include specular and diffuse scatter of the laser beam from the capillary, Raman scatter from the solvent, and luminescence from the optics and the background electrolyte solution. Several detector designs have been developed to minimize background radiation and scattering [36], including axial-beam illumination [37], two-beam line confocal detection geometry [38], noncircular cross-section capillary columns [39], and sheath-flow detection cells [40], which alleviate background drawbacks by focusing the sample into a narrow flow stream at the exit of the capillary column.

Among these, LIF with the use of a sheath-flow detection cell is the detector of choice for ultrasensitive detection in capillary electromigration techniques. A typical sheath-flow cuvette consists of a quartz flow cell with planar surfaces in which the capillary detection end is inserted. The sample stream exiting the capillary column is concentrically joined with a laminar flow of a sheath liquid of same composition of the solution employed for the separation in the capillary column, which flushes throughout the detection flow cell by a pump. The result is the formation of a stable narrow sample stream directed to the center of the flow cell where the excitation laser beam is focused using a microscope objective. Because sample and sheath solution have the same composition, no variations in refractive index and light scatter or reflection occur at their interface with the result of greatly reducing the background signal and improving detection sensitivity, which may lead to detection limits as low as one single molecule [41].

Gas lasers with powers ranging from a few to more than 10 W are the most commonly employed sources of the excitation beam in LIF detection. These include He–Cd laser (325 and 442 nm), He–Ne laser (543.6, 592.6, and 633 nm), KrF excimer laser (248 nm), Nd–YAG (yttrium–aluminum–garnet) laser (266 nm), and Ar^+ ion laser (usually 488 and/or 514 nm) [35]. LEDs are very attractive alternatives to lasers as the excitation radiation source in fluorescence detection, due to their low cost, long lifetime, small size, high stability, and availability in a wide wavelength range [26]. Since their first use in capillary electrophoresis, proposed by Bruno et al. [42], LED-induced fluorescent (LEDIF) detection has started to be used with increasing frequency [43–45]. However, the divergent beam of the light emitted by LEDs require more complicated optical configuration than that

employed with lasers, which are also superior in terms of monochromaticity. Therefore, using LEDs as the light source may necessitate to spectrally filter not only the fluorescence emitted beam but also the excitation light [46].

A more sophisticated mode of LIF detection is the multiphoton-excitation (MPE) fluorescence [47], which is based on the simultaneous absorption of more than one photon in the same quantum event and uses special lasers, such as femtosecond mode-locked laser [48] or continuous wave laser [49]. This mode of LIF detection allows mass detection limits at zeptomole level (1 zeptomole = 10^{-21} mol) due to exceptionally low detection background and extremely small detection volume, whereas detection sensitivity in concentration is comparable to that of traditional LIF detection modes. A further drawback is the poor suitability of MPE-fluorescence detection to the on-column detection configuration, which is frequently employed in conventional LIF detection.

6.3.2.3 Electrochemical

Electrochemical detection is based on the measurement of electrical properties of the solution transporting the analyte throughout the capillary column. The detection signal may originate either from a cumulative property of the solution, determined by its overall composition, such as conductivity, high-frequency impedance, permittivity (measurement of bulk property), or from a specific property of the solution related to the activity or concentration of the analyte of interest, such as the current resulting from the oxidation or reduction of an electroactive species (measurement of specific property). In principle, each of the main modes of electrochemical detection, which are based on conductometric, amperometric, voltametric, and potentiometric measurements, is applicable to capillary electromigration techniques [50]. However, technical limitations occurring in positioning the electrodes and in the isolation of the detection system from the high-voltage drop across the separation capillary are a challenge in adopting electrochemical detection in capillary electromigration techniques.

Conductivity detection is a universal detection mode in which the conductivity between two inert electrodes comprising the detector cell is measured. The different arrangements employed for the construction of these detectors include apparatus with a galvanic contact of the solution with the sensing electrodes (contact conductivity detection) [51] and detection systems without galvanic contact of the solution with the sensing electrodes (contactless conductivity detection) [1].

Contact conductivity detection can be performed in either on-column mode, realizing a direct or a solution-mediated contact of the analytes with the electrodes, or in end-column mode [1]. In the on-column mode, the sensing electrodes can be two platinum wires that are inserted into two holes made through the wall of the capillary tube, aligned with the help of a microscope and then sealed, as reported in one of the first papers describing the construction of an on-column conductivity detector [52]. The variations in the conductivity within the detection zone are measured by applying an alternating voltage between the sensing electrodes, in order to assure that the measurements are not affected by Faradaic reaction at the electrodes but solely by the concentration and mobility of the charged species in the solution.

In the end-column conductivity detection mode a sensing electrode is situated at the outlet of the separation capillary column and the conductivity measurement is made between this electrode and the ground electrode of the electromigration system used as the second sensing electrode. Advantages of the end-column detection in comparison to on-column mode include easier arrangement and minor difficulties in positioning the sensing electrode whereas detection sensitivity obtained with the two configurations is comparable (10^{-6} to 10^{-7} M) [53]. However, the dead volume between the separation column outlet and the sensing electrode is a source of band broadening that may greatly reduce efficiency and resolution.

Contactless conductivity detection mode, based on an alternating voltage capacitively coupled into the detection cell, is the practical and robust arrangement nowadays employed in commercially available detectors that has been independently developed in 1998 by Zemann et al. [54] and by Freacassi da Silva and do Lago [55]. This detection mode is based on two tubular electrodes,

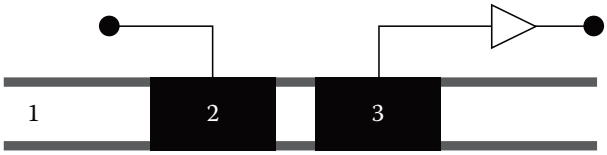

FIGURE 6.5 Schematic representation of contactless conductivity detection cell. (1) Capillary, (2) actuator electrode, and (3) pickup electrode.

consisting of either short metallic tubes [54] or a silver varnish [55], that are placed side by side around the separation capillary tube at a distance of few millimeters, which define the detection volume. Each electrode forms a capacitor with the electrolyte solution contained into the separation capillary whereas the electrolyte solution contained into the capillary forms a resistor. An alternating voltage is applied to one of the galvanically isolated electrodes and the resulting alternating current, which is affected by variations of conductivity into the detection volume, is measured at the second electrode. A schematic representation of a capacitively coupled contactless conductivity detector employing the axial arrangement of two tubular electrodes is reported in Figure 6.5.

Other electrode configurations, such as the radial arrangement consisting of four thin wires placed perpendicularly around the circumference of the separation capillary column, have found less application due to more complicated construction and restriction in space and diameter of the separation capillary [56]. Due to its low cost, robustness, minimal maintenance demands, possibility to be freely moved along the capillary [57], or combined with either UV-absorbance [58] or fluorescence [59] detection, the capacitively coupled contactless conductivity detector has recently gained wide acceptance not only for the determination of inorganic ions but also for biomolecules and organic ions, as it has been recently comprehensively reviewed by Kubáň and Hauser [1].

The amperometric detection modes are suited for monitoring analytes that can be either oxidized or reduced at an electrode surface (the sensing electrode) that is under the influence of an applied direct voltage, which is referred to as the working electrode. The potentiostatic circuitry is completed by the reference and counter electrodes, which, together with the working electrode, comprise the detection cell. Sample detection is carried out by controlling the potential applied to the working electrode, which is usually held at a constant value, and measuring the current resulting from the analyte oxidation or reduction at this potential. The current produced by either the oxidation or the reduction reaction is directly related to the analyte concentration.

Carbon is typically used to construct electrodes and alternative materials include transition or noble metals, such as copper, platinum, and gold. These electrodes are prone to fouling as the oxidation products of the analytes accumulate on the electrode surface. Such problems can be solved by using a pulsed amperometric detector (PAD) [60], in which the applied potential is accompanied by pulsed steps producing the electrode surface activation and electrode cleaning, or an integrated pulsed amperometric detector (IPAD) [61], which incorporates a scanning voltammetry in order to use a potential scan in the detection step along with the pulsed steps for surface activation and electrode cleaning.

The main challenge of coupling capillary electromigration techniques and amperometric detection is the performance of electrochemical measurements in the presence of a high-voltage electrical field. A possible approach to minimizing the interferences of the high-voltage electrical field with the detection circuit consists in making a fracture in the capillary near the end through which the electrophoretic current could be grounded. The fracture divides the capillary into two sections: a "separation capillary" before the fracture and a "detection capillary" beyond it. These two sections are maintained together by a fracture decoupler that in the first configuration described by Wallingford and Ewing was a porous glass capillary forming a joint for the two capillary pieces [62].

A variety of alternative materials can be employed in place of porous glass, including Nefion [63], which is the material of most frequent choice employed today to construct decoupler devices [2]. This arrangement is referred to as the off-column amperometric detection mode [64].

The fabrication and handling of decouplers are quite difficult and require time and manipulative skill. A more straightforward alternative arrangement that avoids the use of a decoupler device is the end-column detection mode, which was first suggested in 1991 by Huang et al. [65] and is widely employed nowadays [66]. In this detection mode, the working electrode is placed near to the outlet of the separation capillary tube and the voltage applied for separation is grounded in the detection reservoir *via* ground electrode. Separation columns of 25 μm internal diameter or smaller are usually employed in order to increase the electrical resistance within the capillary used for separation, with the consequence that the current associated with the electromigration separation system proportionally decreases and the electrical field falls more rapidly at the capillary exit. Typical distance of the working electrode from the outlet of the capillary column is in the order of tens of micrometers and the axial alignment between the capillary exit and the working electrode, which is crucial to achieve optimum detection sensitivity, is carried out by the help of an *x*,*y*,*z*-micropositioner and a microscope. Alignment by this process is quite complex and time consuming and, therefore, a variety of alternative approaches for positioning the working electrode have been developed, such as the use of integrated guiding systems [67] and capillary-electrode holders [68].

6.3.2.4 Other Detection Modes and Hyphenated Techniques

The three main detection techniques described above can also be applied in "indirect" detection mode, which implies to monitor a characteristic property of the background electrolyte solution, such as UV absorbance, fluorescence, or electrochemical property that is altered in the zone of the electrolyte solution containing the separated analytes. This detection mode is typically realized by incorporating into the electrolyte solution a ionic additive that can be easily revealed at low concentration by the selected detection mode, thus giving a highly background detection signal. For electroneutrality reasons, the migration of charged analytes within the electrolyte solution causes the displacement of the ionic additive from the zone where they are present, with consequent production of a negative peak in the background signal, which reveals their presence. Sensitivity is generally lower than that of the corresponding direct detection mode and has to be optimized by minimizing the concentration of the additive, whereas the ratio of background signal to background noise and the number of molecules of the ionic additive that are displayed by a molecule of the analyte (transfer ratio) should be as large as possible. An additional drawback of indirect detection is the linearity of detection response, which has generally a narrower range of that of the corresponding direct detection mode.

Other detection modes employed in capillary electromigration techniques include chemiluminescence [69–71], Raman spectroscopy [72,73], refractive index [74,75], photothermal absorbance [76,77], and radioisotope detection [78]. Some of these detection modes have found limited use due to their high specificity, which restricts the area of application and the analytes that can be detected, such as radioisotope and Raman-based detection that are specific for radionuclides and polarizable molecules, respectively. On the other hand, the limited use of more universal detection modes, such as refractive index, is either due to the complexity of coupling them to capillary electromigration techniques or to the possibility of detecting the analytes of interest with comparable sensitivity by one of the less problematic detection modes described above.

The hyphenation of capillary electromigration techniques to spectroscopic techniques which, besides the identification, allow the elucidation of the chemical structure of the separated analytes, such as mass spectrometry (MS) and nuclear magnetic resonance spectroscopy (NMR) has been widely pursued in recent years. Such approaches, combining the separation efficiency of capillary electromigration techniques and the information-rich detection capability of either MS or NMR, are emerging as essential diagnostic tools for the analysis of both low molecular weight and macromolecular compounds.

Mass spectrometry provides detailed information regarding molecular weights and structures from extremely small quantities of materials. Several types of ionization sources can be employed for the on-line hyphenation of capillary electromigration techniques with MS, which include

electrospray ionization (ESI), atmospheric pressure chemical ionization (APCI), atmospheric pressure photochemical ionization (APPI), MALDI, inductively coupled plasma (ICP), and fast atom bombardment (FAB) [6,79–81]. At present, the most common approaches are based upon the atmospheric pressure ionization (API) interfaces APCI and ESI, whereas the earliest arrangements based on FAB interfaces, which are effected by several drawbacks, such as unstable electrical current, have been progressively abandoned. A major advantage of ESI is the softness of the ionization process by which ions in solution, also of high molecular mass such as proteins, can be transferred to the gas phase [82]. This characteristic results in natural compatibility with both biological samples and liquid-phase separation methods such as capillary electromigration techniques.

Another distinguished characteristic of ESI is the generation of a series of multiply charged intact ions for high molecular mass substances such as proteins. These ions are represented in the mass spectrum as a sequence of peaks, the ion of each peak differing by one charge from those of adjacent neighbors in the sequence. The molecular mass is obtained by computation of the measured mass-to-charge ratios for the multiple charged ions using a "deconvolution algorithm" that transforms the multiplicity of mass-to-charge ratio signals into one single peak on a real mass scale [83]. Obtaining multiple charged ions is advantageous as it allows the analysis of proteins up to 100–150 kDa using mass spectrometers with upper mass limit of 1500–4000 amu.

Several approaches are employed to connect the outlet of the separation capillary column to the MS ion source providing suitable arrangements to apply voltage to the capillary outlet and to obtain the flow rate adjustment between the separation capillary column (in the range of nL min^{-1}) and the MS ion source (in the range of μL min^{-1}), which is usually performed through an additional liquid (sheath liquid). Basically, three major types of interfaces are employed for coupling capillary electromigration systems with MS, which are identified as coaxial sheath-flow [84], sheathless [85], and liquid-junction interfaces [86,87].

In the sheathless interface, the electrical contact is obtained by coating with either a metal [85, 88–90] or a conductive polymer [91] the separation capillary outlet, which is shaped as sharp tip. Also employed are sheathless interfaces in which the electrical contact is established using a metal electrode or a conductive wire inserted into the outlet of the separation capillary [92]. A small gap between the separation capillary and the needle of the ionization device filled by a liquid is the approach made to establish the electrical contact in the liquid junction interface [86,87]. This arrangement is also realized by making porous through chemical etching the tip [93] or a small section of the wall [94] of the separation capillary at its outlet.

The most commonly used arrangement is the coaxial sheath interface, consisting of one or two concentric tubes surrounding the separation capillary through which are flushing the sheath liquid and the nebulizing gas [95,96]. Main advantages of this approach include the possibility of employing for the separation method solutions having limited compatibility with the ionization process and the formation of an electrical contact between the separation capillary and the electrode.

Capillary electromigration technique can also be successfully coupled to MALDI by several arrangements, either off-line [97] or on-line [6]. The off-line coupling is usually realized by collecting the effluent from the capillary column drop wise or by sample deposition from the outlet end of the separation capillary onto the MALDI target, either in the form of spots [98] or as a continuous steak [99], using either appropriated designed tips or sheath-flow-assisted deposition devices [100–103]. The matrix for MALDI is either deposited on the target plate, or mixed with the affluent from the column after the separation or added after sample deposition.

The on-line coupling of CE to MALDI reduces the sample handling steps and, therefore, is expected to be more effective for ultra-trace analysis. Several arrangements have been proposed for such approach including the direct introduction of the end of the separation capillary into the vacuum region of a time-of-flight (TOF) mass spectrometer and desorption of the separated samples by a laser light irradiating the capillary end [104]. A variety of vacuum deposition interfaces has been proposed too, which use either a rotating quartz wheel [105] or a disposable moving tape

[106,107], located in the vacuum of the mass spectrometer, onto which the effluent from the separation capillary is deposited after having been mixed with the matrix solution in a liquid junction located between the above separation capillary and the capillary tube used to deposit the sample–matrix mixture. Other proposed approaches employ a rotating ball interface with an open configuration that allows online sample and matrix contact deposition from the capillaries at atmospheric pressure [108,109].

The on-line approach shows high efficiency and sensitivity. However, off-line cleaning or replacement requirements of the interface result in limited operational time. On the other hand, problems have been reported with the off-line approach too. The essentially arbitrary collection of fractions (spots) clearly offsets the high resolution of the separation. Other problems may arise from the incomplete deposition of the analyte in the form of drops onto the target, which in turn results in a substantial fraction of the analyte being present in the next deposited drop.

Also promising is the hyphenation of capillary electromigration techniques with nuclear magnetic resonance spectroscopy (NMR), which is widely employed for identification and structural elucidation of organic compounds unattainable by other analytical methods. Direct on-line hyphenation can be realized by constructing a solenoidal geometry radio frequency (RF) NMR transmit/receive coil by wrapping a copper or gold wire around the fused-silica capillary at the end of the separation column, which is then located inside the magnet bore of the NMR instrument in position to ensure that the detection zone of the capillary and coil are perpendicular to the static magnetic field, as first reported by Sweedler and coworkers [110,111]. A saddle-type (Helmholtz) RF coil can also be used as the NMR probe [112]. The RF coil is the probe having the function of delivering the radio frequency energy needed to excite NMR active nuclei and of collecting signals from the sample. To gain the maximum NMR signal, a solenoidal RF coil must be aligned perpendicular to the static magnetic field whereas a saddle-type coil must be positioned with its axis parallel to the static magnetic field. Other specific requirements are limited to keeping magnetic objects far away from the magnet, usually several meters depending on the magnet field strength, except with shielded magnets, whereas nonmagnetic plastic electrolyte reservoirs and platinum electrodes can even been located within the magnet bore. Otherwise, the instrumentation employed to perform capillary electromigration techniques can be on-line hyphenated with the NMR spectrometer without major modifications.

Because capillary electromigration techniques employ limited volumes of solvents, their hyphenation with NMR makes economically practicable the use of deuterated solvents, avoiding the elaborate signal suppression techniques requested with the use of protonated solvents that lead to distortion of parts of the NMR spectra. The interpretation of NMR spectra can also be complicated by changes in the chemical shift caused by variations of temperature due to joule heating. Therefore, capillaries of smaller internal diameter are preferred for their higher capability at dissipating heat due to the greater surface-to-area ratio than larger capillaries. On the other hand, because of the low sensitivity of NMR as compared to other detection techniques, ranging between 10^{-9} and 10^{-11} mol [5], capillary of a relatively large internal diameter would be preferred. In practice, capillaries of 75–200 µm internal diameters are generally employed when electromigration separation techniques are hyphenated with NMR.

Using solenoidal RF coils the volume of detection is determined by the diameter of the capillary and the number of turns of the RF coil (determining the length of the probe), whereas the acquisition time of the NMR signal depends on the velocity at which each analyte passes the detection zone. Therefore, with capillary of 75 mm I.D. and solenoidal RF coil of 1 mm length the NMR detection cell volume is about 5 nL and the residence time of the analytes inside the detection cell is usually less than 60 s, which may adversely limit the number of possible NMR acquisitions and therefore the detection sensitivity. Bigger detection cells can be realized by enlarging the inner diameter of the zone of the fused-silica capillary at the end of the separation column where the RF coil is located [112]. Such arrangement results in increasing both detection volume and residence

times at expenses of resolution of closely migrating/eluting analytes. Longer residence times have the effect of enabling prolonged NMR acquisition times and larger detection volumes, resulting in increased mass of the analyte exposed to the mass-sensitive RF coil with the consequence of enhancing sensitivity. However, the enlargement of the inner diameter of the capillary tube brings to a reduction of its thickness at the detection zone with the consequence that the coil comes into closer contact with the sample and magnetic susceptibility effects may occurs, resulting in degraded line shapes and loss of sensitivity. Moreover, a decrease in sensitivity is observed if the volume of the detection cell is larger than the volume occupied by the separated analyte in the capillary separation column due to an increase of the signal-to-noise ratio.

For a given diameter, solenoidal RF coils are 2–3 times more sensitive than saddle-type RF coils [113], which are more difficult to construct than RF coils with solenoidal geometry, especially at small dimensions. Another significant difference between the two RF coils is related to the influence of the magnetic field induced by the current resulting from the electric field applied across the ends of the separation capillary on the acquisition of the NMR spectra. With saddle-type RF coils, the separation capillary is aligned parallel to the NMR static magnetic field, which is practically not affected by the magnetic field induced by the current resulting from the electric field applied across the ends of the separation capillary, perpendicular to the current flow direction and, therefore, to the static magnetic field. On the other hand, using a solenoidal RF coil, positioned perpendicular to the static magnetic field in order to gain the maximum NMR signal, the current associated to the electromigration separation system induces a magnetic gradient along the static magnetic field, which causes the broadening of the NMR signals, resulting in a decrease of sensitivity and a loss of scalar coupling information that are hard to avoid using the shimming procedures generally employed to restore magnetic field homogeneity. Also of limited help are NMR post-processing procedures appositively developed to extract information from NMR spectra distorted by inhomogeneous magnetic field resulting from the magnetic field induced by the current associated to the electromigration separation system [114].

The simplest approach to circumvent the detrimental effect of the magnetic field induced by the electromigration system consists in performing the acquisition of the NMR spectra during periodic interruptions of the applied electric field (stopped-flow method), which have also the beneficial effect of increasing the acquisition times and eliminating the observed degradation of NMR signals acquired with sample movement through the NMR probe [115]. Such procedure is also employed to perform signal acquisitions for two-dimensional NMR investigations [116]. However, the periodic interruption of the applied electric field may adversely affect the separation efficiency and reduce resolution due to the diffusion of the analytes over the stopped-flow periods, in addition to increasing the analysis time. These drawbacks can be avoided by splitting the flow from the separation capillary into two outlets, consisting of two capillaries each holding a RF coil, and alternating electromigration flow and NMR measurements between the two outlets in order to perform continuous electromigration separations with stopped-flow NMR signal acquisition [117].

Alternatively, the electric field can be solely applied along the portion of the capillary column, located outside the magnet bore of the NMR spectrometer, where the separation takes place and not across the whole capillary system. Such splitless arrangement can be realized by inserting between the separation and detection portion of the capillary a short stainless steel capillary tube, by using two zero dead volume unions, which is then electrically connected to the high-voltage power supply to close the electrical circuit of the electromigration separation system, excluding the capillary section holding the RF coil [118]. Besides its role for the identification and structural elucidation of compounds in complex mixtures, the hyphenation of capillary electromigration techniques with NMR is a powerful tool to monitor separation parameters [115] and to elucidate dynamic processes occurring during the separation, such as chiral recognition mechanisms [119] and Joule heating effects [120].

6.4 FACTORS INFLUENCING PERFORMANCE AND SEPARATION PARAMETERS

Besides electroosmosis, other phenomena that may affect the performance of any electromigration technique are the heat generated in the column by Joule effect, the untoward interactions of the analytes with the inner surface of fused-silica capillary tubes, sample diffusion, and electromigration dispersion. This section briefly describes the first two phenomena in Sections 6.4.1 and 6.4.2, respectively, whereas the motion of the analytes within the electrolyte solution due to chaotic Brownian movement (diffusion) and the variations in conductivity and electric field strength occurring in the sample zone during electrophoresis (electromigration dispersion) are discussed in Section 6.4.3 as factors contributing to the band broadening of charged analytes migrating under the influence of the applied electric field. Ssection 6.4.3 describes the separation parameters common to all electromigration techniques having electrophoresis as the dominant separation mechanism, whereas parameters related to a specific separation mode are introduced and discussed in each corresponding subsection.

6.4.1 Joule Heating

A capillary tube filled with an electrolyte solution behaves as a cylindrical electric conductor when an electric field is applied across its ends. Therefore, the passage of an electric current along the capillary generates Joule heat and the temperature of the electrolyte solution inside the capillary tends to increase if the produced heat is not efficiently dissipated through the capillary wall. In an open capillary tube of length L and cross-section A, filled with an electrolyte solution of conductivity σ, the amount of heat Q generated as a function of time depends on the applied electrical potential V and the current i passing through the capillary of resistance R, according to the following equation:

$$Q = i^2 Rt = \frac{V^2 t}{R} = V^2 \lambda t = \frac{V^2 \sigma A t}{L} \tag{6.19}$$

where λ is the conductance of the capillary that, like resistance R, depends upon the capillary dimensions as follows:

$$\lambda = \frac{\sigma A}{L} \tag{6.20}$$

The Joule heat generation in a packed capillary column is given by the following expression, similar to Equation 6.19:

$$Q = \frac{V^2 \sigma_\varepsilon A \varepsilon t}{L} \tag{6.21}$$

where ε is the column porosity, which for an open capillary is unity, and accounts for the reduced cross section in capillary tubes either packed or filled with a stationary phase, whereas σ_ε is an empirical equivalent conductivity parameter that accounts for the influence of the geometrical characteristics of the packed/filled capillary on conductivity and can be calculated from the measurements of current as a function of applied voltage. Therefore, as it can be verified experimentally, Joule heat increases with increasing applied voltage, capillary diameter, and conductivity of the electrolyte solution.

Heat dissipation takes place mainly by conduction through the capillary wall and by convection, radiation, and conduction in the medium surrounding the capillary tube, which can be either air or a cooling fluid, depending on the system employed to control the temperature of the capillary column. In the presence of low Joule heating and efficient heat dissipation, the current resulting from the applied electric field is expected to vary linearly with the applied potential drop, according to Ohm's law. Therefore, the experimental verification of linear increase of the electric current with increasing applied electric potential across the capillary tube is indicative of efficient heat dissipation through the capillary wall.

The generation of Joule heat is expected to produce temperature gradients inside the capillary tube that may affect EOF, migration velocity, band broadening of the analytes, and separation efficiency. As the temperature of the electrolyte solution increases, its viscosity and electrical permittivity decreases, whereas longitudinal diffusion of the analyte and the zeta potential at the solid/liquid interface increase. Therefore, poor repeatability of EOF and migration behavior of analytes may occur, as well as peak broadening of charged analytes due to the different electrophoretic mobility at the center and near the wall of the capillary owing to radial temperature differences inside the capillary tube. Further, peak broadening may occur as a consequence of increased longitudinal diffusion of the analytes.

The effects of Joule heating can be controlled by efficient heat removal using a thermostabilized heat exchanger in contact with the capillary tube and by the appropriate selection of the operational parameters, such as capillary size, composition of the electrolyte solution, and electric field strength. Therefore, Joule heating effects can be minimized by using capillary of small internal diameter, electrolyte solution of low conductivity, and by applying electric potentials which are within the linearity of Ohm's law. In fact, capillaries of smaller internal diameters are more efficient at dissipating heat due to the greater surface-to-volume ratio than larger capillaries and, in addition, less amount of Joule heat is generated in capillary of smaller cross section. Because Joule heating depends on the square of the current flushing through the capillary tube, the use of diluted solutions of low conductive electrolytes should be preferred whenever possible, recalling that in an open capillary tube the conductivity of an electrolyte solution is expressed as

$$\sigma = F^2 C \sum_j z_j^2 \nu_j \chi_j \tag{6.22}$$

where

F is the Faraday constant

C is the molar concentration of the electrolyte

z_j, ν_j, and χ_j are valency, mobility, and number of moles of the jth ionic species per mole of electrolyte, respectively

However, it should be noted that using diluted electrolyte solutions imply lowering ionic strength and buffering capacity, leading to a variety of drawbacks that will be discussed later in this chapter.

Several models have been developed to describe the effects of Joule heating and to calculate the resulting temperature profile in open and packed/filled capillary columns [120–125]. The temperature inside the capillary tube assumes a parabolic profile with the maximum value at the center and drops according to a logarithmic curve in the capillary wall and in the medium surrounding the capillary tube. Accordingly, the temperature gradient between the center of the capillary and the surrounding medium is given by the following equation:

$$\Delta T = \frac{Q r_i^2}{2}\left[\frac{1}{\kappa_s}\ln\left(\frac{r_o}{r_i}\right) + \frac{1}{\kappa_w}\ln\left(\frac{r_c}{r_o}\right) + \frac{1}{r_c}\ln\left(\frac{1}{h}\right)\right] \tag{6.23}$$

where

r_i and r_o are the inner and outer radius of the fused-silica tube

r_c refers to the outer radius of the polyimide coating of the capillary tube

κ_s and κ_w are the thermal conductivities of the electrolyte solution and of the capillary wall, respectively

h is the thermal transfer rate from the capillary wall

Equation 6.23 evidences the importance of efficient heat removal from the outer capillary wall and is in agreement with the above observation on the advantageous use of capillary tubes of smaller inner radius. Capillaries with a larger outer radius reduce the effects of the thermal isolating properties of the external polyimide coating of the capillary tube, facilitating heat dissipation through the capillary wall.

6.4.2 Interactions with the Inner Wall of Fused-Silica Capillaries

Charged compounds bearing different functional groups may interact with a variety of active sites on the inner surface of fused-silica capillaries, which comprise inert siloxane bridges, hydrogen bonding sites, and different types of ionizable silanol groups (vicinal, geminal, and isolated), giving rise to peak broadening and asymmetry, irreproducible migration times, low mass recovery, and in some cases irreversible adsorption. The detrimental effects of these undesirable interactions are particularly challenging in analyzing biopolymers, owing to the general more complex molecular structure of these molecules, and basic compounds. One of the earliest and still more adopted strategy to preclude the interactions of interacting analytes with the wall of bare fused-silica capillaries is the chemical coating of the inner surface of the capillary tube with neutral hydrophilic moieties [126]. The chemical coating has the effect of deactivating the silanol groups by either converting them to inert hydrophilic moieties or shielding all the active interacting groups on the capillary wall. A variety of compounds, including alkylsilanes, carbohydrates, neutral polymers, acrylamide, and acrylamide derivatives can be covalently bonded to the silica capillary wall by using bifunctional reagents to anchor the coating to the wall [127]. Polyacrylamide (PA), poly(ethylene glycol) (PEG), poly(ethylene oxide) (PEO), and polyvinylpyrrolidone (PVP) can be successfully anchored onto the capillary surface treated with several different silanes including 3-(methacryloxy)-propyltrimethoxysilane, 3-glycidoxypropyltrimethoxysilane, trimethoxyallylsilane, and chlorodimethyloctylsilane. Alternatively, a polymer can be adsorbed onto the capillary wall and then cross-linked in situ. Other procedures are based on simultaneous coupling and cross-linking. The use of alternative materials to fused silica such as polytetrafluorethylene (Teflon) and poly(methyl methyacrylate) (PMMA) hollow fibers has found limited application.

The deactivation of the silanol groups can also be obtained by the dynamic coating of the inner wall by flushing the capillary tube with a solution containing a coating agent. A number of neutral or charged polymers with the property of being strongly adsorbed onto the capillary wall are employed for the dynamic coating of bare fused-silica capillaries [128]. Modified cellulose and other linear or branched neutral polymers may adsorb onto the capillary wall with the consequence of modifying the ξ–potential, increasing the local viscosity in the electric double layer and masking silanol groups and other active sites on the capillary surface. Hence, the dynamic adsorption of the coating agent results in lowering or suppressing the EOF and in reducing the interactions with the capillary wall.

Polymeric polyamines are also strongly adsorbed in the compact region of the electric double layer as a combination of multisite electrostatic and hydrophobic interactions. The adsorption results in masking the silanol groups and the other adsorption active sites on the capillary wall and in altering the EOF, which is lowered and in most cases reversed from cathodic to anodic. One of the most widely employed polyamine coating agents is polybrene (or hexadimetrine bromide), a linear hydrophobic polyquaternary amine polymer of the ionene type [129].

Alternative choices are polydimethyldiallylammonium chloride, another linear polyquaternary amine polymer, cationic amine surfactants, and polyethylenimine (PEI) [130]. Also interesting is the dynamic coating obtained with ethylenediamine-derivatized spherical polystyrene nanoparticles of 50–100 nm diameter, which can be successively converted to a more hydrophilic diol-coating by in situ derivatization of the free amino groups with 2,3-epoxy-1-propanol [131]. Particularly attractive is the use of aliphatic vicinal oligoamines, such as triethylenetetramine (TETA) and diethylenetriamine (DIEN), which are effective at masking the silanol adsorption sites of bare fused-silica capillaries for proteins and peptides, while being capable of controlling the protonic equilibrium in a wide pH range, when used as the BGE in combination with a polyprotic acid [132–134]. The pK_a values of the above aliphatic vicinal oligoamines are reported in Table 6.1 and an example of separation of basic proteins performed at pH 4.0 in a bare fused-silica capillary with the BGE consisting of 10 mM *N*,*N*,*N*′*N*′-tetramethyl-1,3-butandiamine incorporated into 40 mM DIEN-phosphate buffer, is reported in Figure 6.6. The efficient separation displayed in Figure 6.6 is the result of the capability of the two aliphatic oligoamines at masking the silanol active sites for proteins on the wall of bare fused-silica capillaries, also at a pH value at which the separation of basic proteins in uncoated capillaries is particularly problematic. This in consequence that at pH 4.0 the capillary wall and the basic proteins are oppositely charged, in view of the isoelectric points of the four proteins, which are ranging from 9.5 (cytochrome *c*) to 11.0 (lysozyme) and the ionization of the silanol groups, already significant at this pH value.

TABLE 6.1
Acronym, Structure, and pK_a Values of the Aliphatic Vicinal Oligoamines Diethylentriamine and Triethylenetetramine

Buffering Agent	Acronym	Structure	pK_a [133]
Diethylentriamine	DIEN	$H_2NC_2H_4NHC_2H_4NH_2$	4.23
			9.02
			9.84
Triethylentetramine	TETA	$H_2NC_2H_4NHC_2H_4NHC_2H_4NH_2$	3.25
			6.56
			9.08
			9.74

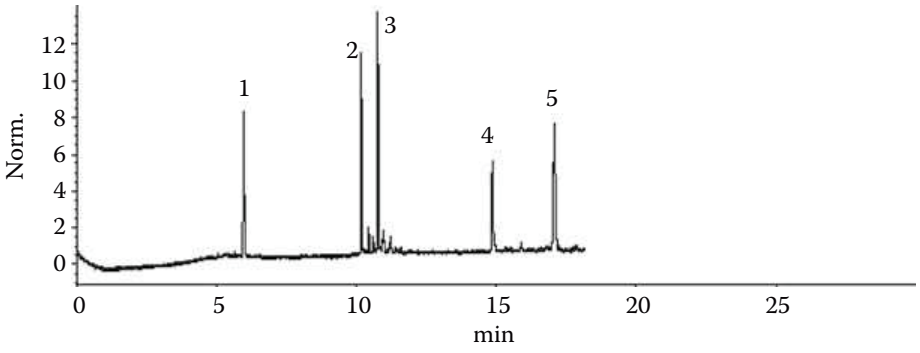

FIGURE 6.6 Separation of standard basic proteins in bare fused-silica capillary with BGE consisting of 10 mM *N*,*N*,*N*′*N*′-tetramethyl-1,3-butandiamine in 40 mM diethylenetriamine-phosphate buffer (pH 4.0). Capillary, bare fused silica 0.050 mm I.D., 0.375 mm O.D., total length 330 mm (245 mm to the detector); applied voltage 15 kV; cathodic detection at 214 nm; temperature of the capillary cartridge, 25°C; samples: (1) phenyltrimethylammonium iodide, (2) cytochrome *c*, (3) lysozyme, (4) ribonuclease A, (5) α-chymotrypsinogen A. (Personal collection).

6.4.3 Separation Parameters

The time required by a given analyte to migrate under the sole influence of the applied electric field across the capillary tube from the injection end of the capillary to the detection windows (migration distance) is defined as the "migration time" (t_m) and, similarly as the retention time in HPLC, is used for identification of sample components. It is given by

$$t_m = \frac{l}{v_{obs}} \tag{6.24}$$

where
l is the migration distance
v_{obs} is the observed migration velocity of the considered analyte

By analogy with chromatography, the record of the electrophoretic process is termed "electropherograms."

In the absence of EOF and separation mechanism other than electrophoresis, each analyte migrates with its own velocity which, according to Equation 6.8, is proportional to the strength of the electric field applied across the capillary tube. The constant of proportionality of the observed velocity of the charged analyte is defined as the "observed mobility" (μ_{obs}) and can be directly calculated by the migration time and the other experimental parameters, according to the following equation:

$$\mu_{obs} = \frac{v_{obs}}{E} = \frac{l}{t_m E} = \frac{lL}{t_m V} \tag{6.25}$$

where
L is the total length of the capillary tube
E is the strength of the applied electric field (V/L)

In the presence of EOF, the observed velocity is due to the contribution of electrophoretic and electroosmotic migration, which can be represented by vectors directed either in the same or in opposite direction, depending on the sign of the charge of the analytes and on the direction of EOF, which depends on the sign of the zeta potential at the plane of share between the immobilized and the diffuse region of the electric double layer at the interface between the capillary wall and the electrolyte solution. Consequently, v_{obs} is expressed as

$$v_{obs} = v_e + v_{eof} \tag{6.26}$$

where
v_e is the electrophoretic velocity of the considered analyte in the absence of EOF
v_{eof} is the velocity of the EOF, which is indicated with negative sign if the EOF is in the opposite direction to the migration of the analyte

The effective mobility, expressed by Equation 6.16, can be directly calculated from the observed mobility by measuring the electroosmotic mobility using a neutral marker, not interacting with the capillary wall, which moves at the velocity of the EOF. Accordingly, the effective mobility μ of cations in the presence of cathodic EOF is calculated from μ_{obs} by subtracting μ_{eof}:

$$\mu = \mu_{obs} - \mu_{eof} \tag{6.27}$$

Neutral substances commonly employed as neutral markers in measuring the EOF are methanol, acetone, mesityl oxide, and dimethylsulfoxide.

The main factor contributing to band broadening of analytes migrating under the sole influence of the applied electric field is longitudinal diffusion, considering negligible contributions due to convective motion, radial diffusion, and Joule heating, which are minimized by the use of a capillary tube. Therefore, under ideal conditions (primarily, small injection plug and absence of interactions of the analyte with the inner surface of the capillary), the variance of the migration band width (σ^2) is expressed similarly to the Einstein equation for diffusion as

$$\sigma^2 = 2Dt_m = 2D\frac{l}{v_{obs}} = 2D\frac{l}{\mu_{obs}E} = 2D\frac{l}{(\mu+\mu_{eof})E} \tag{6.28}$$

The variance of the migration band is related to the efficiency of the separation system, which by analogy with chromatography is expressed in terms of number of theoretical plates (N), according to the following equation [135]:

$$N = \frac{l^2}{\sigma^2} \tag{6.29}$$

Combining Equations 6.29 and 6.28 leads to

$$N = \frac{(\mu+\mu_{eof})El}{2D} = \frac{(\mu+\mu_{eof})V}{2D} \tag{6.30}$$

Since the number of theoretical plates is directly proportional to the strength of the applied electric field, the highest applied voltage possible is recommended to obtain high efficiency. This follows because on increasing the strength of the applied electric field the migration velocity of the analytes increases and, therefore, they have less time to diffuse. In addition, Equation 6.30 predicts better efficiency for larger charged molecules having small diffusion coefficients, which exhibit less dispersion than low molecular weight species.

The efficiency can also be estimated in terms of height equivalent to a theoretical plate, which expresses the differential increase of the band variance during the migration of a given analyte along the capillary and is given by

$$H = \frac{l}{N} = \frac{2D}{(\mu+\mu_{eof})E} \tag{6.31}$$

Both the number of theoretical plates and the height equivalent to a theoretical plate estimate the band broadening occurring in the separation system, either related to the whole capillary tube (N) or to the portion of the capillary occupied by the analyte (H). The higher is N (or lower is H) the narrower are the recoded peaks in the electropherogram.

For analytes migrating as symmetrical Gaussian peaks, the number of theoretical plates can be calculated directly from the electropherograms using the following equations:

$$N = 5.54\left(\frac{t_m}{2.355\sigma}\right)^2 = 5.54\left(\frac{t_m}{w_{1/2}}\right)^2 \tag{6.32}$$

or

$$N = 16\left(\frac{t_m}{4\sigma}\right)^2 = 16\left(\frac{t_m}{w_b}\right)^2 \tag{6.33}$$

where $w_{1/2}$ and w_b are the peak width measured in time units at half-height and at the base of the detected peak, respectively. In practice, the efficiency determined by Equations 6.32 or 6.33 is generally lower than that calculated by Equation 6.31 which accounts only for peak broadening due to longitudinal diffusion whereas additional dispersive processes often contribute to the total variance of the system, according to the following equation:

$$\sigma^2 = \sigma_D^2 + \sigma_E^2 + \sigma_T^2 + \sigma_I^2 + \sigma_S^2 \tag{6.34}$$

where the terms on the right side correspond to the contribution of band broadening due to diffusion (σ_D^2), electrodispersion (σ_E^2), Joule heat (σ_T^2), length of the sample injection plug (σ_I^2), and interactions of the sample with the inner surface of the capillary wall (σ_S^2).

Electrodispersion, also termed electrophoretic dispersion, describes the changes in conductivity and field strength occurring in the sample zone during the electrophoretic process. It conducts to band broadening and peak asymmetry or distortions, which can be controlled by matching sample and electrolyte solution conductivity and minimizing the concentration of the sample. Electrodispersion is almost negligible when the concentration of the sample in the migrating zone is sufficiently lower (generally at least 100 times) than that of the electrolyte solution [136]. Band broadening due to Joule heating is minimized by controlling the parameters influencing its generation (see Section 6.4.1) and by efficient heat removal from the outer capillary wall, whereas the broadening due to sample injection is simply controlled by minimizing the length of the sample plug introduced into the capillary. The untoward interactions of the analyte with the inner surface of the capillary may cause severe peak broadening and tailing, which require complex procedures to be minimized (see Section 6.4.2). If any of the above terms is predominant over the diffusion, only minimal improvements can be obtained by increasing the strength of the applied electric field.

The capability of separating two analytes is evaluated by the resolution (R_s), which can be simply calculated by dividing the distance between the peak maxima (Δx), expressing the difference between the migration distances of two adjacent peaks, to the average peak width at the baseline ($\bar{w}_b = 4\bar{\sigma}$):

$$R_s = \frac{\Delta x}{\bar{w}_b} = \frac{\Delta x}{4\bar{\sigma}} \tag{6.35}$$

From the relationship existing between migration distance and electrophoretic mobility and between peak width and number of theoretical plates, the resolution can be expressed as

$$R_S = \frac{\sqrt{N}}{4}\frac{\Delta v}{\bar{v}} = \frac{\sqrt{N}}{4}\frac{\Delta\mu}{\bar{\mu}_{obs}} = \frac{\sqrt{N}}{4}\frac{\Delta\mu}{(\bar{\mu} + \mu_{eof})} = \frac{\sqrt{N}}{4}\delta_m \tag{6.36}$$

where Δv and $\bar{v}$ are the difference in electrophoretic velocity and the average electrophoretic velocity of the two analytes, respectively. The ratio $\Delta\mu/\bar{\mu}_{obs}$ is the relative mobility difference of the two analytes being separated (δ_m), representing an operational value of selectivity that does not depend only on the properties of the two separated analytes, because it can be affected by the EOF. The number of theoretical plates requested to completely resolve adjacent peaks can be

calculated by the following expression, which indicates the key role of the selectivity parameter δ_m [137]:

$$N = \frac{16R_S^2}{\delta_m^2} \tag{6.37}$$

The ability to separate analytes on the bases of their electrophoretic mobility, in absence of secondary equilibrium in solution and interactions with the capillary wall, is expressed by the inherent selectivity, which is given by the ratio of the motilities of two analytes (1 and 2) migrating as adjacent peaks:

$$\alpha_{2,1} = \frac{\mu_2}{\mu_1} \tag{6.38}$$

The overall separation potential of an electromigration technique can be expressed by the peak capacity (n), which is defined as the maximum number of peaks that can be separated within a given separation time, usually coincident with the time interval between the first and last detected peak in the electropherogram, while retaining unit resolution for all adjacent peak pairs:

$$n = 1 + \frac{\sqrt{N}}{4} \ln t_\omega / \ln t_\alpha \tag{6.39}$$

where t_ω and t_α are the migration times of the last and first detected peak in the electropherogram, respectively [135]. Peak capacity and resolution increase with the number of theoretical plates N and, therefore, an optimization of operational parameters performed to obtain complete resolution and maximum number of separable peaks involves maximizing N.

6.5 SEPARATION MODES

Using the instrumentation described above, capillary electromigration techniques can be performed by a variety of modes, based on different separation mechanisms that can be selected by simply changing the operational conditions, specifically, composition of the electrolyte solution and/or capillary column. A fundamental aspect of each separation mode is the composition of the electrolyte solution, which may consist of either a continuous or a discontinuous electrolyte system. In continuous systems, the composition of the electrolyte solution is constant along the capillary tube, whereas in discontinuous systems it is varied along the migration path. In most capillary electromigration techniques, the same open capillary tube could theoretically be employed in a variety of separation modes, just varying the composition of the electrolyte solution, whereas other separation modes, such as capillary electrochromatography and capillary gel electrophoresis, require dedicated columns.

The names of the different separation modes of the capillary electromigration techniques described below are those recommended by the Analytical Chemistry Division of the International Union of Pure and Applied Chemistry (IUPAC) [138]. According to this recommendation, capillary electrophoresis is not used as a collective term for all capillary electromigration techniques performed in an open capillary tube. However, it should be noted that such term is generally accepted to identify any electromigration technique governed by separation mechanisms mainly based on electrophoretic principles, in analogy to the use of the term electrochromatography, which is referred to capillary electromigration techniques employing chromatographic columns, specifically, capillary tubes either filled, packed, or coated with a stationary phase [139]. Also, to consider is a number of borderline cases existing with respect to the naming of particular electromigration techniques

governed by the simultaneous action of different separation mechanisms, including the cases where chromatographic and electrophoretic phenomena are superimposed.

The following subsections briefly describe the different separation modes of electromigration techniques. Most of the separation parameters utilized to evaluate performance and results of the different separation modes are common to the majority of them and have been discussed above, whereas terms and parameters related to a specific separation mode are introduced and discussed in each specific subsection.

6.5.1 Capillary Zone Electrophoresis

Capillary zone electrophoresis (CZE) is an electromigration separation mode that uses continuous electrolyte solution systems and constant electric field strength throughout the capillary length, either in aqueous or nonaqueous background electrolyte solutions. The separation mechanism is based on differences in the electrophoretic mobilities of charged species and, therefore, on differences in the charge-to-mass ratio (see Section 6.2.2). Under the influence of the electric field applied across the capillary tube, the analytes migrate with different velocities toward the corresponding electrode: the positively charged analytes toward the cathode and negatively charged analyte toward the anode. However, in the presence of sufficiently strong EOF, which is cathodic in bare fused-silica capillaries, cations, anions, and neutral species migrate in the direction of EOF, where sample detection takes place (see Figure 6.7). Consequently, the migration velocity of charged analytes is either the sum or the difference of electrophoretic velocity and EOF, whereas neutral molecules migrate with the velocity of EOF.

The concept of virtual migration distance has been introduced by Rathore and Horváth [140] to distinguish separative and non-separative components of the differential migration process occurring in CZE, as well as in HPLC and in other electromigration techniques. According to this concept, the length of the capillary is divided into two virtual parts, l_S and l_0. The virtual migration distance, l_S, represents the separation component of the overall migration process and it is considered as the virtual distance that the analytes move under the direct influence of the electric field. It is calculated as the product of the electrophoretic mobility of the analyte (μ) and its migration time (t_m):

$$l_S = \mu t_m \tag{6.40}$$

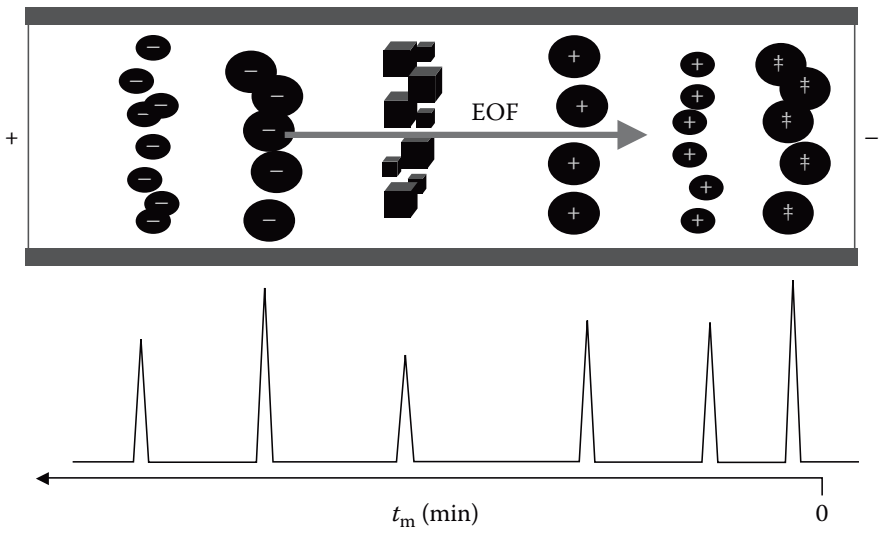

FIGURE 6.7 Representation of the migration behavior of cationic, anionic, and neutral analytes in CZE with sufficiently strong EOF to detect all analytes at the cathodic end of the capillary (panel A) and related electropherogram (panel B). Molecular masses proportional to the symbol size.

The virtual migration distance, l_0, arising from EOF is expressed as the product of the migration time of the analyte (t_m) and the electroosmotic mobility (μ_{eof}):

$$l_0 = \mu_{eof} t_m \tag{6.41}$$

Both l_S and l_0 can be expressed by either positive or negative numbers, depending on the direction of electrophoretic and electroosmotic mobilities and their algebraic addition equal to the real migration distance (L_m), which is the length of the capillary from the injection end to the detection window. Therefore, in co-electroosmotic mode of CZE, which means that the analytes migrate in the same direction of electoosmosis, both l_S and l_0 have the same sign, whereas in counter-electroosmotic mode of CZE, the two virtual migration distances have opposite signs.

The ratio of the two virtual lengths defines a parameter called the electrophoretic velocity factor k_e, which is analogous to the chromatographic retention factor and it is expressed as [140]:

$$k_e = \frac{l_S}{l_0} = \frac{\mu}{\mu_{eof}} = \frac{(L_m/t_m) - (L_m/t_{eof})}{L_m/t_{eof}} = \frac{t_{eof} - t_m}{t_m} \tag{6.42}$$

where t_{eof} is the migration time of the neutral tracer used to measure the EOF and the ratios L_m/t_m and L_m/t_{eof} express the velocity of the charged and neutral components of the sample, respectively. Therefore, the velocity factor k_e can also be considered as the dimensionless electrophoretic velocity of a charged analyte normalized to the velocity of the EOF. It is worth noting that since the analyte may migrate in the opposite direction to that of EOF, the velocity factor k_e can be negative.

The effective mobility relative to the total mobility identifies another dimensionless migration parameter termed electromigration factor (f_m), which is expressed as [141]:

$$f_m = \frac{\mu}{\mu + \mu_{eof}} = \frac{l_S}{(l_s + l_0)} = \frac{l_S}{L_m} \tag{6.43}$$

In terms of virtual migration distance, the electromigration factor is the dimensionless virtual distance of separative migration that measures the separative fraction of the total column length. Table 6.2 summarizes the fundamental migration parameters of CZE expressed according to the conventional formalism and to the concept of virtual migration distances.

In most applications, the electrolyte solution employed in CZE consists of a buffer in aqueous media. Whilst all buffers can maintain the pH of the electrolyte solution constant and can serve as background electrolytes, they are not equally meritorious in CZE. The chemical nature of the buffer system can be responsible for poor efficiency, asymmetric peaks, and other untoward phenomena arising from the interactions of its components with the sample. On the other hand, buffering agents and suitable additives incorporated into the BGE may be effective at preventing or minimizing the interactions of the analytes with the capillary wall, which are particularly challenging for proteins [142,143]. Most of the additives employed for this purpose act either as masking or competing agents for the silanol groups on the inner wall of the capillary, so that they are not accessible to the analytes. Others may function as strong ion-pairing or competing agents for the interacting moieties of the analytes exposed to the electrolyte solution, in order to subtract their availability to the interacting sites on the capillary wall. A schematic representation of the action of additives incorporated into the electrolyte solution on the electrophoretic behavior of analytes bearing multiple interaction sites is depicted in Figure 6.8.

In addition, the composition of the electrolyte solution can strongly influence sample solubility and detection, native conformation of biopolymers, molecular aggregation, electrophoretic mobility, and EOF, which can be altered as a consequence of the adsorption of the components of the BGE onto the capillary wall. Consequently, selecting the proper composition of the electrolyte solution

TABLE 6.2
Separation Parameters in CZE According to (A) Conventional and (B) Virtual Migration Distance Formalism

Parameter	A	B
Electrophoretic velocity factor, k_e	$k_e = \frac{t_{eof} - t_m}{t_m}$	$k_e = \frac{l_S}{l_0}$
Electromigration factor, f_m	$f_m = \frac{\mu}{\mu + \mu_{eof}}$	$f_m = \frac{l_S}{L_m}$
Selectivity, $\alpha_{2,1}$	$\alpha_{2,1} = \frac{\mu_2}{\mu_1}$	$\alpha_{2,1} = \frac{l_{S2} l_{01}}{l_{S1} l_{02}}$
Relative mobility difference, δ_m	$\delta_m = \frac{\Delta\mu}{(\bar{\mu} + \mu_{eof})}$	$\delta_m = \frac{\Delta l_S}{\bar{l}_0}$
Resolution, R_S	$R_S = \frac{\sqrt{N}}{4}\delta_m$	$R_S = \frac{\sqrt{N}}{4}\frac{\Delta l_S}{\bar{l}_0}$
Number of theoretical plates, N	$N = \frac{16R_S^2}{\delta_m^2}$	$N = 16R_S^2\left(\frac{\bar{l}_0}{\Delta l_S}\right)^2$

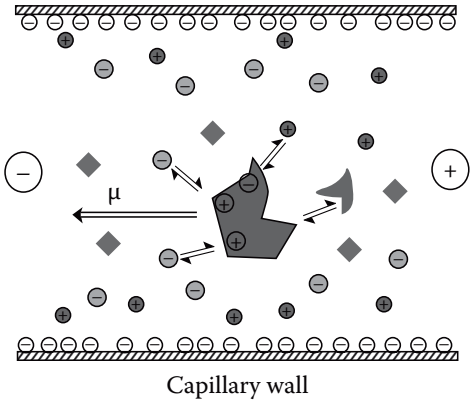

FIGURE 6.8 Schematic representation of the action of additives incorporated into the electrolyte solution on the electrophoretic behavior of analytes bearing multiple interaction sites.

is of paramount importance in optimizing the separation of the analytes in CZE. The appropriate selection of the buffer requires evaluating the physicochemical properties of all components of the buffer system, including buffering capacity, conductivity, and compatibility with the detection system and with the sample.

Additives may also be incorporated into the electrolyte solution to enhance selectivity, which expresses the ability of the separation method to distinguish analytes from each other. Selectivity in CZE is based on differences in the electrophoretic mobility of the analytes, which depends on their effective charge-to-hydrodynamic radius ratio. This implies that selectivity is strongly affected by the pH of the electrolyte solution, which may influence sample ionization, and by any variation of physicochemical property of the electrolyte solution that influences the electrophoretic mobility (such as temperature, for example) [144] or interactions of the analytes with the components of the electrolyte solution which may affect their charge and/or hydrodynamic radius.

Several buffering agents and additives can influence selectivity by interacting specifically or to different extents with the components of the sample, also on the basis of their stereoisomerism. The large selection of compounds that can be employed as additive of the electrolyte solution for this purpose include zwitterions, anionic or cationic ion-pairing agents, complex-forming species, chiral selectors, organic solvents, surfactants, cyclodextrins, denaturing agents, and ionic liquids [145–151]. The related interactions may involve either chiral on non-chiral electrostatic or/and hydrophobic interactions, as well as hydrogen bonding, ion–ion, ion–dipole, dipole–dipole, and ion–dipole/ion-induced-dipole interactions. Moreover, several anions, such as phosphate, citrate, and borate, which are components of the buffer solutions employed as the BGE may act as ion-pairing agents influencing the electrophoretic mobility and, hence, selectivity [133,152].

Organic solvents may also be employed as an alternative to water in preparing the BGE used in CZE, which is referred to as nonaqueous capillary electrophoresis (NACE) [153–155]. The substitution of water by an organic solvent can be advantageous for increasing sample solubility, preserving the stability of analytes having the tendency to decompose in water or improving selectivity, which is expected to be affected by charge and solvation size of the analytes and by their interactions with the other components of the BGE, all influenced by the organic solvent to a different extent than water. In addition, the high volatility and low surface tension of many organic solvents make NACE suitable to be successfully hyphenated with mass spectrometry [156].

6.5.2 Capillary Affinity Electrophoresis

Capillary affinity electrophoresis (CAE), also termed affinity capillary electrophoresis (ACE), is an electromigration separation mode for substances that participate in specific or biological-based molecular interactions, such as receptor–ligand interactions. CAE is widely employed for the characterization of biomolecules, for the analysis of specific interactions of a ligand (proteins, peptides, pharmaceutical active small molecules, etc.) with a receptor (typically a protein or a peptide), and for determining binding constants and binding stoichiometries. The wide array of interactions investigated by CAE include protein–drug, protein–DNA, peptide–carbohydrate, peptide–peptide, DNA–dye, carbohydrate–drug, and antigen–antibody [157–159].

According to the standard approach recalled in the IUPAC definition, CAE is performed incorporating one of the interacting partners into the BGE at varying concentrations, whereas the other specie participating in the specific interactions is injected into the capillary as the sample in mixture with a noninteracting standard and subjected to the electrophoretic run. In most applications, the receptor, which is very often a protein, is used as the sample, whereas the ligand, usually consisting of a less complex molecule, is incorporated into the BGE. When specific interactions between ligand and receptor determine the dynamic formation of a complex having charge-to-size ratio different from that of the receptor, a shift in the migration time of the receptor relative to the standard occurs, whose extension is a function of the ligand concentration. Therefore, the shift in the migration time of the receptor in response to the composition of the running BGE reflects the degree of interactions and, therefore, the binding constant, which can be calculated by linear or nonlinear regression analysis [160,161].

The most frequent deleterious effects that can spoil the estimation of the binding constants include the variations in migration times and losses of the receptor injected as the analyte, due to its interactions with the capillary wall, frequently occurring with uncoated capillaries, especially when the receptor is a protein. Coated capillaries and the experimental arrangement with the protein incorporated into the BGE and the ligand employed as the analyte are used to overcome such drawbacks. However, using UV detection, the high background absorption, due to the protein solution filled in the capillary, may annihilate the theoretical benefit of better peak shape, higher repeatability of migration time, and greater shift of the electrophoretic mobility expected using smaller and less complex molecules than proteins as the injected sample.

The loss in the detection sensitivity can be avoided by using the partial filling technique, in which only a small plug of the BGE containing the protein, or another UV-absorbing receptor, is

introduced in the capillary filled with the BGE without the receptor. The ligand is injected as the sample and the electrophoretic run is performed under the conditions where the UV-absorbing receptor does not migrate toward the detection end of the capillary or migrates at a velocity sufficiently lower than the analyte, which, therefore, can be detected in the neat BGE without the interference of the UV-absorbing receptor [162]. These operational modes of CAE are currently referred to as "dynamic equilibrium capillary affinity electrophoresis" and besides being employed for studying molecular interactions and improving selectivity are widely utilized for the separation of enantiomeric molecules incorporating a chiral selector into the BGE [163].

If the interactions between the ligand and receptor are strong enough leading to the formation of a complex that can be considered irreversible in the capillary electrophoresis timescale, CAE is performed by incubating the interacting partners prior to be injected into the capillary containing the BGE without the interacting species. The separation of free ligand from complexed ligand is subsequently achieved upon application of an electrical field. The concentration of free ligand is determined from peak height or area measurement by the aid of external standards [164]. The third main format of CAE is realized by immobilizing the receptor (or the ligand) onto the capillary wall with the purpose of retaining or retarding the analytes having specific affinity for it, whereas the electrophoretic migration of all other noninteracting species are unaffected by the coating. Such approach is frequently applied using antibodies or antibody-related substances as the selective binding agent. This mode of CAE is also used for the enrichment, prior identification, and/or quantification of analytes present in diluted samples or at low concentration in complex matrices, performed by tandem on-line hyphenation of a packed or monolithic capillary, containing the immobilized selective interacting agent, with the separation capillary [165].

CAE employing antibodies or antibody-related substances is currently referred to as immunoaffinity capillary electrophoresis (IACE), and is emerging as a powerful tool for the identification and characterization of biomolecules found in low abundance in complex matrices that can be used as biomarkers, which are essential for pharmaceutical and clinical research [166]. Besides the heterogeneous mode utilizing immobilized antibodies as described above, IACE can be performed in homogeneous format where both the analyte and the antibody are in a liquid phase. Two different approaches are available: competitive and noncompetitive immunoassay. The noncompetitive immunoassay is performed by incubating the sample with a known excess of a labeled antibody prior to the separation by CE. The labeled antibodies that are bound to the analyte (the immunocomplex) are then separated from the nonbound labeled antibody on the basis of their different electrophoretic mobility. The quantification of the analyte is then performed on the basis of the peak area of the nonbonded antibody.

The competitive immunoassay is performed by incubating the sample with a known fixed quantity of a labeled substance competing with the analyte for the binding sites on the antibody (labeled analog) and a limiting amount of the antibodies that can bind to both the analyte and the labeled analog. The components of the incubating mixture are separated by CE and the amount of the analyte is determined on the basis of the relative amount of the labeled analog that is bound to the antibodies, or that remaining free in solution, in comparison to the amount that is obtained when performing the immunoassay with standard solutions containing known amounts of the analyte [167]. Other formats of CAE, developed to address particular applications, include Hummel–Dreyer method (HD), vacancy affinity capillary electrophoresis (VACE), vacancy peak (VP) method, frontal analysis capillary electrophoresis (FACE), and immunoaffinity capillary electrophoresis (IACE) [168].

6.5.3 Capillary Sieving Electrophoresis

The main separation mechanism in capillary sieving electrophoresis (CSE) is based on differences in size and shape of charged analytes migrating through a sieving matrix that is enclosed in the capillary tube. CSE is successfully employed for separating charged biological macromolecules

having mass-to-charge ratios that do not vary with the molecular size. Typical examples of such compounds are the DNA restriction fragments, which have similar mass-to-charge ratios because each further nucleotide added to a DNA chain introduces an equivalent unit of charge and mass without affecting their ratio and, consequently, their electrophoretic mobility in free solution. Similarly, sodium dodecyl sulfate (SDS) protein complexes, which are generated by the binding of the anionic surfactant SDS to proteins in a constant ratio of 1.4 g of the surfactant per 1.0 g protein, have approximately unvarying mass-to-charge ratios resulting in comparable electrophoretic mobilities. Further examples of analytes having similar electrophoretic mobility in free solution and different molecular size and shape that can be separated by incorporating a sieving matrix in the capillary include oligonucleotides, RNA, double-stranded DNA, complex carbohydrates, and synthetic polyelectrolytes [169,170].

The sieving media may consist of permanent or chemical gels, physical gels, and polymer solutions of suitable viscosity [171–174]. Permanent cross-linked gels are prepared in the capillary by in situ polymerization processes based on adding a catalyst to the monomer solution, which is then pumped into the capillary tube, where the polymerization takes place. The gel is covalently bonded to the inner surface of the capillary to prevent its extrusion. Typical cross-linked sieving matrices are the polyacrylamide gels similar to those employed in slab gel electrophoresis, whose pore size can be adjusted by varying the cross-linker concentration in the reaction mixture and that can be easily anchored to the capillary wall, previously treated with 3-methacryloxypropyltrimethoxysilane.

Such arrangement of CSE is commonly referred to as capillary gel electrophoresis (CGE) and is comparable to conventional slab gel electrophoresis with the advantages of on-capillary detection, full instrumental automation, and the possibility of applying higher electric field, due to the better Joule heat dissipation in the narrow bore capillaries, with consequent shorter analysis time. On the other hand, with cross-linked gels, samples can be introduced in the capillary solely by electrokinetic injection, which is not recommended for sample solutions having high salt concentration. Further drawbacks include the introduction of air bubbles during filling the capillary, the possible shrinkage of the gel during polymerization, gel breaking during subsequent capillary manipulation, and gel degradation by hydrolysis. Clogging of the pores during electrophoresis is another factor which restricts the use of cross-linked capillaries to a limited number of runs.

Replaceable sieving matrices consist of either a physical gel or a polymer solution that can be easily renewed even after each run. Physical gels are formed within the capillary by dynamic noncovalent attractive interactions between the chains of a linear polymer, such as agarose, which is employed to form thermo-reversible gels for both traditional slab gel and capillary electrophoresis. This polysaccharide is not soluble in aqueous solutions at room temperature and goes into solution when heated. Therefore, agarose is dissolved in a warm aqueous electrolyte solution, which is fitted into the capillary. As the heated solution cools, agarose chains hydrogen bond to form double-helical structures, which in turn aggregate to form a three-dimensional network. The EOF should be suppressed to avoid gel extrusion, but the chemical bonding of the gel to the inside wall of the capillary is not required.

Nowadays, the sieving matrices most employed in CSE are polymer solutions that under suitable conditions may form a transient mesh or sieving matrix that provide the size-based separation of charged biopolymers. The polymer solutions can be formulated with linear acrylamide and N-substituted acrylamide polymers, cellulose derivatives, polyethylene oxide, and its copolymers or with a variety of polymers, such as polyvinylpyrrolidone (PVP), polyethylene oxide (PEO), and hydroxypropyl cellulose(HPC), which do not necessitate the preventive coating of the capillary wall due to their ability to dynamically coat the inner surface of the capillary, resulting in suppressed EOF and sample interactions with the capillary wall.

An interesting class of polymer matrices widely employed for CSE consists of temperature–dependent, viscosity-adjustable polymer solutions that are filled into the capillary at one temperature at low viscosities and are used in separation at another temperature at entanglement threshold concentrations and higher viscosities. Such viscosity-adjustable polymers are termed thermoresponsive

and classified as thermoassociating, when viscosity increases and as thermothinning when viscosity decreases with increasing temperature, respectively [175]. Examples of thermoresponsive polymers are the triblock uncharged copolymers of the poly(ethylene oxide)–poly(propylene oxide)–poly(ethylene oxide) type, the block copolymer made of a hydrophilic polyacrylamide backbone grafted with poly-*N*-isopropylacrylamideside chains [176], and the block copolymers of *N*,*N*-dialkylyacrylamide with acrylamide, such as block copolymers of *N*,*N*-diethylacrylamide (DEA) with *N*,*N*-dimethylacrylamide (DMA) [177] and of linear acrylamide (LPA) with dihexylacrylamide (DHA) [178]. Most of these sieving matrices are successfully employed for DNA sequencing using automated multicapillary electrophoresis systems, consisting of an array of capillaries that can be simultaneously operated for increasing the throughput of DNA sequencing [179,180].

6.5.4 Capillary Isoelectric Focusing

In capillary isoelectric focusing (CIEF), amphoteric analytes such as peptides and proteins are separated according to their isoelectric points by the application of an electric field along a pH gradient formed in the capillary tube, which is filled with the electrophoresis medium containing the sample to be analyzed and a mixture of commercially available zwitterionic compounds, known as carrier ampholytes [181]. The anodic end of the capillary is placed into an acidic solution (anolyte), and the cathodic end in a basic solution (catholyte). The carrier ampholytes have closely spaced isoelectric point (p*I*) values encompassing a desired pH range, and upon applying the electric field across the capillary each ampholyte migrates toward the electrode of opposite charge generating a pH gradient.

The basic principle of CIEF is that under the action of an electric field and in the absence of EOF, an analyte migrates as long as it is charged and it stops migrating if it becomes neutral during its migration. Peptides and proteins are amphoteric analytes that are charged at pH values different from their isoelectric points, at which they are electrically neutral. Under the influence of an electric field in a pH gradient between the cathode and the anode, each negatively charged peptide or protein migrates toward the anode encountering progressively lower pH values with the result that its net negative charge and, consequently, its electrophoretic mobility are gradually reduced. When the considered analyte reaches the zone of the electrophoretic medium having pH value corresponding to its p*I*, it becomes neutral and stops migrating. Similarly, each positively charged peptide or protein migrates toward the cathode encountering increasing pH values, with consequent progressive reduction of its net positive charge and cathodic electrophoretic mobility, upon reaching the zone having pH value equal to its p*I*, where it stops migrating.

A steady-state condition is reached when all components of the sample have been focused in the zone of the capillary tube containing the electrophoretic medium at the pH value corresponding to their p*I*. The completion of the focusing procedure is monitored by a drop-off in current. Each sample component stops migrating in a self-sharpened band because if it diffuses out of the focused zone it acquires a charge with the consequence of being pulled back in the focused band where the analyte is electrically neutral. Therefore, a remarkable feature of isoelectric focusing (IEF) is the concentration of the separated analytes within a narrow band [182]. However, in order to avoid the precipitation of the focused analytes, additives, such as nonionic surfactants (e.g., Triton X-100 or Brij-35) and organic modifiers (e.g., glycerol, ethylene glycol) are often incorporated into the electrophoresis medium as dispersants to minimize aggregation.

The resolving power of IEF is measured in terms of minimum difference between the p*I* of two adjacent separated analytes, and is expressed by the following equation:

$$\Delta \mathrm{p}I = 3\left[\frac{D\left(\mathrm{dpH}/\mathrm{d}x\right)}{E\left(-\mathrm{d}\mu/\mathrm{dpH}\right)}\right]^{1/2} \tag{6.44}$$

where

D is the diffusion coefficient of the considered analyte

dpH/d*x* is the rate of variation of pH with distance (pH gradient)

E is the applied electric field

−dμ/dpH is the variation of the electrophoretic mobility with pH in the vicinity of p*I*, which depends on the neat charge of the analyte near its p*I*

The operational parameters to be controlled are the applied electric field, with higher *E* leading to smaller Δp*I*, and pH gradient, which should be as narrower as possible for higher resolution.

A peculiar aspect of performing isoelectric focusing in a capillary tube is that the anticonvective medium (usually a gel), requested in the classical version of the technique, is not used and relatively high electric field can be employed, due to the efficient Joule heat dissipation of small-diameter tubes. Other remarkable features include automation, the requirement of small amount of sample, high resolution, and fast analysis time. On the other hand, in classical gel-IEF, the separated zones are promptly visualized by staining, whereas CIEF performed on most capillary electrophoresis instruments (conventional CIEF) requires an additional step for visualizing the separation. These instruments use a single-point detection system located on one end of the capillary column. Therefore, after the IEF process is completed, a mobilization stage is required to move the focused analyte zones past the detection window. A schematic view of the separation mechanism operating in CIEF is reported in Figure 6.9.

Either two-step or one-step immobilization techniques are generally employed. Using the two-step techniques, the analytes are first focused in the capillary and subsequently displaced toward the detection window by either hydrodynamic or electrophoretic mobilization, as first reported by Hjertén and Zhu [183]. The hydrodynamic flow can be generated by either pressure or gravity, while the applied electric field is maintained to avoid the defocusing of bands by laminar flow. Otherwise, the focused zones can be moved in the direction of the detection window by changing the composition of the anolyte or catholyte solution by adding a salt in the proper reservoir and applying the electric field. This results in a variation of pH in the electrophoresis medium due to the migrations of anions and cations competing with the migration of hydroxyl and hydronium ions, respectively. Thus, as the pH is varied both ampholytes and analytes are charged and move

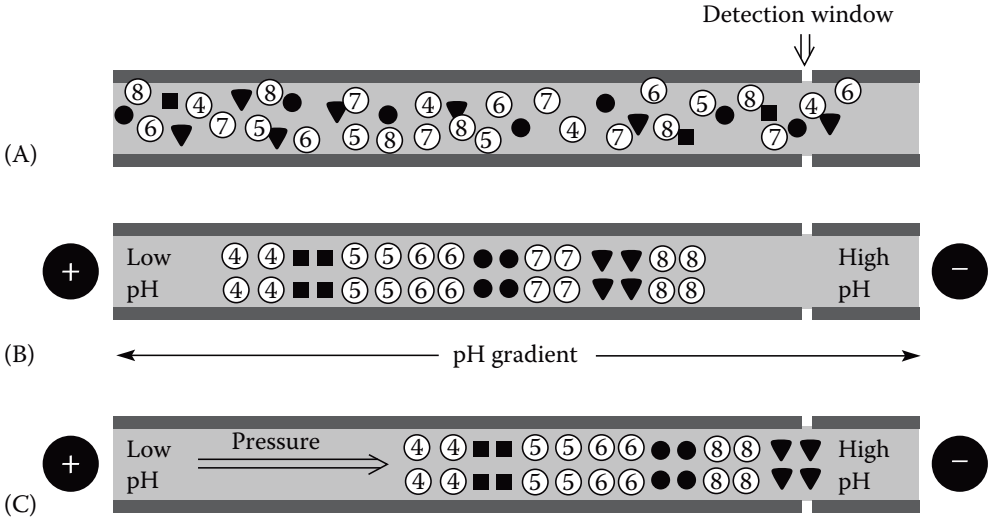

FIGURE 6.9 Schematic representation of CIEF with visualization of the separated analytes by simultaneous pressure–voltage mobilization. The analytes are filled into the capillary mixed with the carrier ampholytes (A). The application of the electric field generates a pH gradient and the analytes focus in narrow bands according to their p*I* (B). Once focused, the analytes are moved toward the detection window by hydrodynamic flow generated by applying pressure, while maintaining the applied electric field (C).

in the direction of the reservoir where the salt has been added. These approaches require the use of coated capillaries to suppress the EOF and to prevent troublesome interactions of the analytes with the inner surface of the capillary tube. A variety of covalent [183–186] and dynamic [187–189] coatings are employed for these purposes. Also popular is the use of capillaries covalently coated with a hydrophilic polymer in combination with a dynamic coating agent, such as zwitterions, polymers, and surfactants [190,191], which is incorporated into the electrophoresis medium.

The alternative approach is using a one-step technique, which allows performing the focusing process and the mobilization of the electrophoresis medium simultaneously. This is obtained by different methods, including the coincident application of electric field and pressure, the use of a catholyte (or anolyte) containing a salt, and performing CIEF with capillaries having a residual EOF, which can be controlled by incorporating an additive into the electrolyte medium [192,193]. One-step mobilization can also be performed with sulfonated polymer–coated capillaries, which provide sufficient and constant EOF for mobilization of the entire pH gradient to the capillary end with the detection windows [194].

Deformation of pH gradient, uneven resolution along the capillary column, and increased analysis times are the main drawbacks of the mobilization techniques used to move the train of focused analytes toward the detection window, which is requested when using classical instrumentation with detection at a fixed point. The ideal alternative is using real-time whole column imaging detectors (WCID), which allow for the simultaneous detection along the entire length of the stationary zones focused within the capillary column by IEF [195,196]. The different types of real-time WCID used in CIEF include refractive index gradient imaging detector, optical absorption imaging detector, and LIF imaging detector, which is the most sensitive detector among them [197–199]. The typical arrangement of a real-time WCI detector, operating in either optical absorption or fluorescence mode, consists of a laser or a LED light source whose beam is projected onto the whole separation length of the capillary column without the outer coating. Either the light intensity passing through the CIEF column or its fluorescence image emission is then focused onto a photodiode array or a charge-coupled device (CCD) camera. In an alternative arrangement, the entire column is transported past a single detection point, using either a modified UV-visible or fluorescence detector. However, in this case, a real-time detection mode is not performed, and the approach is more realistically defined capillary scanning detection. The hyphenation of CIEF with mass spectrometry (MS) is usually performed using electrospray ionization (ESI) or MALDI techniques. However, coupling CIEF with ESI–MS suffers more from signal suppression compared to MALDI-MS [200,201].

CIEF can also be performed in ampholyte-free mode using a tapered capillary column, which takes advantage of the Joule heat to form a pH gradient. Upon applying an electric field along a tapered capillary filled with tris-hydroxymethylaminomethane hydrochloric acid (Tris-HCl) buffer, the heat generated increases along the capillary axis as the inner capillary of the column decreases, forming a temperature gradient along the capillary, which is due to the sensitive variation of the pK_a value of this buffer with temperature [202,203]. Other CIEF modes comprise dynamic isoelectric focusing that employs capillaries having additional electrodes placed between those at the both ends of the capillary, which allow using multiple voltages within one capillary to manipulate the local pH gradient by the proper variation of the electric field [204]. Also attractive is the use of immobilized pH gradient in the form of a capillary monolithic column bearing ampholytes immobilized at different position in the column according to their pI [205].

6.5.5 Electrokinetic Chromatography

Electrokinetic chromatography (EKC) comprises a variety of electromigration techniques that use electrolyte solutions incorporating a separation carrier, which is called the pseudostationary phase, and are based on the distribution of the analytes between this phase and the surrounding solution.

The pseudostationary phases typically used in EKC can be either charged or neutral and comprise micelles, nanometer-sized droplets, nanoparticles, liposomes, etc. Their common characteristic is the capability of establishing a chemical equilibrium with the analytes dissolved in the BGE, which causes the selective variations of their migration velocity due to either electrophoresis or electroosmosis or both. Typically, charged pseudostationary phases migrate at lower velocity than EOF, which is cathodic with anionic and anodic with cationic pseudostationary phases. Therefore, they migrate in the same direction of EOF, but with a lesser velocity, whereas neutral pseudostationary phases migrate with the same direction and velocity of the EOF. Thus, the pseudostationary phase is typically transported through the electrolyte solution at a different rate than the analytes, whose velocity and separation is therefore influenced by their different affinity for the pseudostationary phase, in absence of which neutral analytes migrate unresolved with the same velocity of the EOF.

Therefore, EKC can be considered as a hybrid of electrophoresis and chromatography, separating neutral analytes exclusively on the basis of their differential partitioning between the electrolyte solution and the pseudostationary phase, whereas the charged analytes are separated on the basis of partitioning and electrophoresis. As mentioned above, pseudostationary phases can be either neutral or charged. It is evident that only charged analytes can be separated using neutral pseudostationary phases.

The first introduced and still more diffuse mode of EKC is micellar electrokinetic chromatography (MEKC), also referred to as micellar electrokinetic capillary chromatography (MECC), which employs micelles as the dispersed phase, formed by incorporating a surfactant into the electrolytes solution at a concentration higher than the critical micellar concentration (CMC) [206]. Composition and pH of the electrolyte solution are selected to generate a sufficiently high EOF to transport micelles and analytes toward the detection windows. Sodium dodecyl sulfate (SDS) is by far the most widely used surfactant, due to its relatively low cost, availability in highly purified forms, and low CMC in aqueous solution (8 mM), above which it forms almost spherical anionic micelles with the charged heads oriented toward the solution and the hydrophobic tails pointing inward the aggregate. SDS is incorporated into electrolyte solutions at neutral to alkaline pH values to ensure strong EOF with bare fused-silica capillaries. Under these conditions, the anionic micelles migrate in opposite direction to EOF and, therefore, are transported toward the cathode with a migration velocity slower than the stream of the bulk flow of BGE.

Neutral analytes not interacting at all with the micelles migrate at the same velocity of EOF, whereas the analytes being totally incorporated into the micelle migrate at the same velocity of the micelle. Neutral analytes participating in reversible interactions with the micelles migrate at the velocity of the micelles when they are associated with a micelle and at the velocity of EOF when they are in the bulk solution. Therefore, these analytes migrate at a velocity comprised between that of EOF and that of micelles, which is proportional to the time they spend associated with the micelles and, consequently, to the strength of their interaction with the dispersed phase. The partitioning of neutral analytes in and out of SDS micelles is mainly due to hydrophobic interactions. Therefore, the hydrophobic diazo dye Sudan III and methanol are generally employed as the markers to measure the migration velocity of micelles and EOF, respectively. The time interval between the migration time of methanol (t_0) and Sudan III (t_{psp}) specifies the migration time window within which neutral analytes can be separated by partitioning between the micellar and the aqueous phase (see Figure 6.10).

MEKC is also performed using cationic, nonionic, and zwitterionic surfactants. Widely employed are cationic surfactant consisting of a long chain tetralkylammonium salt, such as cetyltrimethylammonium bromide, which causes the reversal of the direction of the EOF, due to the adsorption of the organic cation on the capillary wall. Other interesting options include the use of mixed micelles resulting from the simultaneous incorporation into the BGE of ionic and nonionic or ionic and zwitterionic surfactants. Chiral surfactants, either natural as bile salts [207] or synthetic [208] are employed for enantiomer separations.

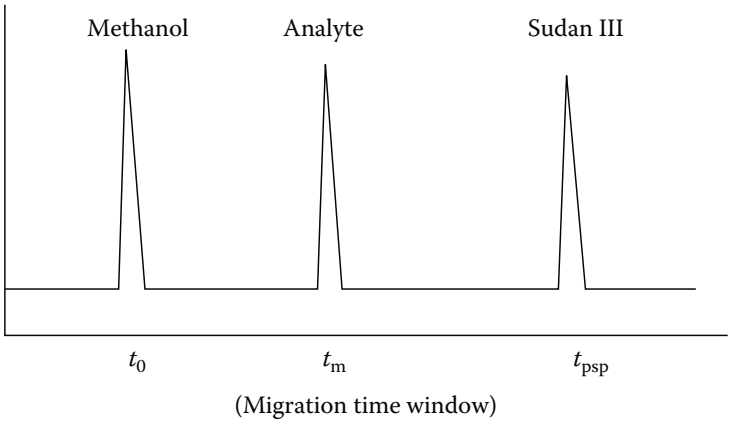

FIGURE 6.10 Schematic representation of the migration time window in MEKC.

The migration behavior of neutral analytes in MEKC can be described by parameters similar to those employed in liquid chromatography [209]. Hence, the ratio of the number of moles of the analyte in the micellar phase, the pseudostationary phase, (n_{psp}) to those in the surrounding solution (n_{lp}) defines the retention factor k:

$$k = \frac{n_{psp}}{n_{lp}} = \frac{t_m - t_0}{t_0\left(1 - (t_m/t_{psp})\right)} \tag{6.45}$$

where
t_m is the migration time of the analyte
t_0 and t_{psp} are the migration times of the markers employed to measure the EOF and the migration rate of the micelles, respectively

The retention factor is related to the distribution coefficient K of the analyte between the micellar phase and the aqueous phase, according to the following equation:

$$k = K\frac{V_{psp}}{V_{lp}} = K\frac{\bar{\nu}\left(C_{sf} - \text{CMC}\right)}{1 - \bar{\nu}\left(C_{sf} - \text{CMC}\right)} \tag{6.46}$$

where
V_{psp} and V_{lp} are the volumes of the micellar and aqueous (liquid) phase, respectively
C_{sf} is the concentration of the surfactant in the BGE
$\bar{\nu}$ is the partial specific volume of the micelle
CMC is the critical micellar concentration

As evidenced by the above equation, the distribution coefficient can be directly calculated from the retention factor and other easily measurable parameters. It is also worth noting that when the concentration of the micellar phase is sufficiently low, the denominator at the last term of the above equation can be approximated to be equal to unity and the retention factor is linearly proportional to the concentration of the surfactant into the BGE. Accordingly, Equation 6.46 is rewritten as

$$k \cong K\bar{\nu}\left(C_{sf} - \text{CMC}\right) \tag{6.47}$$

The degree of separation of two adjacent peaks is evaluated by the parameter resolution (see Section 6.4.3) that in EKC is expressed by the following equation:

$$R_S = \frac{\sqrt{N}}{4}\left(\frac{\alpha-1}{\alpha}\right)\left(\frac{\bar{k}}{1+\bar{k}}\right)\left(\frac{1-t_0/t_{psp}}{1+\left(t_0/t_{psp}\right)\bar{k}}\right) \tag{6.48}$$

where

α is selectivity, given as the ratio of the retention factors of the two adjacent peaks

$\bar{k}$ is the mean retention factor

The above relationship is derived from Equations 6.36 and 6.45 and is similar to the equation correlating resolution to the separation conditions in liquid chromatography [210], except for the addition of the last term on the right-hand side, which accounts for the migration of the pseudostationary phase within the capillary column.

The equations reported above are related to MEKC and all other EKC separation modes performed with pseudostationary phase, analytes, and EOF moving in the same direction at different velocities. Such condition applies when the electroosmotic mobility is higher than the electrophoretic mobility of the pseudostationary phase migrating to the direction opposite to that of EOF.

EKC in the reversed direction mode is performed when analytes and pseudostationary phase move at different velocities in the same direction, which is opposite to that of EOF. In this case, retention factor and resolution are expressed by the following equations [211]:

$$k = \frac{n_{psp}}{n_{lp}} = \frac{t_m + t_0}{t_0((t_m/t_{psp})-1)} \tag{6.49}$$

and

$$R_S = \frac{\sqrt{N}}{4}\left(\frac{\alpha-1}{\alpha}\right)\left(\frac{\bar{k}}{1+\bar{k}}\right)\left(\frac{1+t_0/t_{psp}}{(t_0/t_{psp})\bar{k}-1}\right) \tag{6.50}$$

EKC is not restricted to the separation of neutral analytes, as it is widely employed for the simultaneous separations of charged and neutral analytes as well as of ionizable compounds having similar electrophoretic mobility. The separation of ionizable analytes by EKC is governed by differences in the partitioning between the pseudostationary phase and the surrounding electrolyte solution as well as electrophoretic mobility. For these analytes, the retention factor can be described by the following mathematical model:

$$k = \frac{t_m - t_{0psp}}{t_{0psp}(1-(t_m/t_{psp}))} \tag{6.51}$$

where t_{0psp} is the migration time of the analyte in the absence of the pseudostationary phase, under otherwise identical experimental conditions. However, t_{0psp} cannot be estimated without making several assumptions, such as negligible effect of the pseudostationary phase on the EOF, on viscosity and permittivity of BGE, and, in case of MEKC or microemulsion EKC (see below), absence of interactions of the analytes with surfactant monomers [212]. Also relevant is the influence of pH on

the retention factor of an ionizable analyte, which can be calculated as the weighted average of the retention factor of its undissociated and dissociated forms:

$$k = \frac{k_{HA} + k_A\left(K_a / c\left[H^+\right]\right)}{1 + \left(K_a / c\left[H^+\right]\right)} \tag{6.52}$$

where k_{HA} and k_A are the retention factors of the undissociated (HA) and dissociated forms (A) of the analyte, whose dissociation constant and concentration are K_a and c, respectively, and $[H^+]$ is the concentration of protons [213].

Selectivity in EKC can be modulated by changing the pH of BGE and using either a different pseudostationary phase or incorporating an organic solvent or a suitable additive into the electrolyte solution, such as ion-pairing or complex-forming agents, which are expected to influence the partitioning of the analytes between liquid and pseudostationary phases. A typical application of this approach is the separation of enantiomers, generally performed using electrolyte solutions that incorporate a chiral selector, such as cyclodextrins, crown ethers, or macrocyclic antibiotics. Also, organic solvents influence the analyte interactions with the pseudostationary phase, as well as their mobility and, in case of micelles, vesicles, and other aggregates, the physical structure, conformation, or self-association equilibrium of these pseudostationary phases. Another widely used additive is urea, which increases the solubility of very hydrophobic compounds in aqueous solutions, reducing their interaction with nonpolar pseudostationary phases.

Several limitations and shortcomings are associated with the use of micelles as the pseudostationary phase. Besides the irreversible incorporation of very hydrophobic compounds within the micelles, other analytes such as proteins may strongly interact with the free molecules of the surfactant in solution. Moreover, the significant influence of operational parameters such as temperature, pH, and composition of the BGE on the dynamic aggregation of the surfactant molecules may result in instable micelles and consequent irreproducibility.

One of the possible alternative to micelles are spherical dendrimers of diameter generally ranging between 5 and 10 nm. These are highly structured three-dimensional globular macromolecules composed of branched polymers covalently bonded to a central core [214]. Therefore, dendrimers are topologically similar to micelles, with the difference that the structure of micelles is dynamic whereas that of dendrimers is static. Thus, unlike micelles, dendrimers are stable under a variety of experimental conditions. In addition, dendrimers have a defined number of functional end groups that can be functionalized to produce pseudostationary phases with different properties. Other pseudostationary phases employed to address the limitations associated with the micellar phases mentioned above and to modulate selectivity include water-soluble linear polymers, polymeric surfactants, and gemini surfactant polymers.

Nanoparticles of diameter ranging from decades to hundreds of nanometers, bearing selected functionalities on their surface, such as ionizable groups or chiral selectors, are alternative choices as pseudostationary phases. Either polymer-based or silica nanoparticles are employed [215]. The nanoparticles are suspended in the electrolyte solution to form stable slurries, which are employed as the pseudostationary phase, according to two different operational modes utilizing either the partial or the total filling of the capillary with the slurry solution, as depicted in Figure 6.11. In the partial filling arrangement, a plug of the slurry solution is introduced into the capillary before the sample, and as the electric field is applied, the analytes migrate through the dispersed pseudostationary phase and reach the detection windows prior to the nanoparticle plug. In the total or full-filling arrangement the sample is injected in the capillary completely filled with the slurry solution and the analyte detection takes place in presence of the dispersed nanoparticles [216,217]. The advantage of the partial filling approach include the total absence of detection drawbacks due to light scattering or/and adsorption of the dispersed nanoparticles.

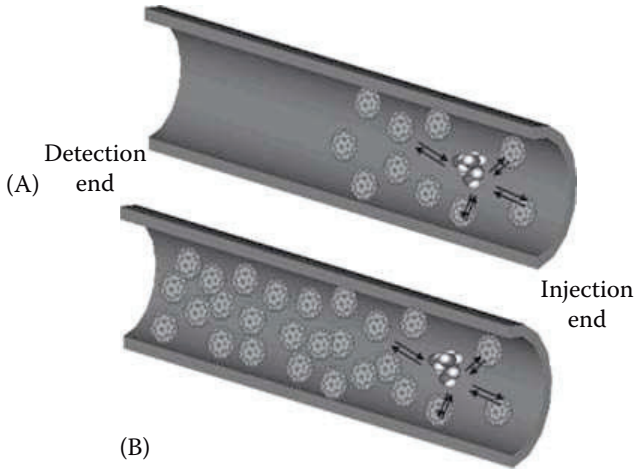

FIGURE 6.11 Schematic representation of (A) partial-filling approach and (B) full-filling approach of EKC with pseudostationary phases consisting of nanoparticles dispersed into the BGE.

As mentioned at the beginning of this section, pseudostationary phases also comprise nanometer-sized oil droplets. These carriers consist of droplets of a water-immiscible liquid dispersed in an aqueous electrolyte solution to form microemulsions. Heptane and octane are the widely used water-immiscible liquids used to form the microemulsion, although diethyl ether, amyl alcohol, cyclohexane, chloroform, methylene chloride, and several chiral compounds, such as (2*R*, 3*R*)-di-*n*-butyl tartrate, are alternative choices. The microemulsion is typically formulated by incorporating, in a suitable ratio, the water-immiscible liquid into the aqueous BGE with a surfactant (e.g., SDS) and a cosurfactant, generally a short-chain alkyl alcohol, such as 1-butanol. The surfactant is incorporated into the BGE to facilitate the formation of the droplets by lowering the surface tension, further lowered by the cosurfactant, which has the function of stabilizing the microemulsion. This EKC mode is termed microemulsion electrokinetic capillary chromatography (MEEKC) or microemulsion electrokinetic capillary chromatography (MEECC) [138]. It employs alkaline electrolyte solutions to generate high cathodic EOF, which transports the SDS-coated (or other anionic surfactant-coated) oil droplets to the cathode, in spite of their superficial negative charges. Neutral analytes are separated according to their partitioning between oil and aqueous phase whereas charged compounds may establish either attractive or repulsive electrostatic interactions with the negatively charged droplets, while attempting to migrate toward the anode against the EOF, which sweeps them through the detector windows at the cathodic end of the capillary. MEEKC offers more operational parameters than MEKC to modulate selectivity and to enlarge the separation windows, which include the concentration and choice of the water-immiscible liquid, surfactant, and cosurfactant. Also, efficiency may result superior in MEEKC than in MEKC due to faster mass transfer between the microemulsion and the surrounding aqueous phase.

The dispersed pseudostationary phase may also consist of liposomes. These are vesicles formed by phospholipids by a self-assembling process in aqueous solutions, which are composed of one or more lipid bilayer membranes that have entrapped a volume of the surrounding aqueous media during the self-assembling process [218]. Liposomes are classified on the basis of size and the number of lipid bilayers. Multilamellar vesicles (MLV) have more than one lipid bilayer and size up to 5.0 μm, whereas unilamellar vesicles consist of a single lipid bilayer and are distinguished in large unilamellar vesicles (LUV) and small unilamellar vesicles (SUV) if their size is in the range of 100–400 nm and 20–50 nm, respectively [219]. EKC using liposomes as the pseudostationary phase can be employed to separate neutral and charged low molecular size analytes [220] as well as proteins [221,222] and to study the interaction between liposomes and drugs [220,223].

6.5.6 Capillary Electrochromatography

Capillary electrochromatography (CEC) can be considered as a variant of capillary HPLC in which the flow of the mobile phase through the column is propelled by electroosmosis instead of a mechanic pump. The capillary column can be either filled, packed, or coated with a stationary phase, which plays the dual role of providing sites for the required interactions with the analytes and charged groups for the generation of the EOF that ensures the movement of the mobile phase though the column. Stationary phases carrying cationic functional groups, such as amino or ammonium groups generate anodic EOF whereas stationary phases with anionic functionalities, such as sulfonic or acetic groups, generate cathodic EOF. The stationary phase may also carry zwitterionic groups and in this case exhibits either cathodic or anodic EOF, according to the pH of the mobile phase.

The capillary format of the column maximizes the surface area-to-volume ratio and, therefore, facilitates the rapid and efficient dissipation of the Joule heat, which can be of a marked extent when applying the elevated voltages requested to obtain high flow rates. As mentioned in Section 6.1, the flow of mobile phase propelled by EOF displays a flat plug-like profile, which does not contribute to peak broadening caused by the sample transport trough the column because the driving force is uniformly distributed along the capillary tube. This is in contrast to the laminar or parabolic flow profile generated in HPLC, where there is a strong pressure drop across the column caused by frictional forces at the liquid–solid boundary. The absence of column backpressure allows performing CEC also with capillary columns of low permeability, such as those packed with particles in the submicron size range [224], whereas the length is mainly limited by the value of the electric field requested to obtain the desired flow rate with commercially available power supplies, which usuallyoperate up to 30 kV.

Capillary columns packed with either silica-based or polymeric particles have been used since the earlier development of CEC [225–227] due to the availability and relatively easy preparation of a wide range of packing material of different diameter, pore size, and surface functionalities tailored for a variety of separation modes, such as in HPLC. Particles are usually packed into a fused-silica capillary tube by a variety of techniques, the most common of which is pressure packing of a liquid slurry using either water, organic solvents [228,229] or supercritical carbon dioxide as the carrier [230]. The generally accepted method employs a packing reservoir, such as a short 2.0 mm I.D. HPLC column, which is connected to the capillary tube to be packed to one end and to a high pressure solvent delivery pump to the other end. The slurry reservoir with the attached column is usually immersed in a ultrasonic bath to maintain the slurry homogeneity during packing, which is carried out by transporting the suspended packing material into the capillary column by pressure, typically between 35.0 and 70.0 MPa (≈5,000 to ≈10,000 psi). Alternative techniques include electrokinetic packing [231], procedures employing centripetal forces [232,233] or combination of high electric field and hydrodynamic flow [234] and packing techniques by gravity [235].

Any of these techniques require the fabrication of retaining frits within the capillary column, which have to posses high permeability to the mobile phase flow and, at the same time, must be mechanically strong to retain the packing material and to resist the pressure generated during the packing process and the flushing procedures requested to fill and condition the column with the mobile phase for its use. The frits are usually fabricated by sintering a plug of silica gel, usually wetted with either water or potassium silicate, introduced into the capillary tube. A heating filament or small coil, rather than the flame of a Bunsen burner used in the earlier methods, are generally employed for sintering the silica plug [236]. When the chromatographic support consists of silica-based material, the frits are generally fabricated by sintering the packing material, having the caution to minimize the degradation of the stationary phase bonded to the silica particles adjacent to the zone of the packing material heated to form the frit. Alternatively, the frits can be produced by polymerization of potassium silicate solution containing formamide, which is introduced into the capillary and polymerized by heating on a steam bath [237].

Sintered frits can be the source of several drawbacks, such as band broadening, bubble formation, EOF inhomogeneity, and insufficient reproducibility of the sintering method. An additional problem is the column fragility at the frit position due to the removal of the polyimide film during the thermal treatment, which may also cause alteration of the surface properties of the packing material when this is used to fabricate the frits. An alternative approach to frit formation is the use of capillaries with a restrictor or a fine tapered end, which retain the packing material inside the capillary column [238]. Tapered capillaries can be produced by drawing the fused-silica capillary through a high-temperature flame or using a laser-based micropipette puller. Such methods produce externally tapered capillaries having reduced outer and inner diameters, which are, therefore, very fragile. The alternative method, producing more robust columns, is carried out by melting the tip of the capillary in a high-temperature flame thereby sealing its end. Then the sealed end is carefully ground to produce an opening of the required diameter. Using this method, only the inner diameter of the capillary is reduced in dimension whereas the outer diameter is unvaried. Packed columns with either external or internal taper at the outlet of the capillary are suitable to be coupled with electrospray ionization and mass spectrometry (CEC-ESI-MS) [238,239].

A capillary restrictor can also be realized by joining two capillaries of same outer diameter (usually 375 μm) and different bore. The two capillaries, having uniform cuts at their ends, are joined by pushing them into a small length of PVC tube of 350 μm I.D. until their ends face each other [240]. Another possible approach is the use of fritless packed capillaries, which are fabricated without the frit at the detection end and with the tapered end at the injection side. These fritless capillaries can only be used with packing materials having electrophoretic mobility larger than EOF and directed to the opposite direction of it. For example, in the case of packing material consisting of negatively charged particles, upon applying the electric field the particles are attracted by the anode. If their electrophoretic mobility is large enough, it prevents the particles being flushed out from the column by the EOF, which transports the mobile phase and the analytes through the CEC column [241]. Besides the above limitations associated with the direction and magnitude of the electrophoretic mobility of the packed charged particles and the EOF, further problems arise from the poor stability of the packing bed when the electric field is not applied and from the fragility of the tapered column inlet.

The problems with packing and retaining particles in capillary tubes are eliminated by the use of columns containing in situ prepared monolithic separation media formed from either organic polymers or silica. Such monolithic columns are characterized by a bimodal pore structure consisting of large pores for flow the mobile phase through the stationary phase and diffusion pores for analyte-stationary phase interactions. The organic-based monolithic columns are generally made of a mixture of monomers, crosslinkers, and porogens by radical polymerization, which is conducted directly within the confine of a capillary. These monolithic columns have excellent pH stability. In addition, porous size and distribution, as well as EOF and retentive properties, can be easily tailored by tuning the composition of the reaction mixture that can be composed of a variety of ionizable monomers, neutral reactants, and porogenic solvents at different percentage [242,243]. The main drawbacks of organic polymer–based monolithic columns are their limited mechanical strength, in addition to the presence of micropores that may negatively affect efficiency and sample recovery. Also challenging is their tendency either to swell or to shrink when exposed to different organic solvents, which can be incorporated into the mobile phase.

Silica-based monolithic CEC column can be prepared by a multistep approach involving the preparation of a silica monolithic skeleton attached to the capillary wall, which is first treated with an alkaline solution to leaching the micropores and then chemically modified with different silylation reagents for binding the functionalities requested to operate the column at different separation modes [244,245]. Alternatively, hybrid organic–inorganic monolithic CEC columns can be prepared by hydrolytic polycondensation of siloxane and organosiloxane precursors, in presence of an acid catalyst and a water-soluble polymer acting as porogen, by one step, in situ, sol-gel process under mild reaction conditions. In such monolithic stationary phases, an organic moiety

is covalently linked by a nonhydrolyzable Si–C bond to a siloxane specie, which hydrolyzes to produce a silica network [246]. The selection of proper sol-gel precursors allows the preparation of silica-based monoliths having ionizable groups and interaction sites that ensure the requested EOF and chromatographic behaviors [247]. Main advantages of silica-based monolithic columns are the high mechanical stability and the presence of surface silanol groups that provide reactive sides for the covalent bonding of an array of functional groups to generate stationary phases having different EOF characteristics and operating in a variety of separation modes.

Another alternative approach to packed capillaries are the so-called open-tubular columns consisting of a capillary tube whose inner surface is coated with a stationary which interacts with the analytes dissolved in the mobile phase transported by the EOF, as first reported by Tsuda et al. for the separation of aromatic compounds using an open silica capillary with octadecylsilane-bonded inner surface [248]. Theoretically, any possible ligand suitable to prepare stationary phases employed in liquid chromatography can be used to make capillary columns for open-tubular capillary electrochromatography (OT-CEC). Also, wide is the array of methods employed for surface modification and immobilization of the stationary phase, which include adsorption [249], covalent bonding of monomers (with or without cross-linking) [250,251] chemical bonding after etching [250,252], grafting polymeric porous layer to the inner surface [253], chemical reactions by sol-gel processes [254], and coating the inner surface of the capillary with nanoparticles [255].

The most important advantages of open-tubular columns over packed capillary columns are common to those reported for monolithic columns, with additional merits arising from the possibility of preparing columns in the small internal diameter range of 20–25 μm, which may be requested in miniaturized analytical techniques. On the other hand, several drawbacks are typical of open-tubular capillary columns, such as the low sample capacity, low phase ratio, and short optical path length for on-column UV-visible and fluorescence detection methods. Therefore, most of the different approaches cited above and recent innovations in developing novel column for OT-CEC have been mainly aimed at increasing the surface area of the bonded stationary phase, besides improving selectivity for a given separation problem.

The separation of uncharged compounds in CEC occurs as in HPLC due to their partitioning between the stationary and the mobile phases, with the only difference that the movement of the mobile phase through the column is propelled by electroosmosis in CEC and by a mechanic pump in HPLC. Consequently, the retention of uncharged analytes can be described by the chromatographic retention factor, k, which is expressed by the well-known equation:

$$k = \frac{t_R - t_0}{t_0} \tag{6.53}$$

where t_R and t_0 are the retention (migration) times of the uncharged analyte and of an unretained uncharged tracer, respectively.

More complex is the separation of charged analytes in CEC, which is the result of the interplay of chromatographic and electrophoretic processes that is considered in the definition of the electrochromatographic retention factor, or overall retention factor, k_c, introduced by Rathore and Horváth [140]:

$$k_c = k + kk_e + k_e \tag{6.54}$$

where

k is the chromatographic retention factor

k_e is the electrophoretic velocity factor (see Equation 6.42) and the product kk_e reflects the simultaneous occurrence of chromatographic and electrophoretic separation processes

It is worth noting that for uncharged compound k_e is zero and the electrochromatographic retention factor is equal to the retention factor defined by Equation 6.53.

The selectivity coefficient or separation factor, α, in CEC is given by the ratio of the electrochromatographic retention factors of the two analytes (1 and 2) migrating as adjacent peaks:

$$\alpha_{1,2} = \frac{k_{c,2}}{k_{c,1}} \tag{6.55}$$

where $k_{c,1}$ and $k_{c,2}$ are the electrochromatographic retention factors for the analytes 1 and 2, respectively, with $k_{c,2} > k_{c,1}$, such that $\alpha_{1,2} > 1$.

The separation factor influences the degree of separation of two adjacent peaks, which is also affected by the number of the theoretical plates, according to the following equation:

$$R_S = \frac{\sqrt{N}}{2}\left(\frac{\alpha_{1,2}-1}{\alpha_{1,2}+1}\right)\left(\frac{\bar{k}_c}{1+\bar{k}_c}\right) \tag{6.56}$$

where $\bar{k}_c$ is the average value of the electrochromatographic retention factors of the two adjacent peaks.

The limits of the electrochromatographic retention factor defined by Equation 6.54 are that both k and k_e must be separately evaluated under specific experimental conditions used in CEC. These limitations can be avoided describing the retention of analytes in CEC by a peak locator that can be evaluated directly from the electrochromatogram as follows [256]:

$$k_{cc} = \frac{t_m - t_0}{t_0} \tag{6.57}$$

where t_m and t_0 are the migration times of the analyte and of a uncharged and chromatographically inert tracer, respectively. This peak locator is expressed in terms typical of retention factor in HPLC, as defined by Equation 6.53. However, in contrast to k in HPLC, k_{cc} may exhibit negative values for charged analytes eluting prior to the marker. It is worth noting that identical resolution values are obtained using either k_c or k_{cc}, whereas the values of selectivity calculated using k_c or k_{cc} differ from each other due to the different definition of the peak locators, as given in Equations 6.54 and 6.57.

A variant of CEC is pressurized capillary electrochromatography (pCEC), in which the mobile phase is propelled by both electroosmosis and pressurized flow generated by an HPLC pump [257,258]. The main advantage of pCEC is the possibility of regulating the flow rate independently by the applied voltage, which offers the opportunity to shortening the analysis time, in addition to minimizing the risk of bubble formation. Such advantages are obtained at the expense of column efficiency, which can be reduced as a consequence of the contribution to band broadening due to the parabolic flow profile produced by the mechanical pump [249]. Capillary electrochromatography is generally performed under isocratic elution mode due to technical difficulty to change the composition of the electrolyte solution at the inlet end of the CEC column, although examples of CEC under either step gradient or linear gradient elution mode have been reported, using appositively modified instruments [260–263].

6.5.7 Capillary Isotachophoresis

Capillary isotachophoresis (CITP) is an electromigration technique, which is performed using a discontinuous buffer system, formed by a leading electrolyte (LE) and a terminating electrolyte

(TE), containing a fast and a slow migrating component of like charge, respectively. The sample is introduced into the capillary filled with the leading electrolyte, which has higher electrophoretic mobility than any of the sample components to be separated. The terminating electrolyte, having electrophoretic mobility lower than any of the sample components, occupies the opposite reservoir. Therefore, the injected sample occupies a zone of the capillary column in between the leading electrolyte and the terminating electrolyte. In each single ITP analysis, either cations or anions can be separated [264].

Highly mobile zones have high conductivity, and as a result, have a lower voltage drop across the band. On the other hand, low mobile zones have low conductivity and consequently a higher voltage drop across the band occurs. Therefore, the electric field varies in each zone that moves as a band. Since the velocity of migration is the product of the electrophoretic mobility and the electric field and conductivity and voltage drop are inversely proportional, the individual band velocities are self-adjusting to a constant value. A consequence of the self-adjusting velocity of migration is that each band maintains very sharp boundaries with the neighboring faster and slower bands. Thus, if an ion diffuses into a neighboring zone, it will either speed up or slow down based on the field strength encountered and it returns to the original band. A schematic representation of the CITP separation process is depicted in Figure 6.12.

The main determining factor in CITP is the composition of the leading electrolyte and of the terminating electrolyte. To separate anions, for example, the LE must be an anion with electrophoretic mobility higher than that of each analyte, whereas the anion acting as TE must have an electrophoretic mobility lower than that of each analyte. When the electric potential is applied, the anionic components of sample, the LE and the TE start to migrate toward the anode. Since the leading anion has the highest electrophoretic mobility, it moves fastest, followed by the anion having the next fastest mobility, which moves faster than the anion having the next fastest mobility, and so on. The result is that the sample components are separated according to the order of their electrophoretic mobility into distinct zones, which are sandwiched between the leading and the terminating electrolyte, forming a front and a rear zone, respectively [265]. The separated zones are surrounded by sharp electrical field differences and their profiles can be negatively affected by the EOF, which is usually regarded as undesirable in CITP, although well-separated bands can be obtained under favorable conditions, such as EOF and isotachophoretic velocities directed in the same direction [266,267]. The EOF is generally suppressed, either using a covalently coated

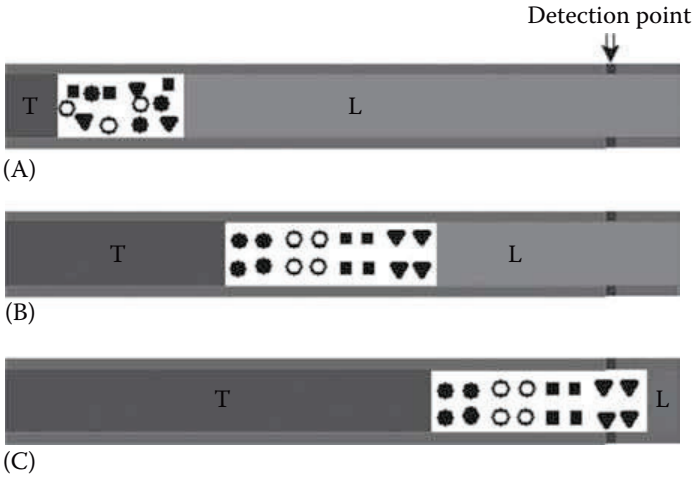

FIGURE 6.12 Schematic view of the CITP separation mechanism. The sample is introduced into the capillary between two electrolyte systems: a leading electrolyte (L), having electrophoretic mobility higher than any of the sample components to be separated and a terminating electrolyte (T), having electrophoretic mobility lower than any of the sample components (A). The sample components are separated according to the order of their individual mobility into distinct zones, which are sandwiched between T and L (B). The separated zones move with the same velocity toward the capillary end where they are detected as bands (C).

capillary or incorporating a suitable additive into the electrolyte solution, such as hydroxyethylcellulose, methylcellulose, and linear polyacrylamide, which increase the viscosity of the BGE and, therefore, minimize the EOF.

Crucial factors that must be considered in selecting the suitable composition of the electrolyte solution for CITP of either cations or anions include the choice of the pH range, which determines the sufficient ionization of the ample components. Another important factor is the range of electrophoretic mobility spanned by the LE and the TE, which determines the so-called mobility window of potential analytes that can be analyzed using a given LE–TE system [268]. Since adjacent bands are in contact with each other, a marker substance (spacer) having a mobility value that falls in between the mobilities of two peaks that need to be resolved is generally added to the sample in order to improve resolution. When UV-visible detection is employed, the spacer is a non-adsorbing substance in order to facilitate the analyte detection, which is otherwise traditionally performed by monitoring the variations in conductivity, although other detection methods are also possible.

Capillary isotachophoresis is usually performed in constant current mode, which implies the invariable ratio between concentration and electrophoretic mobility of ions. Therefore, bands that are less concentrated than the LE are sharpened, whereas those that are more concentrated than the LE are broadened to adapt their concentration to the requested constant value between concentration and electrophoretic mobility. The consequence of this unique property of CITP is that each sample component can be concentrated to an extent that depends on its initial concentration and the concentration of the leading electrolyte. Therefore, the opportune selection of composition and concentration of the leading electrolyte allows the enrichment of diluted analytes.

Sample enrichment techniques based on a transient isotachophoresis step performed in the capillary prior to start the selected electromigration method are widely employed. The transient isotachophoretic step is carried out by incorporating a high concentration of the leading and/or terminating electrolyte in either the sample or the BGE. According to this technique, relatively large volumes of samples introduced into the capillary can be concentrated in the isotachophoresis step by stacking the analytes in a very sharp zone [269–273]. Sample preconcentration can also be performed by coupling two capillary columns [274–276]. According to this approach, the sample migrates between a LE and a TE in the first capillary where it is concentrated by CITP, whereas in the second capillary, which is on-line connected with the exit of the first one, the analysis continues in another electromigration separation mode.

REFERENCES

1. P. Kubáň, P. C. Hauser, *Anal. Chim. Acta* 607, 15–29, 2008.
2. F.-M. Matysik, *Microchim. Acta* 160, 1–14, 2008.
3. X.-J. Huang, Z.-L. Fang, *Anal. Chim. Acta* 414, 1–14, 2000.
4. W. F. Smyth, *Electrophoresis* 27, 2051–2062, 2006.
5. D. A. Jayawickrama, J. V. Sweedler, *J. Chromatogr. A* 1000, 819–840, 2003.
6. C. W. Huck, R. Bakry, L. A. Huber, G. K. Bonn, *Electrophoresis* 27, 2063–2074, 2006.
7. P. C. Hiemenz, *Principles of Colloid and Surface Chemistry*. Marcel Dekker, Inc., New York, 1986.
8. A. W. Adamson, *Physical Chemistry of Surfaces*. John Wiley & Sons, Inc., New York, 1990.
9. R. J. Hunter, *Zeta Potential in Colloid Science*. Academic Press, London, U.K., 1981.
10. P. Jandik, G. Bonn, *Capillary Electrophoresis of Small Molecules and Ions*. VCH Publishers, Inc., New York, 1993.
11. J. P. Landers, *Handbook of Capillary Electrophoresis*. CRC Press, Boca Raton, FL, 1994.
12. D. C. Grahame, *Chem. Rev*. 41, 441–501, 1947.
13. M. von Smoluchowski, in I. Graetz (Ed.) *Handbuch der Elektrizitat und des Magnetismus*, Barth, Leipzig, Germany, 1921, pp. 366–428.
14. W. Schützner, E. Kenndler, *Anal. Chem*. 64, 1991–1995, 1992.
15. E. Sahlin, S. G. Weber, *J. Chromatogr. A*, 972, 283–287, 2002.
16. X. Huang, Cs. Horváth, *J. Chromatogr. A*, 788, 155–164, 1997.

17. T. Tsuda, J. V. Sweedler, R. N. Zare, *Anal. Chem*. 62, 2149–2152, 1990.
18. A. Cifuentes, M. A. Rodriguez, F. J. Garcia-Montelongo, *J. Chromatogr. A* 737, 243–253, 1996.
19. F. E. P. Mikkers, F. M. Everaerts, T. P. E. M. Vergheggen, *J. Chromatogr*. 169, 11–20, 1979.
20. T. Tsuda, T. Mizuno, J. Akiyama, *Anal. Chem*. 59, 799–800, 1987.
21. M. Deml, F. Foret, P. Boček, *J. Chromatogr*. 320, 159–165, 1985.
22. G. B. Gordon, U.S. Patent 5,061,361, October 29, 1991.
23. J. P. Chervet, M. Ursem, J. P. Salzmann, R. W. Vannoort, *J. High Resolut. Chromatogr. Chromatogr. Commun*. 12, 278–281, 1989.
24. T. Wang, J. H. Aiken, C. W. Huie, R. A. Hartwick, *Anal. Chem*. 63, 1372–1376, 1991.
25. Technical Note n. 5965–5984, Agilent Technologies, Santa Clara, CA, 1997.
26. D. Xiao, S. Zhao, H. Yuan, X. Yang, *Electrophoresis* 28, 233–242, 2007.
27. W. Tong, E. S. Yeung, *J. Chromatogr. A* 718, 177–185, 1995.
28. P. A. G. Butler, B. Mills, P. C. Hauser, *Analyst* 122, 949–953, 1997.
29. S. Casado-Terrones, S. Cortacero-Ramírez, *Anal. Bioanal. Chem*. 386, 1835–1847, 2006.
30. C. Johns, M. Macka, P. R. Haddad, *Electrophoresis* 25, 3145-31-52, 2004.
31. J. P. Hutchinson, C. J. Evenhuis, C. Johns, A. A. Kazarian, M. C. Breadmore, M. Macka, E. F. Hilder, R. M. Guijt, G. W. Dicinoski, P. Haddad, *Anal. Chem*. 79, 7005–7013, 2007.
32. M. C. Breadmore, R. D. Henderson, A. R. Fakhari, M. Macka, P. R. Haddad, *Electrophoresis* 28, 1252–1258, 2007.
33. J. S. Frits, G. H. Schenk, *Quantitative Analytical Chemistry*, 5th edn., Allin & Bacon, Inc., Boston, MA, 1987, pp. 369–421.
34. E. Gassmann, J. E. Kuo, R. N. Zare, *Science* 230, 813–814, 1985.
35. A. M. García-Campaña, M. Taverna, H. Fabre, *Electrophoresis* 28, 208–232, 2007.
36. M. E. Johnson, J. P. Landers, *Electrophoresis* 25, 3513–3527, 2004.
37. J. A. Taylor, E. S. Yeung, *Anal. Chem*. 64, 1741–1745, 1992.
38. P. G. Schiro, C. L. Kuyper, D. T. Chiu, *Electrophoresis* 28, 2430–2438, 2007.
39. T. Tsuda, J. W. Sweedler, R. N. Zare, *Anal. Chem*. 64, 967–972, 1992.
40. S. Wu, N. J. Dovichi, *J. Chromatogr*. 480, 141–155, 1989.
41. D. Y. Chen, N. J. Dovichi, *Anal. Chem*. 68, 690–696, 1996.
42. A. E. Bruno, F. Maystre, B. Krattiger, P. Nussbaum, E. Gassmann, *Trends Anal. Chem*. 13, 190–198, 1994.
43. S. Nagaraj, H. T. Karnes, *Biomed. Chromatogr*. 14, 234–242, 2000.
44. B. Yang, H. Tian, J. Xu, Y. Guan, *Talanta* 69, 996–1000, 2006.
45. J. Xu, S. Chen, Y. Xiong, B. Yang, Y. Guan, *Talanta* 75, 885–889, 2008.
46. E. P. Jong, C. A. Lucy, *Anal. Chim. Acta* 546, 37–45, 2005.
47. W. Du, S. Chen, Y. Xu, Z. Chen, Q. Luo, B.-F. Liu, *J. Sep. Sci*. 30, 906–915, 2007.
48. M. L. Gostkowski, J. B. McDoniel, J. Wie, T. E. Curey, J. B. Shear, *J. Am. Chem. Soc*. 120, 18–22, 1998.
49. J. E. Melanson, C. A. Lucy, C. A. Boulet, *Anal. Chem*. 73, 1809–1813, 2001.
50. K. Tóth, K. Štulik, W. Kutner, Z. Fehér, E. Lindner, *Pure Appl. Chem*. 76, 1119–1138, 2004.
51. A. J. Zemann, *Trends Anal. Chem*. 20, 346–354, 2001.
52. X. Huang, T. J. Pang, M. J. Gordon, R. N. Zare, *Anal. Chem*. 59, 2747–2749, 1987.
53. X. Huang, R. N. Zare, *Anal. Chem*. 63, 2193–2196, 1991.
54. A. J. Zemann, E. Schnell, D. Volgger, G. K. Bonn, *Anal. Chem*. 70, 563–567, 1998.
55. J. A. Freacassi da Silva, C. L. do Lago, *Anal. Chem*. 70, 4339–4343, 1998.
56. D. Kaniansky, V. Zelenskaè, M. Masaèr, F. Ivanyi, Sí. Gazdikova, *J. Chromatogr. A* 844, 349–359, 1999.
57. V. Unterholzner, M. Macka, P. R. Haddad, A. J. Zemann, *Analyst* 127, 715–718, 2002.
58. M. Novotný, F. Opekar, I. Jelínek, K. Štulík, *Anal. Chim. Acta* 525, 17–21, 2004.
59. F. Tan, B. C. Yang, Y. F. Guan, *Anal. Sci*. 21, 583–585, 2005.
60. P. L. Weber, T. Kornfelt, N. K. Klausen, S. M. Lunte, *Anal. Biochem*. 225, 135–142, 1995.
61. J. Wen, A. Baranski, R. Cassidy, *Anal. Chem*. 70, 2504–2509, 1998.
62. R. A. Wallingford, A. G. Ewing, *Anal. Chem*. 59, 1762–1766, 1897.
63. T. J. O'Shea, R. D. Greenhagen, S. M. Lunte, C. E. Lunte, M. R. Smyth, D. M. Radzik, N. Watanabe, *J. Chromatogr*. 593, 305–312, 1992.
64. R. Chen, H. Cheng, W. Wu, X. Ai, W. Huang, Z. Wang, J. Cheng, *Electrophoresis* 28, 3347–3361, 2007.
65. X. Huang, R. N. Zare, S. Sloss, A. G. Ewing, *Anal. Chem*. 63, 189–192, 1991.
66. F.-M. Matysik, *Electroanalysis* 12, 1349–1355, 2000.

67. M. Zhong, S. M. Lunte, *Anal. Chem*. 68, 2488–2493, 1996.
68. M. Chen, H. J. Hung, *Anal. Chem*. 67, 4010–4014, 1995.
69. M. Lowry, S. O. Fakayode, M. L. Geng, G. A. Baker, L. Wang, M. E. McCarroll, G. Patonay, I. M. Warner, *Anal. Chem*. 80, 4551–4574, 2008.
70. X. Huang, J. Ren, *Trends Anal. Chem*. 25, 155–166, 2006.
71. X.-B. Yin, E. Wang, *Anal. Chim. Acta* 533, 113–120, 2005.
72. E. V. Efremov, F. Ariese, C. Gooijer, *Anal Chim. Acta* 606, 119–134, 2008.
73. R. J. Dijkstra, F. Ariese, C. Gooijer, U. A. Th. Brinkman, *Trends Anal. Chem*. 24, 304–323, 2005.
74. H. Zhu, I. M. White, J. D. Suter, M. Zourob, X. Fan, *Anal. Chem*. 79, 930–937, 2007.
75. A. E. Bruno, B. Krattiger, F. Maystre, H. M. Widmer, *Anal. Chem*. 63, 2689–2697, 1991.
76. S. E. Johnston, K. E. Fadgen, J. W. Jorgenson, *Anal. Chem*. 78, 5309–5315, 2006.
77. M. Yu, N. J. Dovichi, *Anal. Chem*. 61, 37–40, 1989.
78. S. L. Pentoney Jr., R. N. Zare, J. F. Quint, *Anal. Chem*. 61, 1642–1647, 1989.
79. A. Gaspar, M. Englmann, A. Fekete, M. Harir, P. Schmitt-Kopplin, *Electrophoresis* 29, 66–79, 2008.
80. P. Schmitt-Kopplin, M. Englmann, *Electrophoresis* 26, 1209–1220, 2005.
81. C. W. Klampfl, *J. Chromatogr. A* 1044, 131–144, 2004.
82. M. Yamashita, J. B. Fenn, *J. Phys. Chem*. 88, 4451–4459, 1984.
83. M. Mann, C. K. Meng, J. B. Fenn, *Anal. Chem*. 61, 1702–1708, 1989.
84. R. D. Smith, J. A. Olivares, N. T. Nguyen, H. R. Udseth, *Anal. Chem*. 60, 436–441, 1988.
85. J. A. Olivares, N. T. Nguyen, C. R. Yonker, R. D. Smith, *Anal. Chem*. 59, 1230–1232, 1988.
86. E. D. Lee, W. Muck, J. D. Henion, *J. Chromatogr*. 458, 313–321, 1988.
87. E. D. Lee, W. Muck, J. D. Henion, T. R. Covey, *Biomed. Environ. Mass Spectrom*. 18, 844–850, 1989.
88. J. H. Whal, D. C. Gale, R. D. Smith, *J. Chromatogr. A* 659, 217–222, 1994.
89. M. S. Kriger, K. D. Cook, R. S. Ramsy, *Anal. Chem*. 67, 385–389, 1995.
90. L. Bendahl, H.S. Hansen, J. Olsen, *J. Rapid Commun. Mass Spectrom*. 16, 2333–2340, 2002.
91. E. P. Maziarz, S. A. Lorentz, T. P. White, T. D. Wood, *J. Am. Soc. Mass Spectrom*. 11, 659–663, 2000.
92. P. Cao, M. Moini, *J. Am. Soc. Mass Spectrom*. 9, 1081–1088, 1998.
93. J. P. Quirino, M. T. Dulay, B. D. Bennet, R. N. Zare, *Anal. Chem*. 73, 5539–5543, 2001.
94. J. T. Whitt, M. Moini, *Anal. Chem*. 75, 2188–2191, 2003.
95. R. Mol, G. J. de Jong, G. W. Somsen, *Electrophoresis* 26, 146–154, 2005.
96. C. Rentel, P. Gfrörer, E. Bayer, *Electrophoresis* 20, 2329–2336, 1999.
97. T. Johnson, J. Bergquist, R. Ekman, E. Nordhoff, M. Schürenberg, K.-D. Klöppel, M. Müller, H. Lehrach, J. Gobom, *Anal. Chem*. 73, 1670–1675, 2001.
98. K. L. Walker, R. V. Chiu, C. A. Monnig, C. L. Wilkins, *Anal. Chem*. 67, 4197–4204, 1995.
99. H. Y. Zhang, R. M. Caprioli, *J. Mass Spectrom*. 31, 1039–1046, 1996.
100. K. K. Murray, *Mass Spectrom. Rev*. 16, 283–299, 1997.
101. A. I. Gusev, *Fresenius' J. Anal. Chem*. 366, 691–700, 2000.
102. T. Rejtar, P. Hu, P. Juhasz, J. M. Campbell, M. L. Vestal, J. Preisler, B. L. Karger, *J. Proteome Res*. 1, 171–179, 2002.
103. M. Lechner, A. Seifner, A. M. Rizzi, *Electrophoresis* 29, 1974–1984, 2008.
104. S. Y. Chang, E. S. Yeung, *Anal. Chem*. 69, 2251–2257, 1997.
105. J. Preisler, F. Foret, B. L. Karger, *Anal. Chem*. 70, 5278–5287, 1998.
106. J. Preisler, P. Hu, T. Rejtar, B. L. Karger, *Anal. Chem*. 72, 4785–4795, 2000.
107. J. Preisler, P. Hu, T. Rejtar, E. Moskovets, B. L. Karger, *Anal. Chem*. 74, 17–25, 2002.
108. H. Orsnes, T. Graf, S. Bohatka, H. Degn, *Rapid Commun. Mass Spectrom*. 12, 11–14, 1998.
109. H. K. Musyimi, D. A. Narcisse, X. Zhang, W. Stryjewski, S. A. Soper, K. K. Murray, *Anal. Chem*. 76, 5968–5973, 2004.
110. N. Wu, T. L. Peck, A. G. Webb, R. L. Magin, J. V. Sweedler, *Anal. Chem*. 66, 3849–3857, 1994.
111. N. Wu, T. L. Peck, A. G. Webb, R. L. Magin, J. V. Sweedler, *J. Am. Chem. Soc*. 116, 7929–7930, 1994.
112. K. Pusecker, J. Schewitz, P. Gfrörer, L.-H. Tseng, K. Albert, E. Bayer, *Anal. Chem*. 70, 3280–3285, 1998.
113. D. I. Hoult, R. E. Richards, *J. Magn. Reson*. 24, 71–85, 1976.
114. Y. Li, M. E. Lacey, J. V. Sweedler, A. G. Webb, *J. Magn. Reson*. 162, 133–140, 2003.
115. D. L. Olson, M. E. Lacey, A. G. Webb, J. V. Sweedler, *Anal. Chem*. 71, 3070–3076, 1999.
116. J. Schewitz, K. Pusecker, L.-H. Tseng, K. Albert, E. Bayer, *Electrophoresis* 20, 3–8, 1999.
117. A. W. Wolters, D. A. Jayawickrama, A. G. Webb, J. V. Sweedler, *Anal. Chem*. 74, 5550–5555, 2002.
118. E. Rapp, A. Jakob, A. Bezerra Schefer, E. Bayer, K. Albert, *Anal. Bioanal. Chem*. 376, 1053–1061, 2003.
119. E. Bednarek, W. Bocian, K. Michalska, *J. Chromatogr. A* 1193, 164–171, 2008.
120. A. S. Rathore, *J. Chromatogr. A* 1037, 431–443, 2003.

121. C. J. Evenhuis, R. M. Guijt, M. Macka, P. J. Marriott, P. R. Haddad, *Anal. Chem*. 78, 2684–2693, 2006.
122. G. Chena, U. Tallarek, A. Seidel-Morgenstern, Y. Zhang, *J. Chromatogr. A* 1044, 287–294, 2004.
123. G. Y. Tang, C. Yang, C. J. Chai, H. Q. Gong, *Langmuir* 19, 10975–10984, 2003.
124. W. A. Gobie, C. F. Ivory, *J. Chromatogr*. 516, 191–210, 1990.
125. J. Knox, *Chromatographia* 26, 329–337, 1988.
126. S. Hjerten, *Chromatogr. Rev*. 9, 122–219, 1967.
127. E. A. S. Doherty, R. J. Meagher, M. N. Albarghouthi, A. E. Barron, *Electrophoresis* 24, 34–54, 2003.
128. C. A. Lucy, A. M. MacDonald, M. D. Gulcev, *J. Chromatogr. A* 1184, 81–105, 2008.
129. J. E. Wiktorowicz and J. C. Colburn, *Electrophoresis* 11, 769–773, 1990.
130. A. Eckhardt, I. Mikšík, Z. Deyl, J. Charvátová, *J. Chromatogr. A* 1051, 111–117, 2004.
131. Kleindiest, G., C. G. Huber, D. T. Gjerde, L. Yengoyan, G. K. Bonn, *Electrophoresis* 19, 262–269, 1998.
132. D. Corradini, L. Bevilacqua, I. Nicoletti, *Chromatographia* 62, 43–50, 2005.
133. D. Corradini, L. Sprecacenere, *Chromatographia* 58, 587–596, 2003.
134. D. Corradini, E. Cogliandro, L. D'Alessandro, I. Nicoletti, *J. Chromatogr. A* 1013, 221–232, 2003.
135. J. C. Giddings, *Sep. Sci*. 4, 181–189, 1969.
136. F. E. P. Mikkers, F. M. Everaerts, T. P. E. M. Verheggen, *J. Chromatogr*. 169, 1–10, 1979.
137. J. W. Jorgenson, K. D. Lukacs, *Anal. Chem*. 53, 1298–1302, 1981.
138. M.-L. Riekkola, J. Å. Jönsson, R. M. Smith, *Pure Appl. Chem*. 76, 443–451, 2004.
139. J. H. Knox, *J. Chromatogr. A* 680, 3–13, 1994.
140. A. S. Rathore, Cs. Horváth, *J. Chromatogr. A* 743, 231–246, 1996.
141. J. C. Reijenga, E. Kenndler, *J. Chromatogr. A* 659, 403–415, 1994.
142. D. Corradini, *J. Chromatogr. B* 699, 221–257, 1997.
143. J. Znaleziona, J. P. Radim Knob, V. Maier, J. Ševičik, *Chromatographia* 67, S5–S12, 2008.
144. J. C. Reijenga, L. G. Gagliardi, E. Kenndler, *J. Chromatogr. A* 1155, 142–145, 2007.
145. Z. Wang, J. Ouyang, W. R. G. Baeyens, *J. Chromatogr. B* 862, 1–14, 2008.
146. T. V. Popa, C. T. Mant, R. S. Hodges, *J. Chromatogr. A* 1111, 192–199, 2006.
147. P. Jáč, M. Polášek, M. Pospíšilová, *J. Pharm. Biomed. Anal*. 40, 805–814, 2006.
148. C. M. Shelton1, J. T. Koch, N. Desai, J. F. Wheeler, *J. Chromatogr. A* 792, 455–462, 1997.
149. Y. Yang, R. I. Boysen, J. I.-C. Chen, H. H. Keah, M. T. W. Hearn, *J. Chromatogr. A* 1009, 3–14, 2003.
150. A. Rizzi, *Electrophoresis* 22, 3079–3106, 2001.
151. M. López-Pastor, B. M. Simonet, B. Lendl, M. Valcárel, *Electrophoresis* 29, 94–107, 2008.
152. S. Mohabbati, S. Hjerten, D. Westerlund, *Anal. Bioanal. Chem*. 390, 667–678, 2008.
153. L. Geiger J.-L. Veuthey, *Electrophoresis* 28, 45–57, 2007.
154. S. P. Porras, E. Kenndler, *Electrophoresis* 26, 3203–3220, 2005.
155. H. Cottet, C. Simó, W. Vayaboury, A. Cifuentes, *J. Chromatogr. A* 1068, 59–73, 2005.
156. G. K. E. Scriba, *J. Chromatogr. A* 1159, 28–41, 2007.
157. A. C. Moser, D. S. Hage, *Electrophoresis* 29, 3279–3295, 2008.
158. C. Schou, N. H. H. Heegaard, *Electrophoresis* 27, 44–59, 2006.
159. Y. Tanaka, S. Terabe, *J. Chromatogr. B* 768, 81–92, 2006.
160. M. T. Bowser, D. D. Y. Chen, *J. Phys. Chem*. 103, 197–202, 1999.
161. K. L. Rundlett, D. W. Armstrong, *J. Chromatogr. A* 721, 173–186, 1996.
162. L. Valtcheva, J. Mohammad, G. Peterson, S. Hjerten, *J. Chromatogr*. 638, 263–267, 1993.
163. G. Gubitz, M. G. Scchmid, *Electrophoresis* 28, 114–126, 2007.
164. J. Østergaard, N. H. H. Heegaard, *Electrophoresis* 27, 2590–2608, 2006.
165. N. A. Guzman, T. Blanc, T. M. Phillips, *Electrophoresis* 29, 3259–3278, 2008.
166. L. K. Amundsen, H. Sirén, *Electrophoresis* 28, 99–113, 2007.
167. S. Lin, S.-M. Hsu, *Anal. Biochem*. 341, 1–15, 2005.
168. M. Gayton-Ely, T. J. Pappas, L. A. Holland, *Anal. Bioanal. Chem*. 382, 570–580, 2005.
169. A. Guttman, *LC-GC North Am*. 22, 896–904, 2004.
170. O. Grosche, J. Bohrisch, U. Wendler, W. Jaeger, H. Engelhardt, *J. Chromatogr. A* 894, 105–116, 2000.
171. S. Boulos, O. Cabrices, M. Blas, B. R. McCord, *Electophoresis* 29, 4695–4703, 2008.
172. I. Mikšík, P. Sedláková, K. Mikulíková, A. Eckhardt, T. Cserhati, T. Horváth, *Biomed. Chromatogr*. 20, 458–465, 2006.
173. V. Dolnik, W. A. Gurske, A. Padua, *Electrophoresis* 22, 707–719, 2001.
174. M. Bergman, H. Claessens, C. Cramers, *J. Microcol. Sep*. 10, 19–26, 1998.
175. F. Xu, Y. Baba, *Electrophoresis* 25, 2332–2345, 2004.
176. J. Sudor, V. Barbier, S. Thirot, D. Godfrin, D. Hourdet, M. Millequant, J. Blanchard, J. L. Viovy, *Electrophoresis* 22, 720–728, 2001.

177. C.-W. Kan, E. A. S. Doherty, B. A. Buchholz, A. E. Barron, *Electrophoresis* 25, 1007–1015, 2004.
178. T. Chiesl, W. Shi, A. E. Barron, *Anal. Chem*. 77, 772–779, 2005.
179. B. A. Buchholz, W. Shi, A. E. Barron, *Electrophoresis* 23, 1398–1409, 2002.
180. A. Tsupryk, M. Gorbovitski, E. A. Kabotyanski1, V. Gorfinkel, *Electrophoresis* 27, 2869–2879, 2006.
181. P. G. Righetti, C. Simò, R. Sebastiano, A. Citterio, *Electrophoresis* 28, 3799–2810, 2007.
182. P. G. Righetti, *Isoelectric Focusing: Theory, Methodology and Applications*, Elsevier, Amsterdam, the Netherlands, 1983.
183. S. Hjertén, M. D. Zhu, *J. Chromatogr*. 346, 265–270, 1985.
184. L. Gao, S. Liu, *Anal. Chem*. 76, 7179–7186, 2004.
185. M. Horká, J. Planeta, F. Růzička, K. Šlais, *Electrophoresis* 24, 1383–1390, 2003.
186. H. Tian, L. C. Brody, D. Mao, J. P. Landers, *Anal. Chem*. 72, 5483–5492, 2000.
187. K. K.-C. Yeung, K. K. Atwal, H. Zhang, *Analyst* 128, 566–570, 2003.
188. M. Poitevin, A. Morin, J.-M. Busnel, S. Descroix, M.-C. Hennion, G. Peltre, *J. Chromatogr. A* 1155, 230–236, 2007.
189. M. Horká, F. Růzička, *Anal. Bioanal. Chem*. 385, 840–846, 2006.
190. A. Palm, M. Zaragoza-Sundqvist, G. Marko-Varga, *J. Sep. Sci*. 27, 124–128, 2004.
191. P. G. Righetti, A. Bossi, C. Gelfi, *J. Capillary Electrophor*. 2, 47–59, 1997.
192. W. Thormann, J. Caslavska, R. A. Mosher, *J. Chromatogr. A* 1155, 154–163, 2007.
193. P. Lopez-Soto-Yarritu, J. C. Díez-Masa, A. Cifuentes, M. de Frutos, *J. Chromatogr. A* 968, 221–228, 2002.
194. J. R. Mazzeo, I. S. Krull, *Anal. Chem*. 63, 2852–2857, 1991.
195. J. Wu, J. Pawliszyn, *Anal. Chem*. 64, 224–227, 1992.
196. X.-Z. Wu, N. S.-K. Sze, J. Pawliszyn, *Electrophoresis* 22, 3968–3971, 2001.
197. X.-Z. Wu, T. Huang, Z. Liu, J. Pawliszyn, *Trends Anal. Chem*. 24, 369–382, 2005.
198. J. Wu, C. Tragas, A. Watson, J. Pawliszyn, *Anal. Chim. Acta* 383, 67–78, 1999.
199. X. Fang, C. Tragas, J. Wu, Q. Mao, J. Pawliszyn, *Electrophoresis* 19, 2290–2295, 1998.
200. H. Stutz, *Electrophoresis* 26, 1254–1290, 2005.
201. F. Foret, O. Muller, J. Thorne, W. Gotzngner, B. L. Carger, *J. Chromatogr. A* 716, 157–166, 1995.
202. J. Pawliszyn, J. Wu, *J. Microcol. Sep*. 5, 397–401, 1993.
203. T. Huang, J. Pawliszyn, *Electrophoresis* 23, 3504–3510, 2002.
204. R. Montgomery, X. Jia, L. Tolley, *Anal. Chem*. 78, 6511–6518, 2006.
205. C. Yang, G. Zhu, L. Zhang, W. Zhang, Y. Zhang, *Electrophoresis* 25, 1729–1734, 2004.
206. S. Terabe, K. Otsuka, K. Ichikawa, A. Tsuchiya, T. Ando, *Anal. Chem*. 56, 111–113, 1984.
207. S. Terabe, M. Shibata, Y. Miyashita, *J. Chromatogr*. 480, 403–411, 1989.
208. A. Dobashi, T. Ono, S. Hara, J. Yamaguchi, *Anal. Chem*. 61, 1984–1986, 1989.
209. S. Terabe, K. Otsuka, T. Ando, *Anal. Chem*. 57, 834–841, 1985.
210. G. Guiochon. Optimization in liquid chromatography, in C. Horváth (Ed.) *High-Performance Liquid Chromatography*. Academic Press, New York, 1980, pp. 1–56.
211. P. Gareil, *Chromatographia* 30, 195–200, 1990.
212. H. Corstjens, H. A. H. Billiet, J. Frank, K. Ch. M. Luyben, *J. Chromatogr. A* 753, 121–131, 1996.
213. K. Otsuka, S. Terabe, T. Ando, *J. Chromatogr*. 348, 39–47, 1985.
214. P. G. H. M. Muijselaar, H. A. Classens, C. A. Cramers, J. F. G. A. Jansen, E. W. Meijer, E. M. M. de Brabander-van den Berg, S. van der Wal, *J. High Resolut. Chromatogr*. 18, 121–123, 1995.
215. C. Fujimoto, Y. Muranaka, *J. High Resolut. Chromatogr*. 20, 400–402, 1997.
216. P. Viberg, M. Jornten-Karlsson, P. Petersson, P. Spegel, S. Nilsson, *Anal. Chem*. 74, 4595–4601, 2002.
217. P. Spegel, L. Schweitz, S. Nilsson, *Anal. Chem*. 75, 6608–6613, 2003.
218. U. Sharma, S. Sharma, *Int. J. Pharm*. 154, 123–140, 1997.
219. M. N. Jones, *Adv. Colloid Interface Sci*. 54, 93–128, 1995.
220. Y. Zhang, R. Zhang, S. Hjerten, P. Lundahl, *Electrophoresis* 16, 1519–1523, 1995.
221. D. Corradini, G. Mancini, C. Bello, *Chromatographia* 60, S125–S132, 2004.
222. D. Corradini, G. Mancini, C. Bello, *J. Chromatogr. A* 1051, 103–110, 2004.
223. N. Griese, G. Blaschke, J. Boos, G. Hempel, *J. Chromatogr. A* 979, 379–388, 2002.
224. S. Luedtke, Th. Adam, N. von Doehren, K. K. Unger, *J. Chromatogr. A* 887, 339–346, 2000.
225. V. Preotorius, B. Hopkins, *J. Chromatogr*. 99, 23–30, 1974.
226. J. Jorgenson, K. D. Lukacs, *J. Chromatogr*. 218, 209–216, 1981.
227. S. Zhang, X. Huang, N. Yao, Cs. Horváth, *J. Chromatogr. A* 948, 193–201, 2002.
228. L. A. Colon, T. D. Maloney, A. M. Fermier, *J. Chromatogr. A* 887, 43–53, 2000.
229. F. Lynen, A. Buica, A. de Villiers, A. Crouch, P. Sandra, *J. Sep. Sci*. 28, 1539–1549, 2005.

230. M. M. Robson, S. Roulin, S. M. Shariff, M. W. Raynor, K. D. Bartle, A. A. Clifford, E. Myers, M. R. Euerby, C. M. Johnson, *Chromatographia* 43, 313–321, 1996.
231. C. Yan, U.S. Patent 5,453,163, September 26, 1995.
232. A. M. Fermier, L. A. Colon, *J. Microcol. Sep*. 10, 439–447, 1998.
233. T. D. Maloney, L. A. Colon, *Electrophoresis* 20, 2360–2365, 1999.
234. R. Stol, M. Mazereeuw, U. R. Tjaden, J. van der Greef, *J. Chromatogr. A* 873, 293–298, 2000.
235. K. J. Reynolds, L. A. Colon, *Analyst* 123, 1493–1495, 1998.
236. H. Rebscher, U. Pyell, *Chromatographia* 42, 171–176, 1996.
237. H. J. Cortes, C. D. Pfeiffer, B. E. Richter, T. S. Stevens, *J. High Resolut. Chromatogr. Chromatogr. Commun*. 10, 446–448, 1987.
238. G. A. Lord, D. B. Gordon, P. Myers, B. W. King, *J. Chromatogr. A* 768, 9–16, 1997.
239. G. Choudhary, Cs. Horváth, J. F. Banks, *J. Chromatogr. A* 828, 469–480, 1998.
240. M. E. R. Hows, D. Perrett, *Chromatographia* 43, 200–204, 1996.
241. M. Mayer, E. Rapp, C. Marck, G. J. M. Bruin, *Electrophoresis* 20, 43–49, 1999.
242. C. Fujimoto, *Anal. Chem*. 67, 2050–2053, 1995.
243. I. Gusev, X. Huang, Cs. Horváth, *J. Chromatogr. A* 855, 273–290, 1999.
244. N. Ishizuka, H. Minakuchi, K. Nakanishi, N. Soga, H. Nagayama, K. Hosoya, N. Tanaka, *Anal. Chem*. 72, 1275–1280, 2000.
245. D. Allen, Z. El Rassi, *Electrophoresis* 24, 408–420, 2003.
246. M. T. Dulay, J. P. Quirino, B. D. Bennett, M. Kato, R. N. Zare, *Anal. Chem*. 73, 3921–3926, 2001.
247. G. Ding, Z. Da, R. Yuan, J. J. Bao, *Electrophoresis* 27, 3363–3372, 2006.
248. T. Tsuda, K. Nomura, G. Nakagawa, *J. Chromatogr*. 248, 241–247, 1982.
249. Z. Liu, H. Zou, M. Ye, J. I. Ni, Y. Zhang, *Electrophoresis* 14, 2891–2897, 1999.
250. J. J. Pesek, M. T. Matyska, S. Cho, *J. Chromatogr. A* 845, 237–246, 1999.
251. J. J. Pesek, M. T. Matyska, S. Sentellas, M. T. Galceran, M. Chiari, G. Pirri, *Electrophoresis* 23, 2982–2989, 2002.
252. Z. J. Tan, V. T. Remcho, *Anal. Chem*. 69, 581–586, 1997.
253. X. Huang, J. Zhang, Cs. Horváth, *J. Chromatogr. A* 858, 91–101, 1999.
254. Y. Guo, L. A. Colon, *Anal. Chem*. 67, 2511–2516, 1995.
255. M. C. Breadmore, M. Macka, N. Avdalovic, P. R. Haddad, *Analyst* 125, 1235–1241, 2000.
256. A. S. Rathore, Cs. Horváth, *Electrophoresis* 23, 1211–1216, 2002.
257. T. Tsuda, *Anal. Chem*. 59, 521–523, 1987.
258. Z. Lin, Z. Xie, H. Lü, X. Lin, X. Wu, G. Chen, *Anal. Chem*. 78, 5322–5328, 2006.
259. P. Gfrörer, L.-H. Tseng, E. Rapp, K. Albert, E. Bayer, *Anal. Chem*. 73, 3234–3239, 2001.
260. C. Yan, R. Dadoo, R. N. Zare, *Anal. Chem*. 68, 2726–2730, 1996.
261. C. G. Huber, G. Choudhari, Cs. Horváth, *Anal. Chem*. 69, 4429–4436, 1997.
262. G. Choudhary, Cs. Horváth, J. F. Banks, *J. Chromatogr. A* 828, 469–480, 1998.
263. Q.-H. Ru, J. Yao, G.-A. Luo, Y.-X. Zhang, C. Yan, *J. Chromatogr. A* 894, 337–343, 2000.
264. P. Boček, M. Deml, P. Gebauer, V. Dolnik, *Analytical Isotachophoresis*, VCH, Weinheim, Germany, 1988.
265. A. J. P. Martin, F. M. Everaerts, *Anal. Chim. Acta* 38, 233–237, 1967.
266. J. C. Reijenga, G. V. A. Aben, Th. P. E. M. Verheggen, F. M. Everaerts, *J. Chromatogr*. 260, 241–254, 1983.
267. H. R. Udseth, J. A. Lao, R. D. Smith, *Anal. Chem*. 61, 228–232, 1989.
268. P. Gebauer, P. Boček, *J. Chromatogr*. 267, 49–65, 1983.
269. R. Aebersold, H. D. Morrison, *J. Chromatogr*. 516, 79–88, 1990.
270. M. Dankova, D. Kaniansky, S. Fanali, F. Ivanyi, *J. Chromatogr. A* 838, 31–43, 1999.
271. S. Fanali, C. Desiderio, E. Olvecka, D. Kaniansky, M. Vojtek, A. Ferancova, *J. High Resolut. Chromatogr*. 23, 531–538, 2000.
272. X. Fang, L. Yang, W. Wang, T. Song, C. S. Lee, D. L. DeVoe, B. M. Balgley, *Anal. Chem*. 79, 5785–5792, 2007.
273. P. Mikus, K. Marakova, J. Marak, A. Plankova, I. Valaskova, E. Havranek, *Electrophoresis* 29, 4561–4567, 2008.
274. F. Foret, E. Szoko, B. L. Karger, *J. Chromatogr*. 608, 3–12, 1992.
275. J. Safra, M. Pospisilova, J. Spilkova, *Chromatographia* 64, 37–43, 2006.
276. J. Safra, M. Pospisilova, J. Honegr, J. Spilkova, *J. Chromatogr. A* 1171, 124–132, 2007.

Trends in Analytical Chemistry 164 (2023) 117080

Contents lists available at ScienceDirect

Trends in Analytical Chemistry

journal homepage: www.elsevier.com/locate/trac

Buffering agents and additives for the background electrolyte solutions used for peptide and protein capillary zone electrophoresis

Danilo Corradini

National Research Council (CNR), Institute for Biological Systems, Area della Ricerca Ricerca di Roma 1, 00015, Monterotondo, Rome, Italy

ARTICLE INFO

Article history:
Received 31 December 2022
Received in revised form
24 April 2023
Accepted 26 April 2023
Available online 6 May 2023

Keywords:
Capillary electrophoresis
Peptide separation
Protein separation
Back ground electrolyte solution
Buffering agents
Additives
Separation performance
Selectivity
Resolution
Electroosmotic flow

ABSTRACT

The background electrolyte solution (BGE) has a strong impact on the separation performance of peptides and proteins in all separation techniques governed by electrophoretic principles, due to its considerable influence on the separation mechanism and on the physicochemical properties of both the sample and the inner surface of the separation device, which mostly consists of a fused-silica capillary tube. This review article examines and discusses the effects of composition and pH of BGE on the electrokinetic phenomena taking place at the solid liquid interface within fused-silica capillaries, generating the electroosmotic flow (EOF), and on the separation performance of peptides and proteins in capillary zone electrophoresis (CZE), which is the most used separation mode of capillary electrophoresis for these biopolymers. The paper reviews and discusses literature relevant to explain how pH, ionic strength, conductivity and composition of BGE employed in peptide and protein CZE influence efficiency, selectivity and resolution and other factors affecting the performance of separation, including the electroosmotic flow. Also examined and discussed is the compatibility of BGE composition with the ionization sources employed for the on-line hyphenation of peptides and proteins CZE with mass spectrometry and with the two most popular on-line preconcentration methods field-amplified sample stacking (FASS) and dynamic pH junction.

© 2023 Elsevier B.V. All rights reserved.

1. Introduction

Capillary electrophoresis (CE) is a microscale separation technique based on the differential migration velocity of the analytes in a conductive medium under the action of an electric field (E field). It is widely employed for chemical characterization and routine analysis of therapeutic peptides and proteins, for the investigation of the molecular bases of biological processes and for peptidomics and proteomics studies [1–4]. The technique can be performed according to a variety of modes with different separation mechanisms that can be selected by changing the operational conditions, mainly type and composition of the background electrolyte solution (BGE) [5,6].

The BGE is filled either in capillary tubes or in micro-channels fabricated on plates of reduced dimensions, communally referred to as microfluid chips [7]. Characteristic feature of CE is the possible occurrence of an electrically driven flow of BGE across the separation pathway, the electroosmotic flow (EOF), which is generated by the action of the E field on the electric double layer formed at the interface between the conducting electrolyte solution and the charged surface of either the capillary column or the microfluid chip in contact with the liquid (see Fig. 1).

Capillary tubes and microchannels enable the application of high electric fields with minimal generation of Joule heat, which is efficiently dissipated by transfer through the wall of these separation devices as a result of their large surface-to-volume ratio. Moreover, the microscale format minimizes the convective mixing of the separated zone in the BGE, ensuring high efficiency and resolution, especially for large molecules having small diffusion coefficients. Besides high resolution and efficiency, small sample amount requirement, short analysis time and high throughput are the major common advantages of all CE separation modes. Additional advantages include the use of small amounts of chemicals, reduced waste, automation, and the use of a wide range of detection methods, which include UV, mass spectrometry, fluorescence, and capacitively coupled contactless conductivity detection, among others [8,9]. Possible drawbacks include poor repeatability/reproducibility of the low sample volumes introduced into the separation device (in nanoliter range), low sensitivity of UV detection,

E-mail address: danilo.corradini@cnr.it.

https://doi.org/10.1016/j.trac.2023.117080
0165-9936/© 2023 Elsevier B.V. All rights reserved.

Abbreviations

[bmim][BF4]	1-Butyl-3-methylimidazolium tetrafluoroborate
[emim][BF4]	1-Ethyl-3-methylimidazolium tetrafluoroborate
BGE	Background electrolyte solution
Bis-Tris	1,3-Bis[tris(hydroxymethyl)methylamino]
CA	Carrier ampholytes
CE	Capillary electrophoresis
CHES	2-(Cyclohexylamino)ethanesulfonic acid
CMAs	Critical method attributes
CMVs	Critical method variables
CZE	Capillary zone electrophoresis
DIEN	Diethylenetriamine
DMA	N,N-Dimethylacetamide
DMF	N,N-Dimethylformamide
DoE	Design of experiment
E field	Electric field
EOF	Electroosmotic flow
ESI	Electrospray ionization
FASS	Field-amplified sample stacking
GnRH	Human gonadotropin-releasing hormone
HPLC	High performance liquid chromatography
HP-β-CD	2-Hydroxypropyl-β-cyclodextrin
I	Ionic strength
IEF	Isoelectric focusing
IgG1	Immunoglobulin G1
IL	Ionic liquids
MS	Mass spectrometry
NACE	Nonaqueous capillary electrophoresis
OFAT	One factor at time
PAMAPTAC	Poly(acrylamide-co-(3- acrylamidopropyl) trimethylammonium chloride
pI	Isoelectric point
TEA	Triethanolamine
TETA	Triethylentetramine
Tris	Tris(hydroxymethyl)aminomethane
UV	Ultraviolet
WCID	Whole column imaging detection
β-CD	β-Cyclodextrin

fluctuant EOF, and poor migration time repeatability. Further undesirable features are loss of sample and compromission of separation efficiency ascribable to the interactions of the analytes with the inner surface of microfluid chips or capillary columns. The proper selection of the components of BGE is fundamental to minimize several of the mentioned drawbacks, and to optimize selectivity and separation performance [10,11].

Capillary zone electrophoresis (CZE) is generally performed in capillary columns, using BGE of uniform composition along the separation path and applying a constant E field across the capillary length. The separation mechanism is based on differences in the electrophoretic mobilities of the charged analytes and, therefore, on their charge-to-hydrodynamic radius ratio [5]. Based on the consideration that CZE is the most used separation mode for peptides and proteins capillary electrophoresis, this review article examines the effects of buffering agents and additives incorporated into the BGE on EOF and separation performance of these analytes in CZE. The paper reviews and discusses literature relevant to elucidate the effects of chemical composition, ionic strength, pH, buffering capacity, and electric conductivity of the BGE used in CZE on both EOF and electrophoretic behaviour of peptides and proteins, including their interactions with the inner surface of both bare and coated fused-silica capillary columns. Also discussed are the requirements for the selection of buffering agents and additives compatible with the hyphenation of CZE with mass spectrometry and with the on-line preconcentration methods, widely employed to increase the number of detectable peptides and proteins occurring in diluted samples.

2. Control of the protonic equilibrium

The electrophoretic mobility of peptides and proteins in a conductive medium is influenced by all factors that affect their charge to size ratio and, therefore, by pH and composition of BGE. The changes in the composition and pH of BGE due to electrolysis, frequently taking place in the electrode compartments during the electrophoretic separation, have been extensively investigated and only a selected number of relevant papers covering this subject are herewith cited [12–16]. As a result of electrolysis and production of hydroxonium and hydroxide ions, the pH of BGE on the cathodic side tends to increase while the BGE on the anodic side tends to become more acidic, originating a pH gradient within the capillary tube, which is expected to affect the electrophoretic mobility of the analytes and, to a minor extent, the zeta potential at the solid-liquid interface and, consequently, the electroosmotic flow. Moreover, the altered BGE can be propagate throughout the capillary by EOF and affect the electrophoretic mobility of the analytes, particularly in longer electrophoretic runs [12].

Practical methods proposed to minimize the negative effects of electrolysis include the use of BGEs with high buffering capacity and low electric conductivity, such as zwitterionic organic buffers. Also recommended has been the use of BGE reservoirs of relatively large volume and having the electrodes located at the greatest distance from the inlets of the capillaries. This in order to ensure the dilution of the products of the redox reaction and to prevent their propagation into the capillary column. The replacement of the BGE with a new one before starting each separation has been recommended too [15]. Also proposed has been the use of a salt bridge to isolate the electrolysis region, as well as the use of electrolysis-separated systems constructed by splitting each of the original reservoirs into two compartments with a salt bridge between them [16].

Recently, Novotný and Gaš [12] proposed a theoretical model for quantifying the variations in composition, pH, and conductivity of BGE caused by redox reactions occurring at the electrode compartments. The model considered electromigration and EOF in the separation capillary and the redox reactions of the BGE in the electrode compartments. The BGE consisted of either formic acid-ammonium formate or MES-histidine solution (Good's buffer), which were used to fill both the electrode compartments and the capillary. The pH of BGE in the cathodic and anodic compartments and the conductivity in the separation capillary were experimentally measured by a pH-microelectrode and by a contactless conductivity detector, respectively. The experimental data, measured before and after 1h electrophoretic run, were in good agreement with those theoretically calculated. As predicted by the theoretical model, the variations of pH and conductivity measured with the Good's buffer were much lower than those measured with ammonium formate, composed of a weak acid-strong base pair, confirming the advantages of using BGEs with a high buffering capacity and low specific conductivity, as it is generally recommended [15].

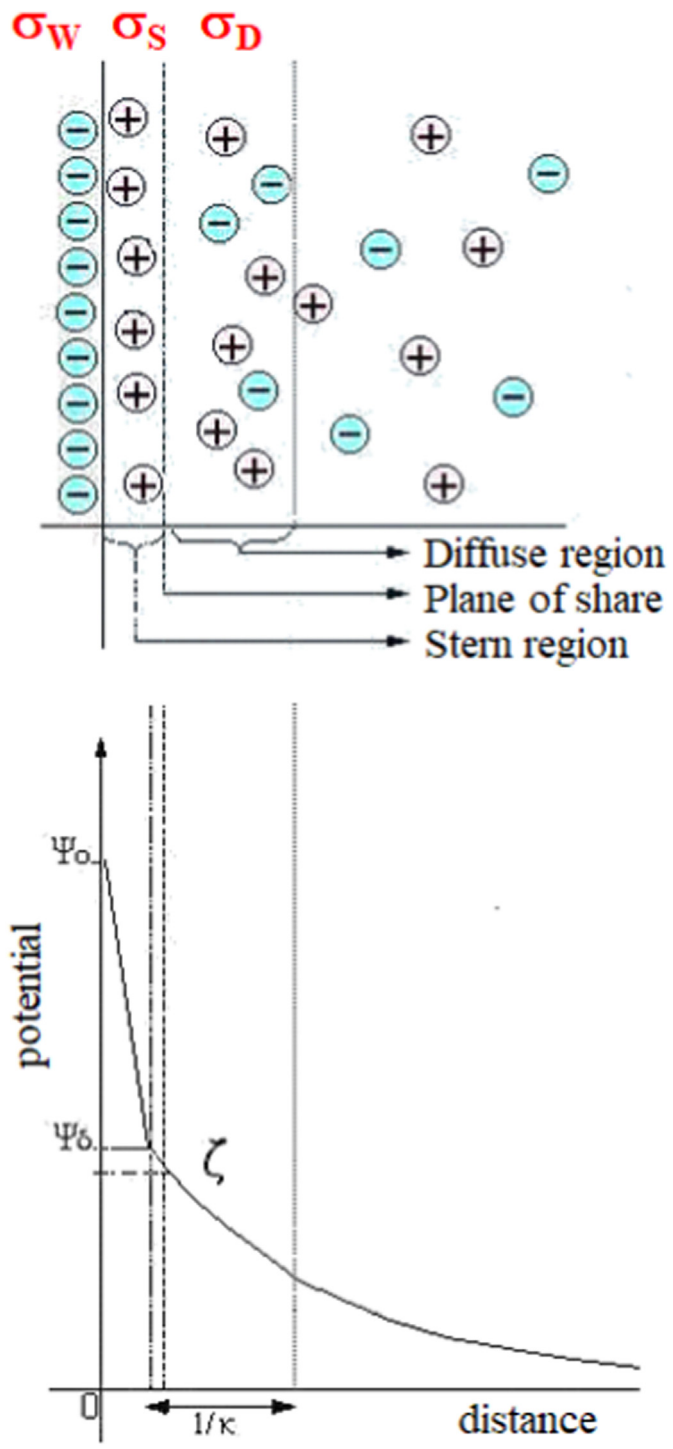

Fig. 1. Graphical representation of the electric double layer at solid-liquid interface of a bare fused silica capillary and decay of the electric potential with distance from the capillary wall. The charge density at the capillary wall and in the Stern and diffuse regions of the electric double layer is indicated as σ_W, σ_S, and σ_D, respectively.

In another study, whole column imaging detection (WCID) was employed to monitor the variations of migration velocity of selected analytes (proteins and pI-standards) across a coated capillary during the electrophoretic run, caused by the redox reactions at the electrode compartments [13]. The impact of electrolysis on the migration behavior of the analytes was evidenced by the non-constant migration velocity of the analytes during the electrophoretic run, which was larger for BGE with lower buffering capacity, especially at pH value closer to the pH region where the ionization of the analyte changes highly with pH. The study confirmed the superiority of zwitterionic buffers, in comparison to traditional ones (phosphate and borate buffers) at contrasting the negative effects of prolonged electrolysis in the BGE vessels.

Zwitterionic compounds possessing at least two of the pKa constants close to their pI exhibit high buffering capacity and low mobility, resulting in low electric current during the electrophoretic separation. These buffering agents have been employed in peptide and protein capillary electrophoresis, since its pioneering applications [17]. The low conductivity of zwitterionic buffers allows their incorporation into BGE at high concentration, increasing the buffer capacity while limiting the electric charges passing throughout the separation channel, which minimize the generation of Joule heat. On the other hand, the low UV-transparency of zwitterionic buffers limits their use at high concentration in capillary electrophoresis with UV detection. This requirement does not apply with other common no UV detection methods, such as laser induced fluorescent [10] or contactless conductivity detection [18].

Several studies have evidenced the strong impact of buffer concentration and ionic strength (I) on the factors influencing the separation performance of peptides and proteins in capillary electrophoresis [11,19]. These include EOF and electrophoretic mobility of the analytes (both decreasing with increasing I), analysis time (longer at higher I), electrostatic interactions with the capillary wall, if any (weaker at higher I), and the production of heating by Joule's effect (increasing with increasing I). Also considered should be the distortion of the mobile ion atmosphere around the analytes (relaxion effect) accompanying the binding of BGE anions to peptides and proteins [20]. Each of these factors affect the separation performance to different extents that depend on the physicochemical properties of the separated peptides and proteins (pI, molecular mass, net-charge, etc.), type of the capillary column (bare or coated fused-silica), and operational conditions (pH and composition of BGE, temperature, applied E field, length and diameter of the capillary, etc.).

The results of two relatively recent studies on the influence of composition and ionic strength of BGE on the separation performance of various peptides and proteins, in either coated or uncoated capillary, are explanatory examples of the different optimal conditions requested for the separation of peptides and proteins under diverse experimental conditions [10,11]. Morani et al. [10] recommended to use the low conductivity zwitterionic buffer Tris/CHES (pH 8.4) at high concentration for the efficient and selective separation of fluorescently labelled amyloid beta peptide Aβ 1–42, trypsin inhibitor and ovalbumin, performed in a bare fused-silica capillary.

Conversely, the results of the study conducted by Bekri and coworkers [11] evidenced that the use of BGE having relatively low ionic strength was preferable to optimize the separation of standard proteins by CZE in counter-electroosmotic mode with either acetate or formate buffers as the BGE. The study was carried out in a successive multi-ionic layer coated capillary, using BGEs at constant pH 2.5 and different values of the ionic strength, which was ranging from 3.1 to 51.1 mM and from 3.4 to 76.6 mM for acetate and formate buffer, respectively.

Amphoteric compounds, having very low electric conductivity and relatively high buffering capacity, originally designed for isoelectric focusing (IEF) and referred to as *carrier ampholytes* (CA), have been proposed as potential buffers in CZE [21]. Their use as low conductivity buffers requires the previous fractionations of the CA solution in portions having narrow pH spreading. Busnel et al.

[22] tested 25 fractions of a wide pH range (pH 3–10) CA solution, obtained by preparative IEF, providing the suitability of some of them for the efficient and fast separation of the nine components of a protein test mixture. The extremely low electric conductivity of the tested ampholyte-based buffers allowed the application of high electric field strength (up to 1000 V/cm), resulting in short analysis time (about 90 s) and negligible Joule heat. Similar results were shown by Solinova et al. [23] who reported the efficient CZE separation of oligopeptide fragments of human gonadotropin-releasing hormone (GnRH), obtained in a bare fused-silica capillary under very high electric field strength (800 V/cm).

Isoelectric buffers and aliphatic oligoamines are other examples of the variety of low conductivity buffers employed in peptide and protein CZE. Several of these compounds act as dynamic coating agents and buffer simultaneously. A practical example are the aliphatic oligoamines triethylentetramine (TETA) [24] and diethylenetriamine (DIEN) [25], which, in combination with the polyprotic phosphoric acid, display an appreciable buffer capacity in a wide pH range while controlling EOF and minimizing the interactions of peptides and proteins with the capillary wall.

3. Suppression of the interactions with the capillary wall and control of EOF

The surface of bare fused-silica capillaries, as well as that of glass and synthetic organic polymers employed to construct microfluid chips, may acquire superficial negative charges that originate cathodic EOF and promote electrostatic interactions with positively charged peptides and proteins. The EOF is proportional to the intensity of the applied electric field, depends on both the surface chemistry of the separation channel and the physicochemical properties of BGE, and may either positively or negatively affect migration behavior and electrophoretic performance of the analytes.

Particularly detrimental for the separation performance of peptides and proteins are the interactions of these analytes with the inner surface of the separation device. Using bare fused-silica capillaries, peptides and proteins may interact with a variety of active sites occurring on their inner surface exposed to the BGE, which comprise inert siloxane bridges, hydrogen bonding sites and different types of ionizable silanol groups (vicinal, geminal, and isolated) [26]. These interactions are expected to cause peak broadening and asymmetry, irreproducible migration times, low mass recovery, and, in some cases, irreversible adsorption. The most popular methods employed to control direction and velocity of EOF and to minimize the untoward interactions of peptides and proteins with the capillary wall is coating the inner surface of the capillary tube, either by permanent or dynamic processes [2,27]. Common alternative approaches include the use of electrolyte solutions at the extreme of the pH scale and/or at increased ionic strength, either using concentrated buffers or incorporating a suitable additive into the BGE.

Permanent and dynamic coatings have the effect of deactivating the original interacting groups on the inner wall of the separation channel by either converting them to inert hydrophilic moieties or shielding them with the coating material. Recent advancements and emerging trends in capillary coatings, both covalently bonded and either permanently or reversibly adsorbed, have been recently illustrated and discussed [2,27–31] and are not reviewed in this paper. However, it is worth noting that a variety of untoward interactions, including hydrogen-bonding and hydrophobic interactions, may also occur in capillaries coated with non-charged material, leading to poor separation performance. Therefore, also for coated capillaries, either neutral or charged, the influence of pH, ionic strength and BGE composition on potential interactions of peptides and proteins with the capillary wall must be considered.

The effect of ionic strength on EOF of coated capillaries was recently reported for fused-silica capillaries covalently modified by the cationic copolymer poly(acrylamide-co-(3-acrylamidopropyl) trimethylammonium chloride) (PAMAPTAC), containing variable ratios of the charged monomer and displaying anodic EOF [30]. The study was carried out with BGEs consisting of sodium phosphate buffer (pH 2.5) at various concentrations, ranging from 10 to 100 mM. The electroosmotic flow decreased with increasing ionic strength, in accordance with the theoretical prediction that EOF is inversely proportional to the square route of ionic strength (Gouy-Chapman-Stern-Grahame model of the electric double layer) [5,6]. Similar results were reported for a noncovalently bounded coating designed to provide a low to moderate EOF and used for CZE analysis of peptides with mass spectrometric detection [31]. The influence of ionic strength on EOF was investigated using BGEs consisting of 3:1 (v/v) acetic acid-formic acid mixtures, each at concentration either 1 M or 2 M. As expected, lower EOF was observed with the BGE at higher ionic strength.

Suppression of EOF and prevention of wall adsorption are also performed by incorporating a suitable additive into the electrolyte solution. These additives may act either as masking or competing agents for the silanol groups on the inner wall of bare fused-silica capillaries, avoiding their availability for electrostatic interactions with positively charged proteins and peptides, while affecting the zeta potential at the solid-liquid interface and altering EOF. Compounds with such properties fall into the family of dynamic coating agents that have been discusses in previous review articles [2,27]. Others additives may function as ion-pairing or competing agents for the basic amino acid moieties of the peptides and proteins exposed to BGE, subtracting their availability for the untoward interactions with the capillary wall [32]. Most of these additives also affect selectivity and resolution, as it is discussed in section 4.

4. Enhancement of selectivity and resolution

Selectivity in CZE depends on differences in the electrophoretic mobility of the analytes and, consequently, on their effective charge-to-hydrodynamic radius ratio. Therefore, the selective separation of peptides and proteins is affected by factors that influence their electrophoretic mobility. They include temperature, pH and composition of BGE, and the interactions of the analyzed biomolecules with the sample matrix, the capillary wall and the components of BGE (see Fig. 2). These parameters, also influence efficiency and EOF, which is expected to improve resolution by strengthening the effect of the differences in the electrophoretic mobility of the analyzed peptides and proteins.

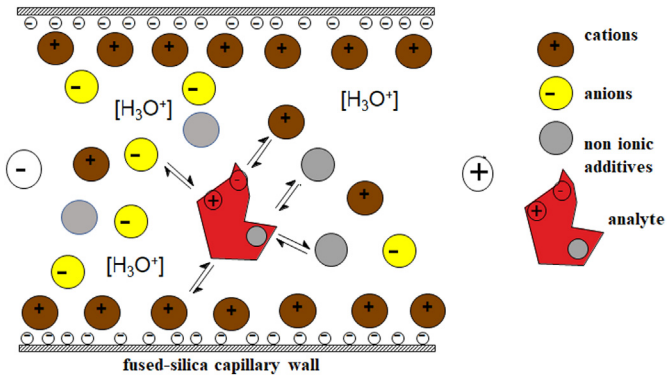

Fig. 2. Schematic representation of the interactions occurring between the components of BGE and the analytes inside a bare fused-silica capillary column.

Besides buffering agents and the variety of compounds that are employed for the dynamic capillary wall coatings [27], a variety of chemicals have been proposed as additives of BGE to enhance selectivity and resolution in peptide and proteins CZE [33,34]. Among them, ionic liquids (IL), diluted in aqueous solutions and no used as pure solvents, have received increasing interest as both dynamic coating agents and BGE additives to enhance selectivity and resolution in CZE [35,36].

The ionic liquids 1-ethyl-3-methylimidazolium tetrafluoroborate ([emim][BF4]) and 1-butyl-3-methylimidazolium tetrafluoroborate ([bmim][BF4]) were recently used as dynamic coating agents and as BGE components for the separation of the standard proteins cytochrome *c*, lysozyme, myoglobin, trypsin, and apo-transferrin, as well as for the separation of proteins in real biological samples (chicken egg white and human tears) [37]. The study evidenced the reversal of the direction of EOF from cathodic to anodic, indicative of the adsorption onto the capillary wall of the cationic constituent of IL, and a significant contribution of [emim][BF4] and [bmim][BF4] to separation performance and selectivity that the authors attributed to electrostatic and hydrogen bond interactions between proteins and the ionic-liquid components.

Similar results were obtained by Jiang et al. [38] who reported the separation of basic proteins in fused silica capillaries dynamically coated with 1-alkyl-3-methylimidazolium-based ionic liquids, whose aqueous solutions, at concentration ranging from 30 to 110 mM, were also used as BGE. Under these conditions, the direction of EOF was reversed from cathodic to anodic and the observed efficient separation of proteins was attributed to the electrostatic repulsion of the positively charged proteins by the positively charged capillary wall, without excluding the occurrence of non-electrostatic interactions of the analytes with the IL, either in solution or adsorbed onto the capillary wall.

In another study, bare fused silica capillaries dynamically coated with three 1-alkyl-3-methylimidazolium tetrafluoroborate ionic liquids, differing from each other by the length of the alkyl group on the imidazolium cation, were employed for the co-electroosmotic separation of basic model proteins using acetate buffer solutions at pH 4.0 as the BGE, either without or with the incorporation of the IL at concentrations ranging from 0.2 to 6.0 mM [39]. The ionic strength of BGE was maintained at a constant value in all experiments in order to level off its contribution to both EOF and electrophoretic mobility of proteins. IL-coated capillaries exhibited lower (but still cathodic) EOF and better protein peak shape than that observed with the bare fused-silica capillary. Upon incorporating the IL into BGE, peak shape and resolution varied to different extents depending on type and concentration of IL. The observed different variations of resolution and peak shape were attributed to a combination of selective electrostatic and hydrophobic interactions between the proteins and the three 1-alkyl-3-methylimidazolium ionic liquids, which appeared to be influenced by the length and, consequently, by the hydrophobicity of the alkyl chain bonded to the imidazolium ring of the different ILs.

Guo et al. [40] reported the successful separation of basic proteins in a bare fused-silica capillary using the ionic liquid N-methyl-2-pyrrolidonium methyl sulfonate as an additive incorporated at low concentration (0.02%, w/v) into the BGE, consisting of 40 mM Na_2HPO_4–H_3PO_4 solution at pH 4.0. The study evaluated the dependence of separation performance on concentration and pH of the phosphate-based BGE, which were varied within the ranges 20–50 mM and pH 2.0–6.0, respectively. It was concluded that the ionic liquid established both hydrogen bonding and electrostatic interactions with the capillary wall, whereas hydrogen bonding, ion-dipole/ion-induced-dipole, and hydrophobic interactions were hypnotized to occur between proteins and ionic liquid, with the result of influencing selectivity and resolution.

The synergistic effect of chiral ionic liquids composed of tetraalkylammonium ions and the amino acids Asn, Asp or Pro on the enantio-separations of dipeptides in capillary electrophoresis, mediated by β-cyclodextrin (β-CD) and 2-hydroxypropyl-β-cyclodextrin (HP-β-CD) was recently investigated too [41]. The study evidenced that the incorporation of an amino acid-derived chiral ionic liquid into the BGE containing either β-CD or HP- β-CD at pH 2.5 and 3.5 led to a concentration-dependent increase in the resolution of the dipeptide enantiomers.

Other studies have investigated the contribution to selectivity and resolution given by either the cationic or the anionic component of the buffer, as a consequence of their interactions with peptides and proteins, in addition to their effect on EOF. The dependence of EOF and separation performance on borate buffer, containing as the counterion a basic polyol, such as tris(hydroxymethyl)aminomethane (Tris) or 1,3-bis(tris(hydroxymethyl) methylamino)propane (Bis-Tris propane), was recently described by Dolnik [34]. The study attributed the observed variations of EOF to the strong interactions of boric acids with both the inner surface of bare fused-silica capillaries and the basic polyol counterions. Borate ions were also expected to interact with the carbohydrate moieties of ovalbumin isoforms, which were separated into at least five major peaks using 200 mM Bis-Tris propane and 400 mM boric acid (pH 7.2) as the BGE.

An example of how apparently slight dissimilarities in the BGE composition can have a strong impact on EOF and separation performance is depicted by the CZE separation of protein tryptic digests obtained with two tetraborate-based buffers, in which either sodium or barium was the counterion [42]. This study, carried out at alkaline pH, evidenced that tetraborate buffer, in which the typical sodium counterion was replaced by barium, caused the reversal of the EOF from cathodic to anodic. This effect was ascribed to the binding of barium cations to ionized silanol groups, with consequent variation of zeta potential and inhibition of peptide adsorption onto the capillary wall, evidenced by their sharp and symmetric peaks.

The dependence of electrophoretic behavior of basic proteins and closely related decapeptides on the anionic component of buffers was investigated using a polyacrylamide coated fused-silica capillary (suppressed EOF) and, as BGE, three low conductivity buffers consisting of the aliphatic tetramine triethylenetetramine (TETA) as the common cation, and either phosphate or perchlorate or citrate as the different negatively charged counterion [24]. All buffers used as BGE were prepared at pH 4.0 with same concentration (50 mM) and ionic strength (136 mM). The occurrence of selective interactions between the analytes and the buffer anions was evidenced by remarkable differences in the migration times and migration order, which were ascribed to specific interactions between the analytes and either the phosphate, perchlorate, or citrate ions, such as ion-pair formation. Discriminating interactions were also described for other anionic components of low conductively buffers, such as formic, acetic, and trifluoroacetic acid [43] and for additives incorporated into the BGE to enhance selectivity, which, among other, included cyclodexitrins [44], ion-pairing agents [45], and aprotic-dipolar solvents (N,N-dimethylacetamide and N,N-dimethylformamide) [46].

5. Compatibility with mass spectrometry

Mass spectrometry plays a fundamental role in the characterization of therapeutic and diagnostic peptides and proteins and in peptidomics and proteomics studies [47]. Hence, an additional aspect to be considered in selecting the proper composition of BGE is its compatibility with the ionization sources employed for the online hyphenation of capillary zone electrophoresis with mass

spectrometry (CZE-MS), generally performed using electrospray ionization (ESI) with either sheathless flow interface or sheath flow interface, which complete the electrical circuit for CZE separation and provide voltage for ESI [48,49].

Technical aspects and pros and cons of sheath flow and sheathless interfaces have been illustrated and discussed in several review articles [50,51]. It is worthy of attention the sample dilution occurring in the sheath flow interface due to the addition of the sheath liquid, causing a potential loss in sensitivity, which is the main disadvantage of this interface. However, this drawback is compensated by the possibility of improving both spray and ionization processes by the proper selection of the sheath liquid. On the other hand, in the sheathless interface no-sample dilution occurs, as the BGE is the only liquid in the system involved in the separation, vaporization and ionization of the analytes. Therefore, in this interface spray properties and sample ionization cannot be tuned by an auxiliary liquid and the composition of the BGE must be suitable for both CZE separation and ESI-MS detection.

BGEs containing volatile buffers are requested to prevent the contamination of ESI and to facilitate the ionization process and evaporation of droplets. Most of the methods for peptide and proteins CZE-ESI-MS employ both coated and uncoated capillaries and BGEs consisting of either aqueous solutions or water-organic solvent mixtures of volatile electrolytes, such as formic and acetic acid and their ammonium salts, or volatile alkylamine salts. The use of ammonium hydrogen carbonate is generally not recommended because of the potential gas bubbles formation. Also common is the approach of controlling the protonic equilibrium by incorporating into the BGE a pure acid or base, instead than a true buffer. Recent examples of this approach include the analysis of intact proteins [52], a proteomics study of thin zebrafish brain tissue sections [53], and a large-scale top-down delineation of histone proteoforms [54], which were performed with aqueous BGEs consisting of 1.0 M formic acid, 10% (v/v) acetic acid, and 5% (v/v) acetic acid, respectively. Since high acid concentrations might lead to low detection sensitivity, due to signal suppression, all BGEs in the above examples were diluted by the sheath liquid before entering the ionization interface, which is a common option to minimize the concentrations of BGE components interfering with the ionization process and/or the MS detection.

The incorporation of an organic solvent into BGE (mainly methanol or isopropanol) can have a beneficial effect on the ionization process and allow the use of BGE and sheath flow of identical composition. Moreover, organic solvents alter permittivity, viscosity, zeta potential, and conductivity of BGE, in addition to influence the ionization of peptides and proteins, with consequent impact on their electrophoretic mobility and, therefore, on separation selectivity and/or efficiency and resolution. Mixtures of water and the aprotic dipolar organic solvents N,N-dimethylacetamide (DMA) and N,N-dimethylformamide (DMF) were investigated as BGEs for peptide CZE-MS [46,55]. These studies evidenced that BGEs consisting of DMA or DMF in water (up to 20%, v/v), containing either acetic or formic acid, were suitable to perform CZE-MS peptide mapping of either a monoclonal antibody [55] or a recombinant IgG1 protein conjugated to a highly hydrophobic pyrrolobenzodiazepine dimer [46], both used as therapeutic proteins. The enhanced selectivity observed by incorporating either DMA or DMF into BGE was ascribed to the ability of these organic solvents to affect peptide selectivity through differential changes in the pKa of the analyzed peptides produced by proteolytic digestion.

The hyphenation of MS with nonaqueous capillary electrophoresis (NACE-MS) is an alternative approach that uses BGEs consisting of solutions of volatile electrolytes in organic solvents, which offer a wide range of physicochemical parameters, such as viscosity, dielectric constant and polarity, that influence EOF and electrophoretic mobility and solubility of the analytes to different extents [56]. Moreover, due to their low surface tension, volatile organic solvents are expected to form stable ESI sprays [57]. However, the low solubility of most peptides and proteins in organic solvents limits the application of NACE-MS for the separation and characterization of these biopolymers. Exceptions include the separation of temporins, a family of natural bioactive highly hydrophobic peptides, which was obtained by NACE using a bare fused-silica capillary and BGE consisting of 78% (v/v) methanol, 20% (v/v) acetonitrile, and 2% (v/v) formic acid containing 20 mM ammonium formate [58].

Further requirements for the proper selection of BGE composition might be requested by the on-line preconcentration method frequently needed to increase the number of peptides and proteins that can be identified in diluted samples, conventionally injected in amounts lower than 1% of the total capillary column volume (i.e. ~10 nL). Among the current preconcentration methods described in literature, those based on discontinuous BGE systems, such as field-amplified sample stacking (FASS) and dynamic pH junction, are the most simple and practical and are widely employed for peptide and protein CZE either with MS or UV detection [59,60]. An overview of current on-line preconcentration techniques employed in capillary electrophoresis of complex samples is reported in the recent review article by Jarvas et al. [60].

The field-amplified sample stacking preconcentration technique uses conductivity gradients generated into the capillary, filled with a high conductive BGE, and is performed by hydrodynamically injecting the sample dissolved in a low-conductivity solution and using a high conductivity BGE. As a result, the electrophoretic mobility of peptides and proteins in the sample plug is higher than in BGE, causing the sample analytes to be focused at sample plug/BGE boundaries, as it is depicted in Fig. 3.

The dynamic pH junction method is performed by establishing a pH discontinuity in the capillary, which can be obtained by hydrodynamically injecting the sample dissolved in a basic electrolyte solution and carrying out the separation using an acidic BGE. The application of a positive potential across the capillary causes the

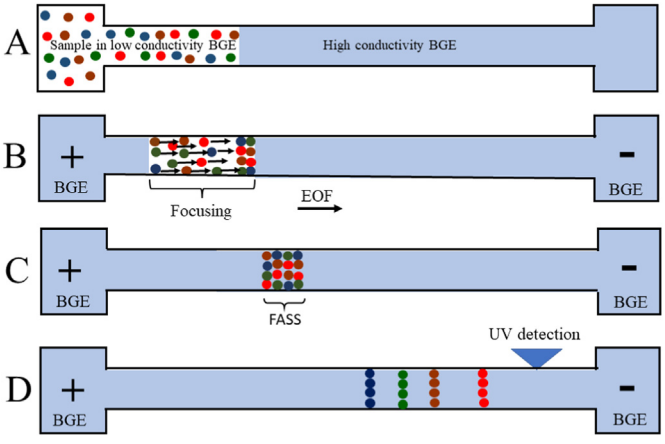

Fig. 3. Scheme of field-amplified sample staking (FASS) technique for on-line preconcentration of diluted peptide and protein samples in capillary zone electrophoresis. A: a long plug of sample, solubilized in a low conductivity solution, is introduced by hydrodynamic injection into the bare fused-silica capillary, which is filled with a high conductivity BGE. B and C: upon application of a high positive voltage, the analytes migrate faster in the sample plug than in BGE, due to the higher electric field developed in the low conductivity solution and are focused into narrow zones at the boundaries with the high conductivity BGE (front and rear boundaries, depending on the analyte charge). D: the concentrated analytes are then separated in the remaining length of the capillary according to their electrophoretic mobility in the high conductivity BGE (negatively charged analyte migrate against EOF).

migration of the negatively charged analytes toward the anode, where they come in contact with the acidic BGE, acquiring positive charge and, therefore, focusing at the boundary between the acidic BGE and the basic sample electrolyte solution (see Fig. 4). The dynamic pH junction preconcentration method can also be performed in low pH sample electrolyte and high pH BGE mode [61].

Recently, Zhang et al. [62] identified over 4400 phosphopeptides by CZE–ESI–MS/MS from a 220 ng sample, which was enriched by on-line dynamic pH junction pre-concentration method, using 30 mM ammonium bicarbonate (pH 8.2) as the sample electrolyte and 1 M acetic acid as the BGE. Large sample volume capacity (1 μL) and high peak capacity (~280) were obtained for a dynamic pH junction-based CZE-MS/MS method, which used 50 mM ammonium bicarbonate (pH 8.0) as the sample buffer and 5% (v/v) acetic acid as the BGE [63]. This paper also reported a comparison between on-line FASS and dynamic pH junction pre-concentration methods, showing that the dynamic pH junction method allowed larger sample loading and better separation of proteins than FASS method.

6. Conclusions and future perspectives

Composition and pH of the electrolyte solution are the most critical parameters for the optimization of capillary electrophoretic methods for a given separation problem. This is particularly true for the separation of complex multifunctional molecules, such as peptides and proteins, whose electrophoretic properties strongly depend on protonic equilibrium and on a variety of interactions that these biopolymers can establish with the capillary wall and with the chemicals comprising both BGE and sample solution. Presently, the selection of all components of BGE, as well as the optimization of pH and the other electrophoretic experimental conditions, depend on human experience and the majority of CZE methods are optimized by the "one factor at time" (OFAT) approach, which is performed by varying an experimental factor while the others are kept constant. The optimization of CZE methods by OFAT requires a relatively large number of experiments and does not permit to evaluate the interactions between experimental factors, leading to the insufficient understanding of multiparameter interaction effects and possible poorly optimized methods.

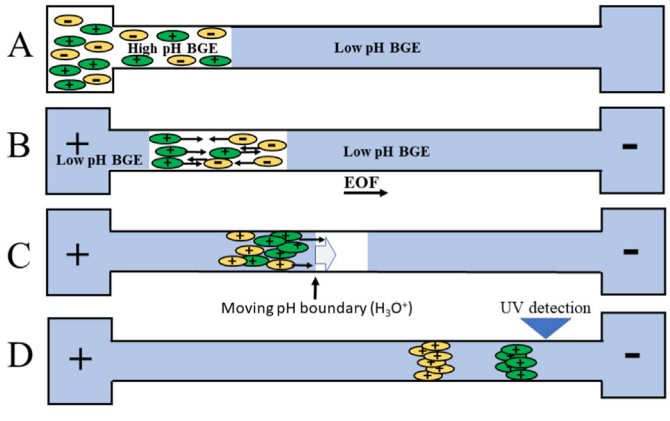

Fig. 4. Scheme of dynamic pH junction technique for on-line preconcentration of diluted peptide or protein samples in capillary zone electrophoresis. A: a relatively large volume of sample, dissolved in a high-pH solution, is introduced (by pressure) into a bare fused-silica capillary, which is filled with a low-pH BGE. B: after the introduction into the capillary of a plug of the low-pH BGE, a positive high voltage is applied across the capillary, causing the migration of the negatively charged analytes toward the anode, where they come in contact with the acidic BGE, acquiring positive charge and, therefore, inverting their migration toward the cathode. C: the acidic BGE titrate the sample solution and all analytes with pI higher than the acidic BGE acquire positive charge. D: the focused analytes migrate toward the cathode according to CZE separation mechanism.

Design of experiment (DoE) techniques, which use statistical tools for designing experiments and mathematical modelling, are a valuable tool to optimize analytical methods, including those based on high performance liquid chromatography (HPLC) and capillary electrophoresis separations [64–66]. Recent applications of DoE approaches for the optimization of CZE methods for peptides and proteins separations comprise the protein profiling of peanut flour [33], the separation of proteins in chicken egg white and human tears samples [37], and the separation of insulin analogs in pharmaceutical preparations [67]. DoE techniques are expected to gain increasing acceptance in capillary electrophoresis as a powerful tool for the development of robust analytical methods, of paramount importance for the characterization of biotherapeutic products, and for the evaluation of interactions between the main factors that affect selectivity and separation performance of peptide and protein CZE.

Funding

This research did not receive any specific grant from funding agencies in the public, commercial, or not-for-profit sectors.

Declaration of competing interest

I declare that I have no known competing financial interests or personal relationships that could have appeared to influence the work reported in this paper. I also declare that the research did not receive any specific grant from funding agencies in the public, commercial, or not-for-profit sector.

Data availability

No data was used for the research described in the article.

References

[1] R. Kumar, A. Guttman, A.S. Rathore, Applications of capillary electrophoresis for biopharmaceutical product characterization, Electrophoresis 43 (2022) 143–166. https://doi.org/10.1002/elps.202100182.
[2] S. Štěpánová, V. Kašička, Applications of capillary electromigration methods for separation and analysis of proteins (2017-mid 2021)-A review, Anal. Chim. Acta 1209 (2022), e339447. https://doi.org/10.1016/j.aca-2022.339447.
[3] V. Kašička, Peptide mapping of proteins by capillary electromigration methods, J. Separ. Sci. 45 (2022) 4245–4279. https://doi.org/10.1002/jssc.202200664.
[4] H. Kaur, J. Beckman, Y.T. Zhang, Z.J. Li, M. Szigeti, A. Guttman, Capillary electrophoresis and the biopharmaceutical industry: therapeutic protein analysis and characterization, TrAC, Trends Anal. Chem. 144 (2021), e116407. https://doi.org/10.1016/jtrac.2021.116407.
[5] F. Foret, L. Křivánková, P. Boček, Capillary Zone Electrophoresis, VCH Verlagsgesellshaft mbH, Weinheim, 1993.
[6] D. Corradini, Capillary electromigration techniques, in: D. Corradini, T.M. Phillips (Editors), Handbook of HPLC –, second ed., CRC Press, Boca Raton, 2010, pp. 155–206.
[7] X. Ou, P. Chen, X. Huang, S. Li, B.-F. Liu, Microfluidic chip electrophoresis for biochemical analysis, J. Separ. Sci. 43 (2020) 258–270. https://doi.org/10.1002/jssc.201900758.
[8] J.P. Smithers, M.A. Hayes, Interfacing microfluidics with information-rich detection systems for cells, bioparticles, and molecules, Anal. Bioanal. Chem. 414 (2022) 4575–4589. https://doi.org/10.1007/s00216-022-04043-1.
[9] I. Mikšík, Coupling of CE-MS for protein and peptide analysis, J. Separ. Sci. 42 (2019) 385–397. https://doi.org/10.1002/jssc.201800817.
[10] M. Morani, M. Taverna, T.D. Mai, A fresh look into background electrolyte selection for capillary electrophoresis-laser induced fluorescence of peptides and proteins, Electrophoresis 40 (2019) 2618–2624.
[11] S. Bekri, L. Leclercq, H. Cottet, Influence of the ionic strength of acidic background electrolytes on the separation of proteins by capillary electrophoresis, J. Chromatogr. A 1432 (2016) 145–151. https://doi.org/10.1016/j.chroma.2015.12.060.
[12] T. Novotný, B. Gaš, Electrolysis phenomena in electrophoresis, Electrophoresis 41 (2020) 536–544. https://doi.org/10.1002/elps.201900411.

[13] A.V. Stoyanov, J. Pawliszyn, Buffer composition changes in background electrolyte during electrophoretic run in capillary zone electrophoresis, Analyst 129 (2004) 979–982. https://doi.org/10.1039/B406307D.
[14] A. Oki, Y. Takamura, Y. Ito, Y. Horiike, pH change of buffer solution in a microcapillary chip and its suppression, Electrophoresis 23 (2002) 2860–2864. https://doi.org/10.1109/JSSC.2002.801174.
[15] M.A. Kelly, K.D. Altria, B.J. Clark, Approaches used in the reduction of buffer electrolysis effects for routine capillary electrophoresis procedures in pharmaceutical analysis, J. Chromatogr. A 768 (1997) 73–80. https://doi.org/10.1016/S0021-9673(97)00054-X.
[16] D.P. de Jesus, J.G.A. Brito-Neto, E.M. Richter, L. Angnes, I.G.R. Gutz, C.L. do Lago, Extending the lifetime of the running electrolyte in capillary electrophoresis by using additional compartments for external electrolysis, Anal. Chem. 77 (2005) 607–614. https://doi.org/10.1021/ac0486645.
[17] P.G. Righetti, C. Gelfi, A. Bossi, E. Olivieri, L. Castelletti, B. Verzola, A.V. Stoyanov, Capillary electrophoresis of peptides and proteins in isoelectric buffers: an update, Electrophoresis 21 (2000) 4046–4053. https://doi.org/10.1002/1522-2683(200012)21:18<4046::AID-ELPS4046>3.0.CO;2-5.
[18] P. Kuba, P.C. Hauser, 20th anniversary of axial capacitively coupled contactless conductivity detection in capillary electrophoresis, TrAC, Trends Anal. Chem. 102 (2018) 311–321. https://doi.org/10.1016/j.trac.2018.03.007.
[19] H. Cottet, H. Wu, S.A. Allison, On the ionic strength dependence of the electrophoretic mobility: from 2D to 3D slope-plots, Electrophoresis 38 (2017) 624–632. https://doi.org/10.1002/elps.201600329.
[20] S.A. Allison, C. Perrin, H. Cottet, Modeling the electrophoresis of oligolysines, Electrophoresis 32 (2011) 2788–2796. https://doi.org/10.1002/elps.201100006.
[21] J.-M. Busnel, M.-C. Hennion, G. Peltre, Carrier ampholytes as potential buffers in electrophoresis: physico-chemical study, J. Chromatogr. B 818 (2005) 99–107. https://doi.org/10.1016/j.chromb.2004.09.036.
[22] J.-M. Busnel, F. Kilár, V. Kašička, S. Descroix, M.-C. Hennion, G. Peltre, Carrier ampholytes-based capillary electrophoresis as an alternative to capillary zone electrophoresis in classical background electrolytes, J. Chromatogr. A 1087 (2005) 183–188. https://doi.org/10.1016/j.chroma.2005.03.109.
[23] V. Šolínová, M. Poitevin, D. Koval, J.-M. Busnel, G. Peltre, V. Kašička, Capillary electrophoresis in classical and carrier ampholytes-based background electrolytes applied to separation and characterization of gonadotropin-releasing hormones, J. Chromatogr. A 1267 (2012) 231–238. https://doi.org/10.1016/j.chroma.2012.07.059.
[24] D. Corradini, E. Cogliandro, L. D'Alessandro, I. Nicoletti, Influence of electrolyte composition on the electroosmotic flow and electrophoretic mobility of proteins and peptides, J. Chromatogr. A 1013 (2003) 221–232. https://doi.org/10.1016/S0021-9673(03)01496-1.
[25] D. Corradini, L. Bevilacqua, I. Nicoletti, Separation of basic proteins in bare fused-silica capillaries with diethylentriamine phosphate buffer as the background electrolyte solution, Chromatographia 62 (2005) S43–S50. https://doi.org/10.1365/s10337-005-0579-7.
[26] C. Senn, P.J. Pigram, J. Liesegang, Surface electrical resistivity and wettability study of fused silica, Surf. Interface Anal. 27 (1999) 835–839. https://doi.org/10.1002/(SICI)1096-9918(199909)27:9<835::AID-SIA642>3.0.CO;2-T.
[27] L. Hajba, A. Guttman, Recent advances in column coatings for capillary electrophoresis of proteins, TrAC, Trends Anal. Chem. 90 (2017) 38–44. https://doi.org/10.1016/j.trac.2017.02.013.
[28] M. Meixner, M. Pattky, C. Huhn, Novel approach for the synthesis of a neutral and covalently bound capillary coating for capillary electrophoresis-mass spectrometry made from highly polar and pH-persistent N-acryloylamido ethoxyethanol, Anal. Bioanal. Chem. 412 (2020) 561–575. https://doi.org/10.1007/s00216-019-02286-z.
[29] S. Meyer, D. Clases, R.G. de Vega, M.P. Padula, P.A. Doble, Separation of intact proteins by capillary electrophoresis, Analyst 147 (2022) 2988–2996. https://doi.org/10.1039/d2an00474g.
[30] R. Konásová, M. Butnariu, V. Solínová, V. Kašička, D. Koval, Covalent cationic copolymer coatings allowing tunable electroosmotic flow for optimization of capillary electrophoretic separations, Anal. Chim. Acta 1178 (2021), e338789. https://doi.org/10.1016/j.aca.2021.338789.
[31] M. Pattky, C. Huhn, Advantages and limitations of a new cationic coating inducing a slow electroosmotic flow for CE-MS peptide analysis: a comparative study with commercial coatings, Anal. Bioanal. Chem. 405 (2013) 225–237. https://doi.org/10.1007/s00216-012-6459-84.
[32] D. Corradini, Buffer additives other than the surfactant sodium dodecyl sulfate for protein separations by capillary electrophoresis, J. Chromatogr. B 699 (1997) 221–256. https://doi.org/10.1016/S0378-4347(97)00301-0.
[33] L. Villemet, A. Cuchet, C. Desvignes, C.E. Sänger-van de Griend, Protein mapping of peanut extract with capillary electrophoresis, Electrophoresis 43 (2022) 1027–1034. https://doi.org/10.1002/elps.202100004.
[34] V. Dolnik, Borate-containing background electrolytes to improve CE separation in bare capillaries, Electrophoresis 41 (2020) 1073–1080. https://doi.org/10.1002/elps.201900470.
[35] S. Krait, M.-L. Konjaria, G.K.E. Scrib, Advances of capillary electrophoresis enantio-separations in pharmaceutical analysis (2017–2020), Electrophoresis 42 (2021) 1709–1725. https://doi.org/10.1002/elps.202000359.
[36] P.Y. Quintas, E.F. Fiorentini, M. Llaver, R.E. Gonz, R.G. Wuilloud, State-of-the-art extraction and separation of enantiomers through the application of alternative solvents, TrAC, Trends Anal. Chem. 157 (2022), e116733. https://doi.org/10.1016/j.trac.2022.116733.
[37] E. Mező, C. Páger, L. Makszin, F. Kilár, Capillary zone electrophoresis of proteins applying ionic liquids for dynamic coating and as background electrolyte component, Electrophoresis 41 (2020) 2083–2091. https://doi.org/10.1002/elps.202000204.
[38] T.F. Jiang, Y.L. Gu, B. Liang, J.B. Li, Y.P. Shi, Q.Y. Ou, Dynamically coating the capillary with 1-alkyl-3-methylimidazolium-based ionic liquids for separation of basic proteins by capillary electrophoresis, Anal. Chim. Acta 479 (2003) 249–254. https://doi.org/10.1016/S0003-2670(02)01537-4.
[39] D. Corradini, I. Nicoletti, G.K. Bonn, Co-electroosmotic capillary electrophoresis of basic proteins with 1-alkyl-3-methylimidazolium tetrafluoroborate ionic liquids as non-covalent coating agents of the fused-silica capillary and additives of the electrolyte solution, Electrophoresis 30 (2009) 1869–1876. https://doi.org/10.1002/elps.200800447.
[40] X.-F. Guo, H.-Y. Chen, X.-H. Zhou, H. Wang, H.-S. Zhang, N-methyl-2-pyrrolidonium methyl sulfonate acidic ionic liquid as a new dynamic coating for separation of basic proteins by capillary electrophoresis, Electrophoresis 34 (2013) 3287–3292. https://doi.org/10.1002/elps.201300369.
[41] M.-L. Konjaria, G.K.E. Scriba, Effects of amino acid-derived chiral ionic liquids on cyclodextrin-mediated capillary electrophoresis enantioseparations of dipeptides, J. Chromatogr. A 1652 (2021), e462342. https://doi.org/10.1016/j.chroma.2021.462342.
[42] M.E. Mendieta, P. Antonioli, P.G. Righetti, A. Citterio, S. Descroix, R. Sebastiano, Effect of barium tetraborate on the separation of tryptic digests of proteins by zone electrophoresis in uncoated capillaries, Electrophoresis 27 (2006) 4016–4024. https://doi.org/10.1002/elps.200600054.
[43] D. Corradini, A. De Rossi, I. Nicoletti, Interactions of proteins with the acidic components of the electrolyte solution and their role in the performance of separations by CZE, Chromatographia 73 (2011) S103–S111. https://doi.org/10.1007/s10357-011-2018-2.
[44] A.S. Rathore, Cs Horváth, Cyclodextrins as selectivity enhancers in capillary zone electrophoresis of proteins, Electrophoresis 19 (1998) 2285–2289. https://doi.org/10.1002/elps.1150191306.
[45] J. Charvatova Miksik, A. Eckhardt, T. Cserhati, E. Forgacs, Z. Deyl, Capillary electrophoretic separation of proteins and peptides by ion-pairing with heptanesulfonic acid, J. Chromatogr. B 800 (2004) 161–167. https://doi.org/10.1016/j.jchromb.2003.09.041.
[46] O.O. Dada, Y. Zhao, N. Jaya, O. Salas-Solano, High resolution capillary zone electrophoresis with mass spectrometry peptide mapping of therapeutic proteins: improved separation with mixed aqueous-aprotic dipolar solvents (N,N-dimethylacetamide and N,N-dimethylformamide) as the background electrolyte, Anal. Chem. 89 (2017) 11227–11235. https://doi.org/10.1021/acs.analchem.7b03405.
[47] X. Shen, Z. Yang, E.N. McCool, R.A. Lubeckyj, D. Chen, L. Sun, Capillary zone electrophoresis-mass spectrometry for top-down proteomics, TrAC, Trends Anal. Chem. 120 (2019), e115644. https://doi.org/10.1016/j.trac.2019.115644.
[48] Z. Zhang, Y. Qu, N.J. Dovichi, Capillary zone electrophoresis-mass spectrometry for bottom-up proteomics, TrAC, Trends Anal. Chem. 108 (2018) 23–37. j.trac.2019.115644.
[49] F.P. Gomes, J.R. Yates III, Recent trends of capillary electrophoresis-mass spectrometry in proteomics research, Mass Spectrom. Rev. 38 (2019) 445–460. https://doi.org/10.1002/mas.21599.
[50] S. Štěpánová, V. Kašička, Recent developments and applications of capillary and microchip electrophoresis in proteomics and peptidomics (mid-2018–2022), J. Separ. Sci. (2023), e2300043. https://doi.org/10.1002/jssc.202300043.
[51] D. Chen, E.N. McCool, Z. Yang, X. Shen, R.A. Lubeckyj, T. Xu, Q. Wang, L. Sun, Recent advances (2019–2021) of capillary electrophoresis-mass spectrometry for multilevel proteomics, Mass Spectrom. Rev. 42 (2023) 617–642. https://doi.org/10.1002/mas.21714.
[52] N. Hamidli, M. Andrasi, C. Nagy, A. Gaspar, Analysis of intact proteins with capillary zone electrophoresis coupled to mass spectrometry using uncoated and coated capillaries, J. Chromatogr. A 1654 (2021), e462448. https://doi.org/10.1016/j.chroma.2021.462448.
[53] R.A. Lubeckyj, L.L. Sun, Laser capture microdissection-capillary zone electrophoresis-tandem mass spectrometry (LCM-CZE-MS/MS) for spatially resolved top-down proteomics: a pilot study of zebrafish brain, Mol. Omics 18 (2022) 112–122. https://doi.org/10.1039/d1mo00335f.
[54] D. Chen, Z. Yang, X. Shen, L. Sun, Capillary zone electrophoresis-tandem mass spectrometry as an alternative to liquid chromatography-tandem mass spectrometry for top-down proteomics of histones, Anal. Chem. 93 (2021) 4417–4424. https://doi.org/10.1021/acs.analchem.0c04237.
[55] O.O. Dada, Y.M. Zhao, N. Jaya, O. Salas-Solano, High-resolution capillary zone electrophoresis with mass spectrometry peptide mapping of therapeutic proteins: peptide recovery and post-translational modification analysis in monoclonal antibodies and antibody–drug conjugates, Anal. Chem. 89 (2017) 11236–11242. https://doi.org/10.1021/acs.analchem.7b03643.
[56] E. Kendler, A critical overview of non-aqueous capillary electrophoresis. Part I: mobility and separation selectivity, J. Chromatogr. A 1335 (2014) 16–30. https://doi.org/10.1016/j.chroma.2014.01.010.
[57] K.E. Scriba, Nonaqueous capillary electrophoresis–mass spectrometry, J. Chromatogr. A 1159 (2007) 28–41. https://doi.org/10.1016/j.chroma.2007.02.005.
[58] J. Cheng, D.D.Y. Chen, Nonaqueous capillary electrophoresis mass spectrometry method for determining highly hydrophobic peptides, Electrophoresis 39 (2018) 1216–1221. https://doi.org/10.1002/elps.201700364.

[59] H. Wu, K. Tang, Highly sensitive and robust capillary electrophoresis-electrospray ionization-mass spectrometry: interfaces, preconcentration techniques and applications, Rev. Anal. Chem. 39 (2020) 45–55. https://doi.org/10.1515/revac-2020-0112.
[60] G. Jarvas, A. Guttman, N. Miękus, T. Bączek, S. Jeong, D.S. Chung, V. Pätoprstý, M. Masár, M. Hutta, V. Datinská, F. Foret, Practical sample pretreatment techniques coupled with capillary electrophoresis for real samples in complex matrices, TrAC, Trends Anal. Chem. 122 (2020), e115702. https://doi.org/10.1016/j.trac.2019.115702.
[61] M.R.N. Monton, K. Imami, M. Nakanishi, J.-B. Kim, S. Terabe, Dynamic pH junction technique for on-line preconcentration of peptides in capillary electrophoresis, J. Chromatogr. A 1079 (2005) 266–273. https://doi.org/10.1016/j.chroma.2005.03.069.
[62] Z. Zhang, A.S. Hebert, M.S. Westphall, J.J. Coon, N.J. Dovichi, Single-shot capillary zone electrophoresis–tandem mass spectrometry produces over 4400 phosphopeptide identifications from a 220 ng sample, J. Proteome Res. 18 (2019) 3166–3173. https://doi.org/10.1021/acs.jproteome.9b00244.
[63] R.A. Lubeckyj, E.N. McCool, X. Shen, Q. Kou, X. Liu, L. Sun, Single-shot top-down proteomics with capillary zone electrophoresis-electrospray ionization-tandem mass spectrometry for identification of nearly 600 escherichia coli proteoforms, Anal. Chem. 89 (2017) 12059–12067. https://doi.org/10.1021/acs.analchem.7b02532.
[64] L. Peng, X. Gao, L. Wang, A. Zhu, X. Cai, P. Li, W. Li, Design of experiment techniques for the optimization of chromatographic analysis conditions: a review, Electrophoresis 43 (2022) 1882–1898. https://doi.org/10.1002/elps.202200072.
[65] G. Hancu, S. Orlandini, L.A. Papp, A. Modroiu, R. Gotti, S. Furlanetto, Application of experimental design methodologies in the enantioseparation of pharmaceuticals by capillary electrophoresis: a review, Molecules 26 (2021), e4681. https://doi.org/10.3390/molecules26154681.
[66] S. Orlandini, R. Gotti, S. Furlanetto, Multivariate optimization of capillary electrophoresis methods: a critical review, J. Pharm. Biomed. Anal. 87 (2014) 290–307. https://doi.org/10.1016/j.jpba.2013.04.014.
[67] B. Pajaziti, M. Andrási, D. Nebija, B.A. Pajaziti, L. Anastasova, R. Petkovska, Chemometrics approach for optimization of capillary electrophoretic conditions for the separation of insulin analogues, Pharmazie 76 (2021) 528–531. https://doi.org/10.1691/ph.2021.1758.

Fundamental and Practical Aspects of Liquid Chromatography and Capillary Electromigration Techniques for the Analysis of Phenolic Compounds in Plants and Plant-Derived Food, Part 2: **Capillary Electromigration Techniques**

Danilo Corradini[1], Francesca Orsini[2], Laura De Gara[2], and Isabella Nicoletti[1], [1]CNR, Institute of Chemical Methodologies, Area della Ricerca di Roma 1, Monterotondo Stazione (Rome), Italy, [2]Unit of Food Science and Nutrition, University Campus Bio-Medico of Rome, Rome, Italy

Analytical separation techniques based on the differential migration velocities of analytes under the action of an electric field are gaining increasing acceptance for the analysis of phenolic compounds in edible and medicinal plants and in plant-derived food products. In Part 2 of this review article the authors discuss the fundamental principles and practical aspects of electromigration techniques, including capillary zone electrophoresis (CZE), micellar electrokinetic chromatography (MEKC), and capillary electrochromatography (CEC). The development of two-dimensional systems, performed by coupling either liquid chromatography (LC) with an electromigration technique or two electromigration techniques, operated under different separation mechanisms, is also discussed.

The first part of this review article focused on fundamental concepts and practical aspects of liquid chromatography (LC) applied to the analysis of phenolic compounds in edible and medicinal plants and in plant-derived food products (1). The paper also briefly discussed the chemical structure and the distribution of the major phenolic compounds occurring in the plant kingdom—which are divided into different subclasses—and how they form an integral part of the human diet and possess a variety of health-promoting properties. This review also briefly addressed the main methods employed for sample preparation and extraction.

A variety of microscale analytical separation methods use a pool of techniques based on the differential migration velocities of analytes under the action of an electric field, which are referred to as capillary electromigration (CE) techniques. These separation techniques are performed in capillary tubes, typically with an internal diameter (i.d.) of 20–100 µm, and may depend on electrophoresis, the transport of charged species through a medium by an applied electric field, or on electrically driven mobile phases to achieve an effective chromatographic separation. Therefore,

KEY POINTS

- This article discusses the main CE techniques employed for the analysis of phenolic compounds in edible and medicinal plants and in plant-derived food.
- CE is performed by a variety of modes, operated under different separation mechanisms, which can be selected by the proper choice of the operational conditions, mainly the chemical composition of the background electrolyte solution filled in an open capillary tube.
- CEC uses capillary chromatographic columns, either packed or monolithic, eluted by liquid mobile phases that are flushed through them by the electroosmotic flow, rather than by a mechanical pump as in nano-LC.
- Most of the CE methods employed for the analysis of phenolic compounds use either CZE or MEKC, which can also be combined together or with LC to perform two-dimensional separations.

Photo Credit: Skyler Ewing/Shutterstock.com

the electric field may either cause the separation mechanism or just promote the flow of a solution throughout the capillary tube, in which the separation takes place—or both.

Part 2 discusses fundamental and practical aspects of a variety of instrumental analytical separation techniques, based on electromigration principles that, as well as LC, are suitable for the separation, identification, and quantification of phenolic compounds in plant materials and plant-derived food products.

Capillary Electromigration Techniques

In addition to high performance liquid chromatography (HPLC) and ultrahigh-pressure liquid chromatography (UHPLC), which are still the techniques of choice for the analysis of phenolic compounds, CE using capillary tubes with a typical internal diameter and length of 20–100 µm and 20–100 cm, respectively, are gaining increasing interest in this field. Capillary electromigration techniques can be performed using a variety of modes, based on different separation mechanisms that can be selected by simply changing the operational conditions, in particular the composition of the electrolyte solution, which may consist of either a continuous or a discontinuous electrolyte system (2). The separation modes mostly employed for the analysis of phenolic compounds are capillary zone electrophoresis (CZE) and micellar electrokinetic chromatography (MEKC), also referred to as micellar electrokinetic capillary chromatography (MECC). Both separation modes use continuous electrolyte systems, which involves background electrolyte (BGEs) solutions whose composition is constant along the capillary tube.

As in HPLC and UHPLC, the detectors primarily used are variable-wavelength and photodiode array (PDA) spectrophotometers. The detection is performed on-column through a "window" obtained by removing a small portion of the polyimide external coating of the fused-silica capillary tube, usually the cathodic end, where the detection takes place. The main drawback of photometric on-column detection is the short distance the light travels through the capillary (the optical path length), corresponding to the internal diameter of the capillary tube. Other detection modalities include electrochemical detection, which is based on conductometric, amperometric, voltametric, and potentiometric measurements, and hyphenation with mass spectrometry (MS), whereas the hyphenation with other techniques, such as mid-infrared (MIR) spectroscopy is limited (3–4).

Capillary electromigration techniques are commonly hyphenated with MS by two major types of electrospray ionization (ESI) interfaces, which are identified as coaxial sheath-flow and sheath-less interfaces (5). The most commonly used arrangement is the coaxial sheath-flow interface, consisting of two concentric tubes surrounding the separation capillary, which are devoted to delivering the sheath-liquid and the nebulizing gas. The function of the sheath liquid is to provide electrical contact, compatible solvent composition for ionization, and evaporation independent of the nature of the BGE, as well as flow rate matching the requirements of the ionization interface. Moreover, sheath-flow interfaces offer the possibility to add a reagent capable of undergoing specific reactions with certain analytes to the sheath-liquid. For example, the addition of DPPH (2,2-diphenyl-1-picrylhydrazyl) to the sheath-liquid has been proven to be a fast screening tool for studying antioxidant characteristics of plant phenolic compounds (6).

Capillary Zone Electrophoresis

Phenolic compounds are separated by CZE using continuous electrolyte solution systems and constant electric field strength throughout the capillary length, either in aqueous or nonaqueous BGEs. The separation mechanism is based on differences in the electrophoretic mobilities of charged species and, therefore, on differences in their charge-to-mass ratio. Under the influence of the electric field applied across the capillary tube, the charged analytes migrate with different velocities towards the corresponding electrode—positively charged analytes towards the cathode and negatively charged analytes towards the anode. However, in the presence of sufficiently strong electroosmotic flow (EOF)—the stream of liquid induced by the applied potential across the capillary tube—cations, anions, and neutral species migrate in the direction of EOF, where the sample detection takes place.

In general, phenolic compounds are assayed by CZE using an alkaline buffer to promote their ionization, which mostly depends on their pK_a values, ranging between approximately 7 and 12 for flavonoids and between approximately 4 and 12 for phenolic acids, respectively, depending on the molecular structure of the phenolic compounds. However, pH values higher than 10 are generally avoided to prevent the possible oxidation of these compounds, which are known to be rather reactive with the dissolved oxygen in alkaline solutions. In addition, the ability of borate ions to form negatively charged complexes with vicinal –OH groups of polyhydric phenolic compounds has been used to modulate the electromigration behaviour of these analytes, which are typically analyzed in tetraborate buffer at pH values ranging between 9 and 10.

The CZE separation of phenolic compounds as borate complexes is usually optimized by incorporating an organic solvent into the BGE, which influences the formation of the borate complexes and changes viscosity and relative permittivity of the buffer solution, with consequent selective variations of the electrophoretic mobility of the charged analytes. The additional positive effects of the incorporation of an organic solvent into the BGE are the decrease in the electrical current, with consequent reduction of Joule heating and peak band broadening, and the reduction of EOF, resulting in an increase of the analyte migration time window. The influence of the content of ethanol incorporated into the BGE on conductivity and EOF is depicted by the plots displayed in Figures 1 and 2, respectively.

By increasing the borate concentrations in the BGE, the extent of complex formation with vicinal diol groups is expected to increase, leading to longer analysis time and larger differences in separation selectivity. Nevertheless, limited practical effects on resolutions are obtained by increasing the concentration of the borate buffer, as well as by changing its pH, which can be varied within the range of the buffering capacity of the borate solutions and the limits of concentration compatible with the requested low electrical conductivity of the BGE.

The electropherograms reported in Figure 3 represent an example of standard phenolic compounds separated by CZE as borate complexes without and with the incorporation

Figure 1: Influence of the content of ethanol incorporated into the BGE on conductivity. Capillary, bare fused-silica 0.050-mm i.d., 0.375 mm o.d., total length = 405 mm (320 mm to the detector); BGE, 50-mM borate buffer pH = 9.5; and applied voltage = 25 KV.

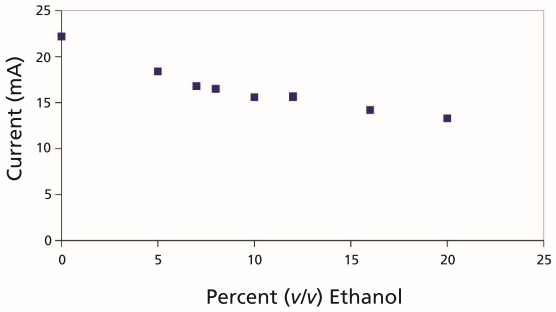

Figure 2: Influence of the content of ethanol incorporated into the BGE on EOF. Capillary, BGE, and experimental conditions as in Figure 1.

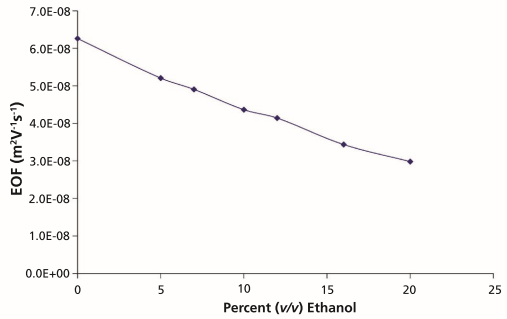

of an organic solvent into the BGE, consisting of 50-mM borate buffer at pH 9.5. It is observed (Figure 3[b]) that the incorporation of 16% (*v/v*) ethanol into the BGE brings about the complete resolution of the selected 11 phenolic compounds, otherwise only partially separated in the absence of ethanol (Figure 3[a]).

CZE methods based on the analytical approach described above have been developed for the analysis of phenolic compounds occurring in a variety of plants and plant-derived food, including herbal teas (7), olive oil (8), and medicinal plants (9–10). Proposed modifications of this approach include the use of mixed phosphate-borate buffers (11), and the incorporation of additives into the borate buffer, such as the ionic liquid 1-butyl-3-methylimidazolium tetrafluoroborate for the separation of isoflavones (12) or the chiral selector 2-hydroxypropyl-γ-cyclodextrin for the separation of flavanone enantiomers (13). In addition to the well established BGEs discussed previously, phosphate buffer was recently employed in CZE for analyzing phenolic acids in Italian wheat samples (14) and in Irish whiskies by a field amplified sample staking (FASS) pre-concentration method (15).

Micellar Electrokinetic Chromatography

Micellar electrokinetic chromatography uses electrolyte solutions incorporating a surfactant at a concentration higher than its critical micelle concentration (CMC) that forms micelles acting as a pseudo-stationary phase dispersed into the BGE. This separation mode extends the application of the electromigration techniques to noncharged molecules. The mechanism of separation is based on the distribution of the analytes between the pseudo-stationary phase, formed by the dispersed micelles and the surrounding solution. Noncharged analytes that do not interact at all with the micelles migrate at the same velocity of EOF, whereas those participating to reversible interactions with the micelles migrate at the velocity of the micelles when they are associated with them and at the velocity of EOF when they are in the bulk solution. Therefore, the migration velocity of these analytes, which is comprised between EOF and the electrophoretic mobility of micelles, is proportional to the time they migrate associated with the micelles and, consequently, to the strength of their interaction with the dispersed phase (2).

Composition and pH of the electrolyte solution employed in MEKC are selected to generate a sufficiently high EOF to transport micelles and analytes towards the detection windows. Sodium dodecyl sulphate (SDS) is by far the most widely used surfactant because of its relatively low cost, its availability in highly purified forms, and low CMC in aqueous solution (8 mM), above which it forms almost spherical anionic micelles with the charged heads oriented towards the solution and the hydrophobic tails pointing towards the aggregate. SDS is incorporated into the BGE at neutral to alkaline pH values to ensure strong EOF with bare fused-silica capillaries. Under these conditions, the anionic micelles migrate in the opposite direction to EOF and, therefore, are transported towards the cathode with a migration velocity slower than the stream of the bulk flow of BGE.

The use of acidic BGEs has been rarely applied for the separation of phenolic compounds by MEKC, mainly as a result of the low EOF generated at low pH values, which hinders the migration of the negatively charged micelles towards the cathodic end of the capillary, where the detection take place. Nevertheless, procyanidins have been efficiently separated by MEKC using 100-mM SDS in 0.1 M acetate buffer pH 5.0 (16).

MEKC is particularly suitable to separate phenolic compounds with similar structure but different lipophilicity. Generally, unsaturation of the C-ring lowers hydrophobicity and, consequently, the migration time; methylation of the hydroxyl group increases the hydrophobicity of the analyte and, accordingly, its affinity to the micelles, which results in increasing migration times; glycosylation and higher number of –OH groups increases hydrophilicity and therefore the migration time decreases.

The on-line hyphenation of MEKC with mass spectrometry (MEKC–MS) is often hampered by the incorporation of the surfactant into the BGE, which suppresses ionization efficiency and contaminates the inlet of the mass spectrometer. Possible approaches to overcome these limitations include the selection of the (semi)volatile surfactants perfluorooctanic acid and perfluorooctane sulfonic acid (17), the use of anodically migrating micelles (18), and the use of either a sheathless porous-tip interface (19) or a desorption electrospray ionization (DESI) interface (20).

As well as the surfactant, a variety of additives or organic solvents can also be incorporated into the BGE to modulate selectivity and peak capacity. The formation of inclusion complexes of cyclodextrins with charged and uncharged phenolic compounds have been widely studied for their ability

to influence the migration behaviour of these compounds in MEKC. For example, the incorporation of β-cyclodextrin into the BGE has proven to improve the resolution of flavonoids in MEKC, performed with phosphate-borate buffer at pH 9.8 containing 100-mM SDS (21). Moreover, the formation of inclusion complexes of sulphated-β-cyclodextrin with catechins has been used to improve the separation of these phenolic compounds extracted from green tea infusions by MEKC (22). Also effective in improving the separation of flavonoids—extracted from the aerial part of an Argentinian medicinal plant (*Ligaria cuneifolia*)—has been the incorporation of a mixture of β-cyclodextrin (5 mM) and sulphated-β-cyclodextrin (2% w/v) into the BGE, consisting of 50-mm SDS in 20-mm borate buffer (pH 8.3) (23).

The suitability of β-cyclodextrin as an additive of the BGE employed in MEKC has also been explored in combination with the ionic liquid 1-butyl-3-methylimidazolium tetrafluoroborate. Both additives have been incorporated into the BGE—consisting of SDS in phosphate-borate buffer—to improve the simultaneous separation by MEKC of seven phenolic acids and four diterpene quinones in three *Salvia* species (24). The same ionic liquid has also been incorporated into the BGE—consisting of polyoxyethylene sorbitan monolaurate (Tween 20) and sodium borate at pH 9.2—to modify the separation performance of phenolic acids in MEKC (25).

The separation window, corresponding to the time difference between the velocity of EOF and anionic micelles, and resolution of phenolic compounds in MEKC are also modulated by incorporating an organic solvent into the BGE. The organic solvents influence EOF, the rate of inclusion complex formation, the hydrophobic interactions of phenolic compounds with nonpolar additives, and the CMC of the surfactant. Methanol and acetonitrile are the organic solvents most often used in MEKC of phenolic compounds (26), although the influence of other organic solvents has been tested too (27).

CE in Two-Dimensional Separation Systems

Phenolic compounds are separated by CZE according to differences in their mass-to-charge ratio, whereas their separation by reversed phase-HPLC depends on differences in their hydrophobicity. These two diverse separation mechanisms are independent of each other and, consequently, provide complementary selectivity. This can be witnessed by plotting the migration times of phenolic compounds in CZE versus their retention times in reversed phase-HPLC, as shown in Figure 4. Significant differences in selectivity are also expected between CZE and MEKC, whose separation mechanism for uncharged analytes is based on their distribution between the dispersed micelles and the surrounding solution.

Thus, two-dimensional (2D) separation systems, performed by coupling LC with CE, appear to be an interesting option, offering a potentially high degree of orthogonality. However, the direct hyphenation of LC with CE requires a variety of problems to be overcome. These arise from the differences between the dimensions of the chromatographic column and

YMC
EUROPE GMBH

BioLC Innovations...
...with Incredible Reproducibility!

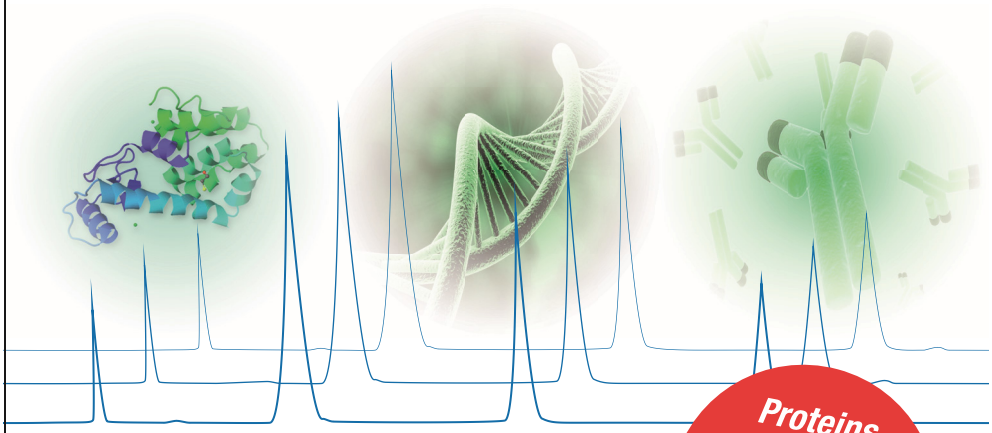

- SEC for high resolved MAbs
- HIC with exceptional efficiency
- RP-C4-Widepore with superior stability
- IEX for high recovery

Discover more at **www.ymc.de**

Figure 3: Separation by CZE of standard phenolic compounds as borate complexes (a) without and (b) with the incorporation of 16% (*v/v*) ethanol into the BGE, consisting of 50-mM borate buffer pH 9.5. Phenolic compounds: (1) *trans*-piceide, (2) *trans*-resveratrol, (3) rutin, (4) naringenin, (5) chlorogenic acid, (6) kaempferol, (7) ferulic acid, (8) myricetin, (9) quercitin, (10) cumaric acid, (11) caffeic acid. Capillary, BGE, and experimental conditions as in Figure 1.

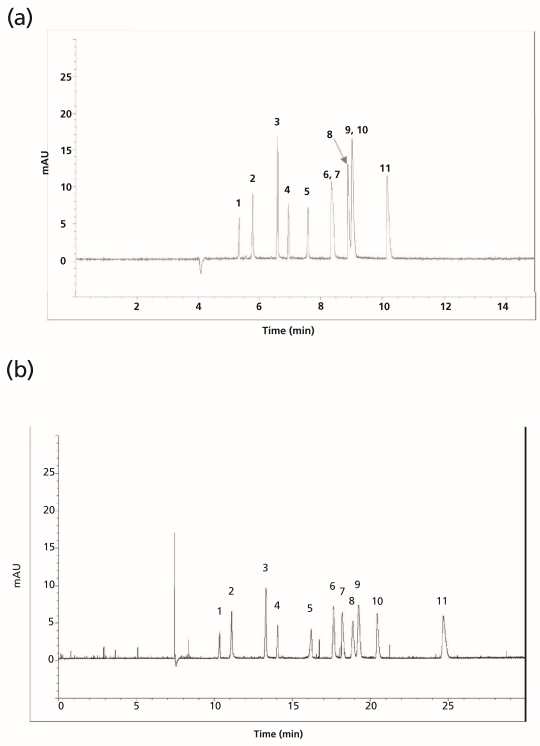

Figure 4: Complementary selectivity between reversed phase-HPLC and CZE. Separation of phenolic compounds by reversed phase-HPLC, column: 2.1 mm × 150 mm, 5-µm Polaris C18, eluted by a multisegment gradient of increasing concentration of acetonitrile in water containing 0.5% (*v/v*) formic acid; flow rate = 0.2 mL/min. Separation of phenolic compounds by CZE, capillary: bare fused-silica 0.050 mm i.d., 0.375 mm o.d. total length 405 mm (320 mm to the detector); BGE: 50 mM borate buffer pH = 9.5; applied voltage = 25 KV. Phenolic compounds: (1) *trans*-piceide, (2) *trans*-resveratrol, (3) rutin, (4) naringenin, (5) chlorogenic acid, (6) kaempferol, (7) ferulic acid, (8) myricetin, (9) quercitin, (10) caffeic acid.

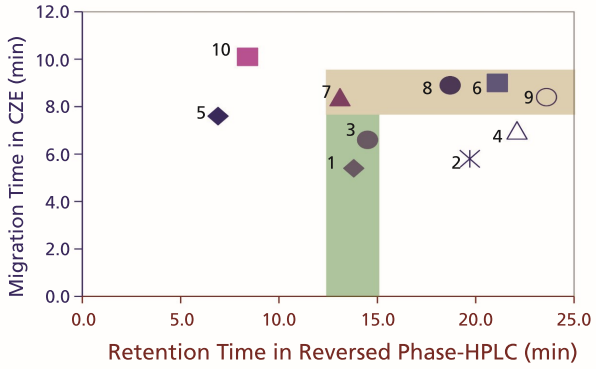

the capillary tube used in CE, the different flow rates and composition of the liquid phase passing throughout them, and the need to complete the electric circuit to apply the high voltage across the capillary tube for electrophoresis. Although CE can be used either in the first or in the second dimension, its use in the second dimension is more common, as first proposed by Jorgenson (28).

It is noteworthy that CE offers the possibility of performing two-dimensional separations using either a single capillary column (29) or, as in 2D LC, two different columns coupled by an interface or a multiple-port switching valve (30–31). The alternative and more applied approach is the offline hyphenation of LC and CE, in which only the fractions of the effluent from the first dimension—those containing the analytes of interest—are collected and subsequently separated in the second dimension.

The majority of the 2D separation systems containing at least one electromigration separation technique have been developed for peptide and protein analysis and proteome investigations. Nevertheless, remarkable applications of these 2D systems for the analysis of phenolic compounds in plants and food matrices of plant origin have been reported. Reversed phase-HPLC has been successfully combined offline with CZE for the separation and identification of phenolic compounds extracted from extra virgin olive oil. The 2D separation system involved the use of a semipreparative reversed phase column in the first dimension, the manual collection of the fractions containing unresolved phenolic compounds, and their subsequent analysis in the second dimension by CZE with on-line quadrupole time-of-flight (QTOF)-MS detection, using an orthogonal electrospray interface (32).

Complex mixtures of phenolic compounds have also been successfully separated coupling offline reversed phase chromatography with MEKC, as reported by Jandera *et al.* (33). They developed an automated offline LC-MEKC system for the separation of flavones and phenolic acid by reversed phase chromatography in the first dimension and MEKC in the second dimension. Reversed phase chromatography was performed with a polyethylene glycol (PEG) reversed phase column, eluted by a gradient of increasing concentration of acetonitrile in the mobile phase, whereas SDS and heptakis(6-O-sulfo)-β-cyclodextrin were incorporated into the BGE used for the MEKC separation. An autosampler was used as the interface between the LC and the MEKC separation systems and the outlet of the reversed phase column was connected to the autosampler via a six-port switching valve. The fractions of the effluent from the LC column, collected into the vials of the autosampler, were subsequently analyzed in the MEKC second dimension, using spectrophotometric UV detection at 280 nm.

Applications of 2D systems in a single capillary have been reported for the separation and quantification of flavonoids in the herbaceous perennial plants *Leonurus cardiaca* (34), using MEKC as the first dimension and CZE with electrochemical detection as the second dimension. A 2D MEKC–CZE system in a single capillary, involving the on-line combination of sweeping with electrokinetic injection and analyte focusing by micelle collapse, has also been reported for the separation and quantification of flavonoids in the medicinal plant *Herba Leonuri* (35).

Capillary Electrochromatography

Capillary electrochromatography (CEC) uses capillary columns similar to those employed in nano-LC, with the difference being that in CEC the mobile phase is flushed through the column by EOF, rather than by a mechanical pump. The result is that the flow of the mobile phase passing throughout the CEC capillary column displays a flat plug-like profile, which does not contribute to peak broadening. This is in contrast to the laminar or parabolic flow profile generated in LC, where there is a strong pressure drop across the column caused by frictional forces at the liquid–solid boundary. Moreover, the absence of column backpressure also allows CEC to be performed with capillary columns of low permeability, such as those packed with sub-2-µm particles. On the other hand, the column length is limited by the value of the electric field requested to obtain the desired flow rate with commercially available power supplies, which usually consent to applying up to 30 kV. It is also noteworthy that only the isocratic elution mode is allowed with common commercially available instrumentation.

The capillary column can be either filled, packed, or coated with a stationary phase, which provides the sites for the required interactions with the analytes and charged groups for the generation of the EOF needed to ensure the movement of the mobile phase through the column. Stationary phases carrying cationic functional groups, such as amino or ammonium groups, generate anodic EOF, whereas stationary phases with anionic functionalities, such as sulphonic or acetic groups, generate cathodic EOF. The stationary phase may also carry zwitterionic groups and in this case exhibits either cathodic or anodic EOF, according to the pH of the mobile phase.

Capillary columns containing *in situ* prepared monolithic separation media, formed from either organic polymers or silica, offer the advantage of circumventing the fabrication of frits at both ends of the capillary tube, which is otherwise necessary to retain the particles inside the packed columns—a critical step in the preparation of homemade CEC columns. The organic-based monolithic columns are generally made of a mixture of monomers, crosslinkers, and porogens by radical polymerization, which is conducted directly within the confine of a capillary. Porous size and distribution, as well as EOF and retentive properties of polymer-based monolithic columns, can be easily tailored by tuning the composition of the reaction mixture, which can be composed of a variety of ionizable monomers, neutral reactants, and porogenic solvents at different percentages.

A homogeneous monolithic CEC column, prepared by photo-polymerization of (3-allyl-1-imidazol)propane sulfonate, has recently been used for the efficient separation of phenolic acids in coffee beans (36). The separation was performed using a mixture of acetonitrile and water, containing 12-mM ammonium acetate at pH 8.5, as the mobile phase. The on-column revelation of the separated phenolic acids was performed by PDA detection at 280 nm. A combination of hydrophobic and electrostatic interactions between the zwitterionic stationary phase and the charged phenolic acids was considered to influence the separation mechanism.

Other applications of CEC using polymer-based monolithic capillary columns include the separation of coumarins extracted from *Fructus cnidii*, using a poly(butyl methacrylate-*co*-ethylene dimethacrylate-*co*-[2-(methacryloyloxy)ethyl] trimethylammonium chloride) homemade monolithic column (37). The separation and quantification of isopimpinelline, bergapten, imperatorin, and osthole was obtained in less than five minutes using an hydro-organic mobile phase, containing 50% (*v/v*) acetonitrile and aqueous 10 mM sodium dihydrogen phosphate solution at pH 4.95. A lauryl acrylate ester-based monolithic column has been developed for studying the phenolic fraction of extra virgin olive oils (EVOO). Using a linear discriminant analysis, the phenolic profiles determined by CEC were able to classify the EVOO samples belonging to three different geographical origins (Croatia, Italy, and Spain), without identifying the separated phenolic compounds (38).

A method for the identification and quantification of 10 phenolic compounds in EVOO by CEC has been developed by Fanali *et al.* using silica-based reversed phase columns (39). The study evaluated the performance of several types of C8 and C18 stationary phases and the optimum separation was obtained using bidentate C18 particles packed in a 23-cm silica tube (75-mm i.d.) and eluted by a hydro-organic mobile phase. The method allowed the efficient separation, identification, and quantification of protocatechuic, p-coumaric, o-coumaric, vanillic, ferulic, caffeic, syringic acids, hydroxytyrosol, tyrosol, and oleuropein in less than 35 min.

A capillary column packed with bidentate C18 particles has also been successfully used in CEC for the rapid and efficient separation and quantification of catechins and methylxantines in green and black teas, including (+)-catechin, (–)-epicatechin, (–)-epigallocatechin, theophylline, and caffeine (40). Fanali has also developed an amino-functionalized spherical ordered mesoporous silica that, when packed in 100-µm i.d. fused-silica capillary tubes, has been successfully used in CEC for enantio- and diastereomeric separations (41). Efficient and rapid stereoisomer resolution of a variety of flavonoids and flavanones glycosides has been obtained in reversed phase mode, using a mixture of methanol–water as the mobile phase with ammonium acetate buffer at pH 4.5 and at different volume ratios.

Conclusions

CZE and MEKC are the most popular separation modes employed using CE for phenolic compounds, which are generally separated by CZE as borate complexes at alkaline conditions (pH 9–10). Borate buffer is also the BGE of choice when using MEKC for neutral phenolic compounds as a result of its optimum buffering capacity at pH values that ensure strong EOF and the capability of the borate ions to form negatively charged complexes with vicinal –OH groups of polyhydric phenolic compounds. However, borate buffer, as well as other nonvolatile buffers, and the majority of surfactants employed in MEKC are not suitable for on-line hyphenation of this technique with MS, which has found limited applications for the analysis of phenolic compounds.

As well as the surfactant, several additives and organic solvents are currently incorporated into the BGE to modulate selectivity and peak capacity. Examples of this approach include the use of cyclodextrins, which form inclusion complexes with charged and uncharged phenolic compounds and, therefore, influence their migration behaviour in MEKC.

A high degree of orthogonality is potentially possible by the hyphenation of reversed phase chromatography with either

CZE or MEKC, as well as by the combination of two different electromigration separation techniques, such as MEKC and CZE, either using one single or two different capillary tubes. However, the direct hyphenation of LC with CE is hampered by the need to solve several technical problems arising from instrumental and operational differences, limiting its applications. Also modest are the applications of CEC for the analysis of phenolic compounds occurring in edible and medicinal plants and in plant-derived food and dietary supplements, mainly because isocratic elution mode is solely possible with common commercially available CEC instrumentation and the restricted number of commercially available CEC columns.

Currently, a wide selection of techniques are available for the separation and identification of natural phenolic compounds. However, the ever increasing interest of scientists, food producers, and society in healthy food and dietary supplements is expected to boost the development of more advanced methods for both sample preparation and analysis of phenolic compounds, as well as other plant specialized metabolites with health-promoting properties.

References

(1) D. Corradini, F. Orsini, L. De Gara and I. Nicoletti, *LCGC Europe* **31**(9), 480–490 (2018).
(2) D. Corradini, in *Handbook of HPLC,* D. Corradini, Ed. (CRC Press, Boca Raton, USA, 2nd ed., 2010), pp.155–206.
(3) A. Beutner, R. Rodrigues Cunha, E.M. Richter, and F.M. Matysik, *Electrophoresis* **37**, 931–935 (2016).
(4) J. Kuligowski, A. Quintás, M. de la Guardia, and B. Lendl, *Anal. Chim. Acta* **679**, 1640–1652 (2017).
(5) G. Bonvin, J. Schappler, and S. Rudaz, *J. Chromatogr. A* **1267**, 17–31 (2012).
(6) L. Maringer, E. Ibáñez, W. Buchberger, C.W. Klampfl, and T.J. Causon, *Electrophoresis* **36**, 348–354 (2015).
(7) W.J. Arries, A.G.J. Tredoux, D. de Beer, E. Joubert, and A. de Villiers, *Electrophoresis* **38**, 897–905 (2017).
(8) M. de los Angeles de Fernandez, V.C. SotoVargas, and M.F. Silva, *J. Am. Oil Chem. Soc.* **91**, 2021–2033 (2014).
(9) L.S. Müller, G. Domingos da Silveira, V. Dal Prá, O. Lameira, C. Viana, and L. Machado de Carvalho, *J. Liq. Chromatogr. Relat. Technol.* **39**, 13–20 (2016).
(10) Y. Deng, S.-C-Lam, J. Zhao, and S.P. Li, *Electrophoresis* **38**, 2654–2661 (2017).
(11) Z.-Y. Ren, Y. Zhang, and Y.P. Shi, *Talanta* **78**, 959–963 (2009).
(12) W. Xiao, F.Q. Wang, C.H. Li, Q. Zhang, Z.N. Xia, and F.Q. Yang, *Anal. Methods* **7**, 1098–1103 (2015).
(13) J. Pan, S. Zhang, L. Yan, J. Tai, Q. Xiao, K. Zou, Y. Zhou, and J. Wu, *J. Chromatogr. A* **1185**, 117–129 (2008).
(14) R. Gotti, E. Amadesi, J. Fiori, S. Bosi, V. Bregola, I. Marotti, and G. Dinelli, *J. Chromatogr. A* **1532**, 208–215 (2018).
(15) B. White, M.R. Smyth, and C.E. Lunte, *Anal. Methods* **9**, 1248–1252 (2017).
(16) A. Cifuentes, B. Bartolomé, and C. Gómez-Cordovés, *Electrophoresis* **22**, 1561–1567 (2001).
(17) Y. Ishihama, H. Katayama, and N. Asakawa, *Anal. Biochem.* **287**, 45–54 (2000).
(18) L. Yang, A.K. Harrata, and C.S. Lee, *Anal. Chem.* **69**, 1820–1826 (1997).
(19) D. Moreno-González, R. Haselberg, L. Gámiz-Gracia, A.M. Garcìa-Campaña, G.J. de Jong, and G.W. Somsen, *J. Chromatogr. A* **1524**, 283–289 (2017).
(20) G.K. Barbula, S. Safi, K. Chingin, R.H. Perry, and R.N. Zare, *Anal. Chem.* **83**, 1955–1959 (2011).
(21) L. Jiang, G. Fang, Y. Zhang, G. Cao, and S. Wang, *J. Agric. Food Chem.* **56**, 11571–11577 (2008).
(22) R.G. Peres, F.G. Tonin, M.F.M. Tavares, and D.B. Rodriguez-Amaya, *Food Chem.* **127**, 651–655 (2011).
(23) B. Dobrecky, S.A. Flor, P.G. Lopez, M.L. Wagner, and S.E. Lucangio, *Electrophoresis* **38**, 1292–1300 (2017).
(24) J.L. Cao, J. Hu, J. Wei, B.C. Li, M. Zhang, C. Xiang, and P. Li, *Molecules* **20**, 15304–15318 (2015).
(25) L. Liu, B. Wu, K. Liu, C.-R. Li, X. Zhou, P. Li, and H. Yang, *J. Pharm. Biomed.* Anal. **126**, 1–8 (2016).
(26) R. Martí, M. Valcárcel, J.M. Herrero-Martínez, J. Cebolla-Cornejo, and S. Roselló, *Food Chem.* **221**, 439–446 (2017).
(27) M. Ganzera, C. Egger, C. Zidorn, and H. Stuppner, *Anal. Chim. Acta* **614**, 196–200 (2008).
(28) M.M. Bushey and J.W. Jorgenson, *Anal. Chem.* **62**, 978–984 (1990).
(29) C. Kukusamude, S. Srijaranai, and J.P. Quirino, *Anal. Chem.* **86**, 3159–3166 (2014).
(30) L. Ranjbar, A.J. Gaudry, M.C. Breadmore, and R.A. Shellie, *Anal. Chem.* **87**, 8673–8678 (2015).
(31) Y. Li, X. Fang, S. Zhao, T. Zhai, X. Sun, and J.J. Bao, *Chem. Lett.* **39**, 983–985 (2010).
(32) R. Garcia -Villalba, A. Carrasco-Pancorbo, A. Vázquez-Martìn, C. Oliveras-Ferraros, J.A. Menéndez, A. Segura-Carretero, and A. Fernández-Gutiérrez, *Electrophoresis* **30**, 2688–2701 (2009).
(33) P. Cesla, J. Fischer, and P. Jandera, *Electrophoresis* **31**, 2200–2210 (2010).
(34) X. Zhang and Z. Zhang, *J. Chromatogr. B* **879**, 1641–1646 (2011).
(35) Z. Zhang, X. Du, and X. Li, *Anal. Chem.* **83**, 1291–1299 (2011).
(36) A. Murauer, R. Bakry, H. Schottenberger, C. Huck, and M. Ganzera, *Anal. Chim. Acta* **963**, 1336–1342 (2017).
(37) J. Wang, D. Chen, Z. Chen, G. Fan, and Y. Wu, *J. Sep. Sci.* **33**, 1099–1108 (2010).
(38) M.J. Lerma-García, C. Lantano, E. Chiavaro, L. Cerretani, J.M. Herrero-Martínez, and E.F. Simó-Alfonso, *Food Res. Int.* **42**, 1446–1452 (2009).
(39) Z. Aturki, S. Fanali, G. D'Orazio, A. Rocco, and C. Rosati, *Electrophoresis* **29**, 1643–1650 (2008).
(40) U.D. Uysal, Z. Aturki, M.A. Raggi, and S. Fanali, *J. Sep. Sci.* **32**, 1002–1010 (2009).
(41) M. Silva, D. Pérez-Quintanilla, S. Morante-Zarcero, I, Sierra, M.L. Marina, Z. Aturki, and S. Fanali, *J. Chromatogr. A* **1490**, 166–176 (2017).

Danilo Corradini earned his Ph.D. in chemistry at Sapienza University of Rome (Italy) and received postdoctoral education in separation science at the Department of Chemical Engineering, Yale University (USA). His research interests include the study of fundamental and practical aspects of HPLC and electromigration techniques for analytical separations of biomolecules, mainly of plant origin. In recognition of his scientific contributions, he has received the Csaba Horváth Memorial Award in 2009, the Central European Group for Separation Science Award in 2011, and the Arnaldo Liberti Medal in 2014.

Francesca Orsini is a registered nutritionist in the register of the Italian Biologists. She received her bachelor degree in food science and human nutrition in 2012 and master's degree in food technology and science nutrition in 2014. She completed her education with a Ph.D. in bioengineering and biosciences in 2018 at the University Campus Bio-Medico of Rome. Her research domains include development of sample preparation procedures and chromatographic analytical methods for bioactive compounds in plant material.

Laura De Gara is Full Professor of plant physiology and head of the master's degree in food science and human nutrition at the Campus Bio-Medico University of Rome. She has almost 30 years of experience in studying plant metabolism with particular attention to redox homeostasis and signalling in response to environmental conditions. She is also interested in plant metabolites with nutritional and healthy effects, in particular polyphenols, fructans, and other fibres, as well as antioxidant vitamins.

Isabella Nicoletti was educated as a biologist at Sapienza University of Rome, where she was also a postdoctoral fellow at the Department of Chemistry from 1982 to 1985. Since 1985 she has been a research scientist at the Institute of Chemical Methodologies of the Italian Research Councilin Montelibretti (Rome). She is an expert in the field of separation science, and is interested in the development of chromatographic techniques for innovative analytical methods for foods with determined healthy prerogatives.